INFORMATION TO USERS

This manuscript has been reproduced from the microfilm master. UMI films the text directly from the original or copy submitted. Thus, some thesis and dissertation copies are in typewriter face, while others may be from any type of computer printer.

The quality of this reproduction is dependent upon the quality of the copy submitted. Broken or indistinct print, colored or poor quality illustrations and photographs, print bleedthrough, substandard margins, and improper alignment can adversely affect reproduction.

In the unlikely event that the author did not send UMI a complete manuscript and there are missing pages, these will be noted. Also, if unauthorized copyright material had to be removed, a note will indicate the deletion.

Oversize materials (e.g., maps, drawings, charts) are reproduced by sectioning the original, beginning at the upper left-hand corner and continuing from left to right in equal sections with small overlaps. Each original is also photographed in one exposure and is included in reduced form at the back of the book.

Photographs included in the original manuscript have been reproduced xerographically in this copy. Higher quality 6" x 9" black and white photographic prints are available for any photographs or illustrations appearing in this copy for an additional charge. Contact UMI directly to order.

UMI

A Bell & Howell Information Company
300 North Zeeb Road, Ann Arbor MI 48106-1346 USA
313/761-4700 800/521-0600

Flashing Flow of Refrigerant HFC-134a through a Diabatic Capillary Tube

De-Kang Chen

A Thesis
in
The Department
of
Mechanical Engineering

Presented in Partial Fulfillment of the Requirements
for the Degree of doctor of Philosophy at
Concordia University
Montreal, Quebec, Canada

April 1997

ABSTRACT

Flashing Flow of Refrigerant HFC-134a through a Diabatic Capillary Tube

De-Kang Chen, Ph.D.
Concordia University, 1997

Capillary tubes are components in refrigerating systems which act as expansion and flow-rate controlling devices. The proper design of capillary tubes is an important factor in performance efficiency of these systems.

An experimental test loop was designed and built for testing the capillary tube. This test loop simulated the actual refrigeration system that normally supplied refrigerant with or without oil to the capillary tube, while providing easily controlled boundary conditions. Pressures and temperatures along the capillary tube and suction line were also instrumented. The capillary tube was tested for a wide range of conditions including: subcooled inlet, diabatic and adiabatic capillary tube, refrigerant HFC-134a flow with and without oil.

The process of refrigerant flow through a capillary tube is a flashing process, in which the state of the refrigerant changes from subcooled liquid to a vapor-liquid mixture. Metastable phenomena in the flow, i.e. a thermal nonequilibrium phenomena, may exist within a flashing process. Whereas a

literature survey showed that the metastable flow of refrigerant was only observed in adiabatic capillary tubes, the experiment demonstrated metastable flow through the diabatic capillary tube for the first time. It is found from the experiment that the metastable flow will vanish when $G_o/G_s < 77.8$. A correlation of the underpressure of vaporization (a characteristic quantity for metastable flow) for a diabatic capillary tube, based on homogeneous nucleation theory, was developed to consolidate this new result.

The flow in the capillary tube was numerically modeled by dividing the flow into two regions: single-phase and two-phase. The liquid single-phase flow region was described by four governing differential equations and boundary conditions. The numerical model for the two-phase flow region used one-dimensional nonequilibrium two-fluid equations which accounted for the relative velocity and the temperature difference between the vapor and liquid phases. Results of the numerical models compared satisfactorily with measured experimental data. The results indicated that the vaporization occurred near the capillary tube exit with a strong heat transfer between the capillary tube and suction line; the mass flux of refrigerant in the capillary tube without oil was about 2.2% higher than that with oil.

ACKNOWLEDGMENTS

I would especially like to acknowledge Professor S. Lin' s professional and personal support. This thesis is a product of both.

I would also like to acknowledge my father, Professor Z. H. Chen for his support and encouragement.

Dr. R. Y. Li and Senior Engineer H. L. Yu at Two-Phase Flow Laboratory in East China University of Technology, Shanghai, helped significantly by making available to me test facilities and measuring equipment for the experiment.

I would, above all else, like to thank my wife, Meice, for her patience and love while I was completing my thesis.

TABLE OF CONTENTS

LIST OF FIGURES

LIST OF TABLES

NOMENCLATURE

A	availability	(J)
A_a	area	(m^2)
a	interfacial area/unit volume	(1/m)
B	collision frequency of molecules	(1/s)
C	constant	
C_D	drag coefficient	
Cf	interfacial friction coefficient	
c_p	specific heat	(J/kg °C)
D	tube inside diameter	(m)
D'	reference length	(m)
d	average bubble diameter	(m)
erfc( )	complementary error function	
F_{gl}	interfacial drag force	(Pa/m)
F_{wl}	force due to frictional pressure drop	(Pa/m)

f_o	cross-sectional factor	
G	mass flux	(kg/s m^2)
Gb	Gibbs number	
Gr	Grashof number	
g	acceleration of gravity	(m/s^2)
g_n	Gibbs function	
h	enthalpy	(J/kg)
h_{gl}	latent heat	(J/kg)
$\bar{h}$	heat transfer coefficient	(W/m^2 °C)
K	Boltzmann's constant	(J/K)
k	thermal conductivity	(W/m °C)
L	tube length	(m)
m	mass	(kg)
m_n	molecule number	
$\dot{m}$	mass flow rate	(kg/s)
N	molecule density	($1/m^3$)
N_A	Avogadro constant	(1/mol)
N_R	bubble density	($1/m^3$)

Nu	Nusselt number	
n	rate of formation of activated cluster	(1/s m^3)
Pr	Prandtl number	
p	pressure in capillary tube	(Pa)
$p_{sat} - p_v$	underpressure of vaporization	(Pa)
Q	heat flow rate	(W)
q	heat transfer rate	(W/m^3)
q_{amb}	heat loss from the insulation surface	(W/m^2)
Re	Reynolds number	
r	radius of activated cluster	(m)
s	entropy	(J/kg °C)
T	temperature	(°C)
ΔT_{csub}	subcooling at the capillary tube inlet	(°C)
V	axial velocity in the tube	(m/s)
v	specific volume	(m^3/kg)
W	reversible work	(J/kg)
x	quality	
z	distance along the tube	(m)

Δz_{sv}	distance between the saturated point and inception of vaporization	(m)

Greek letters

α	void fraction	
β	coefficient of thermal expansion	(1/°C)
ε	roughness of the tube wall	(m)
ϕ	heterogeneous factor	
ϕ_{lo}^2	multiplier	
η	energy redistribution coefficient	
λ	frictional pressure drop coefficient	
μ	viscosity	(kg/s m)
ρ	density	(kg/m^3)
σ	surface tension	(N/m)
τ	time	(s)

Superscripts

- activated cluster

Subscripts

air	air
amb	ambient

b	bubble
c	capillary tube
cri	critical
e	equilibrium
exit	exit
f	friction
g	vapor
i	initial
ins	insulation
inter	interface of vapor and liquid
l	liquid
o	at the capillary tube inlet
s	saturated
t	two-phase state
v	position of the inception of vaporization
w	wall
σ	interface of activated cluster

CHAPTER 1

INTRODUCTION

1.1 Description of capillary tube and suction line

Currently, capillary tubes have been widely applied as throttling devices in refrigerators, air-conditioners and heat pumps (Sweedyk, 1981 and ASHRAE Handbook,1983). In a small refrigeration system, the capillary tube can replace the expansion valve, while at the same time reducing the starting torque of the compressor. Consequently, this would provide the opportunity for reduced motor sizes and the elimination of compressor unloaders. As a result, the refrigeration equipment with capillary tubes is a simple construction, small in size, and cheap in cost.

Figure 1.1 shows a schematic of a typical refrigeration system which consists of compressor, condenser, evaporator, capillary tube and suction line. The capillary tube is basically a long (1.5 m for this study) of small

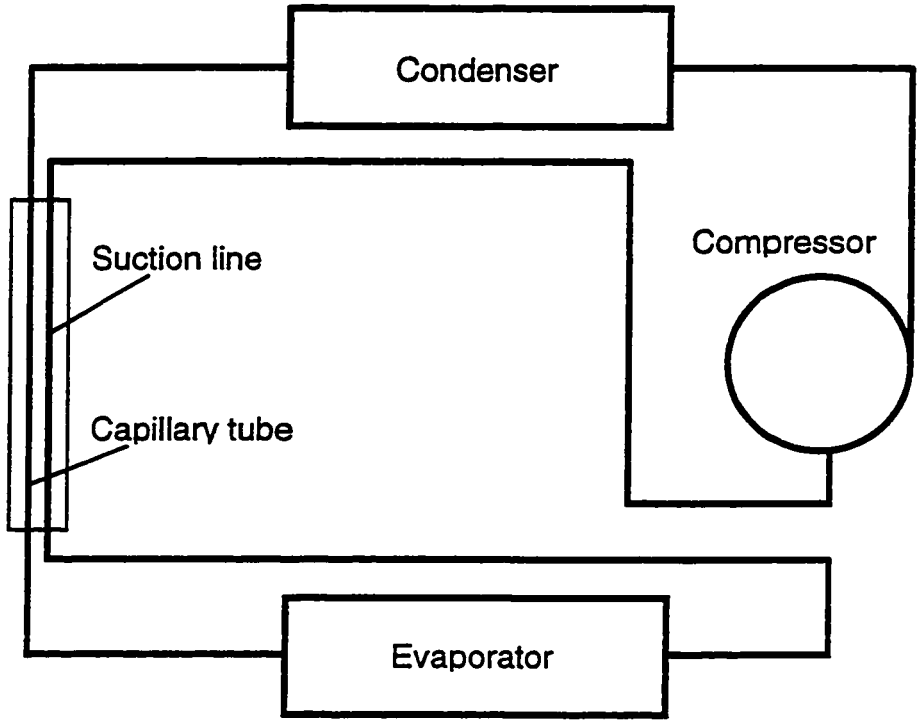

Figure 1.1 Refrigeration system schematic

diameter (0.6 mm for this study) drawn copper tubing. Refrigerant flows through a capillary tube and changes from a subcooled liquid at high pressure to a mixture of vapor and liquid at low pressure.

Besides the function of throttling, the other function of the capillary tube is to balance the flow of refrigerant in the refrigeration system by acting as a self-controlling flow restrictor. The self-controlling flow restriction is based on the principle that the refrigerant in the capillary tube reaches a point of vaporization which then divides the capillary tube flow into regions of liquid single-phase flow and vapor-liquid two-phase flow whose flow length determines the amount of flow restriction. If the mass flow rate increases above the given flow rate, then the condenser will be overloaded resulting in only a small amount of subcooled flow or possible two-phase flow entering the capillary tube. This in turn increases both the two-phase length and the restriction which then reduces the previously high flow rate. Having just the advantages mentioned above, capillary tubes began to be supported by Buchanan (1938). Almost at the same time, McCloy (1939) applied the principle of the capillary tube-suction line heat exchangers in the throttling process, and then diabatic throttling occurred. This results in a great increase in the performance of small refrigeration systems.

The suction line is essentially a drawn copper tube that transports refrigerant vapor from the evaporator to the suction side of the compressor. The capillary tube and suction line form a heat exchanger and are installed in virtually every household refrigerator and freezer. It is a combination of counter flow heat

exchanger and flow restrictor formed by soldering a small diameter capillary tube to the wall of a larger diameter suction line. Heat transfer from the capillary tube to the suction line increases the refrigerating effect because the quality x entering the evaporator is reduced. Heat transfer flow also ensures that any liquid in the suction line is vaporized and that only superheated refrigerant vapor enters the compressor.

Although the geometry of the capillary tube is very simple, the flow and heat transfer phenomena of refrigerant in it are fairly complex. The small diameter in the capillary tube results in a significant pressure drop with the pressure eventually decreasing to the inception of vaporization. From the inlet to the exit, the capillary tube experiences nonequilibrium liquid single-phase flow, nonequilibrium vapor-liquid two-phase flow and equilibrium vapor-liquid two-phase flow. Additionally, entrance conditions, metastable flow, oil in the refrigerant, and the fact that the refrigerant experiences a flashing flow which is simultaneously being cooled by heat transfer to a well, bring about more difficulties to capillary tube two-phase flow research.

1.2 Alternative refrigerant HFC-134a

In the mid 1970's, scientific investigations indicated that some refrigerants, mainly of the CFC type, when released into the atmosphere, destroyed the earth's ozone layer which was important from the viewpoint of atmospheric protection. The so-called "ozone layer" is present in the

stratosphere between 7 and 28 miles in altitude. Ozone, or O_3, is formed by the interaction of ultraviolet radiation from the sun with oxygen (O_2) (Figure 1.2). Harmful ultraviolet radiation is absorbed during this formation process. Ozone is unstable and eventually will revert back to O_2. So, there is a balance between its continuous creation and destruction. The presence of CFC in the upper atmosphere will catalyze the destruction of ozone and thus upset the balance, of course, through a complicated series of chemical reactions. The evidence from satellite measurements indicated that global levels of ozone had decreased by 4 - 5 percent during the past six to eight years. It would cause "millions" of additional skin cancer cases and deaths due to damaging ultraviolet radiation. It would also be harmful to agriculture and so on.

In 1987, the Montreal agreement was signed with the purpose of eliminating the refrigerants CFC-11, CFC-12, CFC-113, CFC-114 and CFC-115 due to their high level of Potential Ozone Depletion (POD). The POD of CFC-11 is set at one and other values of CFC are expressed as a ratio of POD to that of CFC-11 (Table 1.1).

Table 1.1 Potential Ozone Depletion of refrigerants

CFC	POD
11	1.00
12	0.86
113	0.80
114	0.60
115	0.32
502	0.19
22	0.05

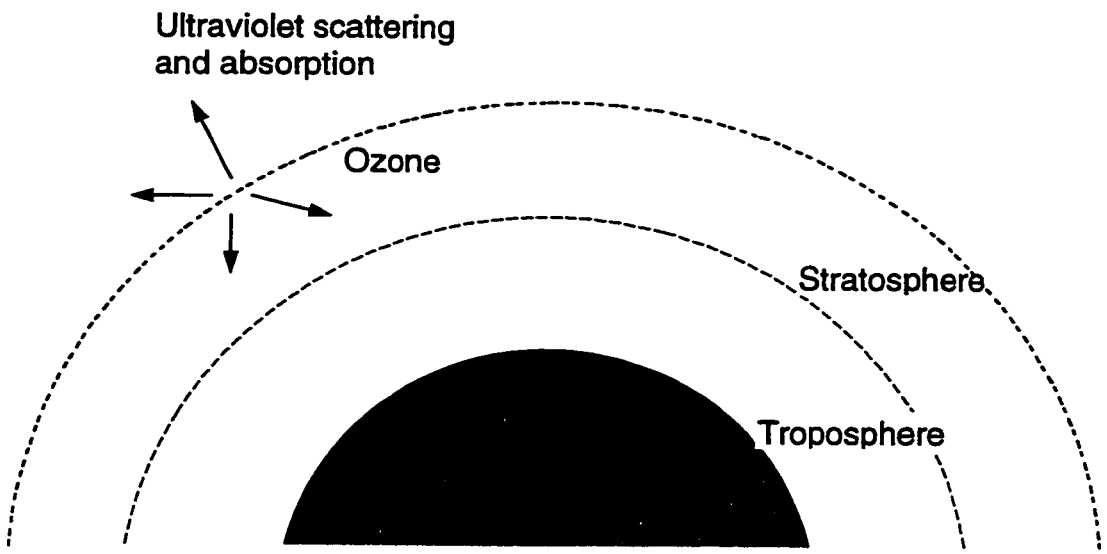

Figure 1.2 Ozone layer in the stratosphere

CFC-12 is the most widely used refrigerant in domestic appliances. Many alternative refrigerants have been investigated for replacing CFC-12. After comparing their chemical stability, safety, thermodynamic properties and so on, most researchers now concentrate on HFC-134a as an alternative refrigerant for replacing CFC-12. In this study, HFC-134a is used as the working refrigerant.

1.3 Literature review

1.3.1 Metastable flow in capillary tube

The process of refrigerant flow through a capillary tube is a flashing process, in which the state of the refrigerant changes from subcooled liquid to a vapor-liquid mixture. Metastable phenomenon in flow, i.e. a thermal nonequilibrium phenomenon, may exist within a flashing process. This means that the inception of vaporization does not take place at the location, a, of the thermodynamic saturated state with a pressure p_{sat}, but take place at a location with a pressure p_v downstream from the thermodynamic saturated point (Figure 1.3). The pressure difference, p_{sat} - p_v, is a characteristic quantity for the metastable flow or a degree of the thermal nonequilibrium of refrigerant flowing through a capillary tube, and is designated as the underpressure of vaporization. It has a significant effect on the mass flow rate, the exit pressure and the exit quality of the refrigerant.

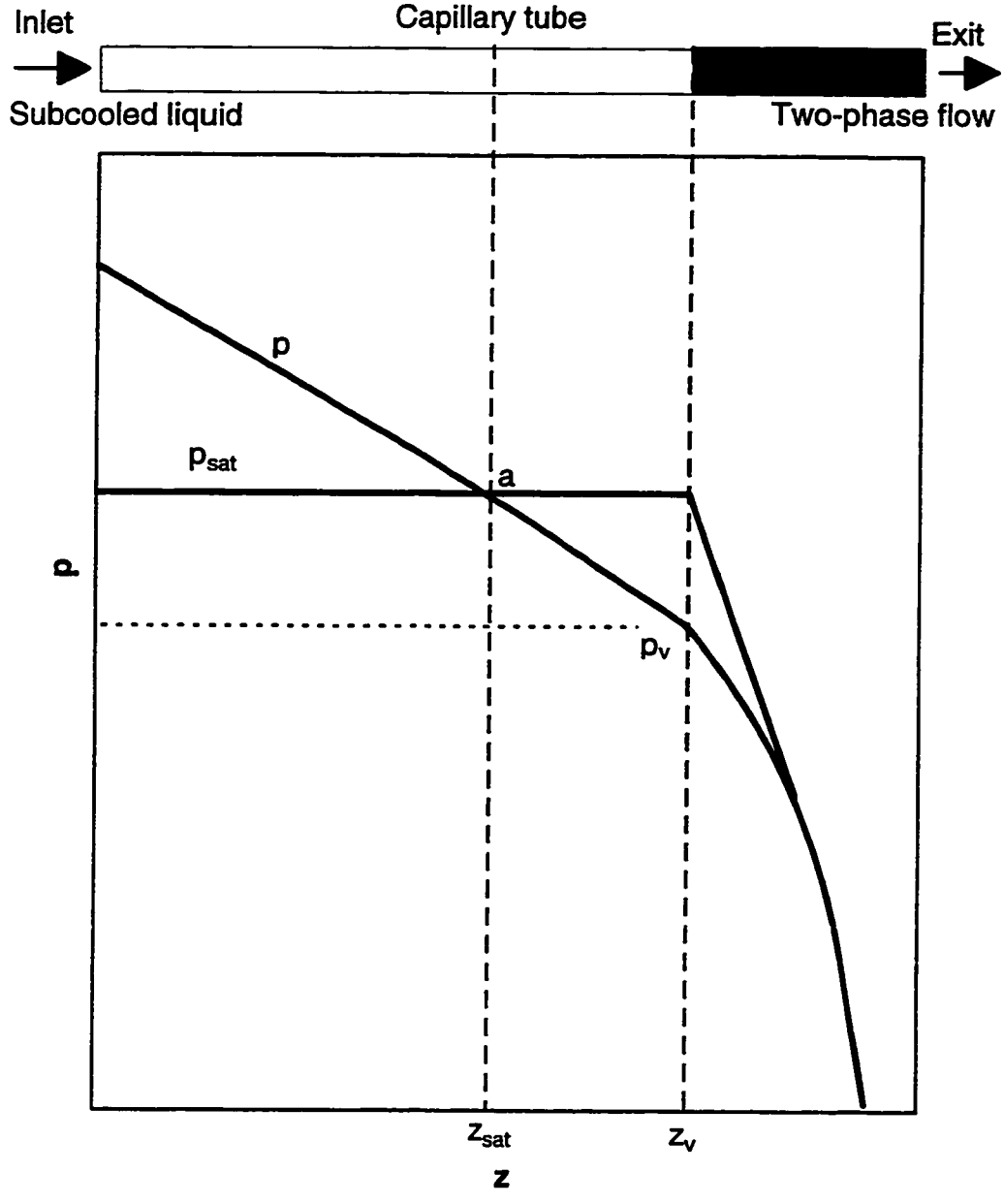

Figure 1.3 Metastable flow of refrigerant through an adiabatic capillary tube

In 1948, Bolstad and Jordan performed the first major study on capillary tube flow and tried to explain that an undetermined error of flow rate prediction of refrigerant in an adiabatic capillary tube might be due to the assumption of the thermal equilibrium in two-phase flow. However, metastable flow was not found in their research. Pasqua (1953) discovered the effect of thermal nonequilibrium in his research on the critical flow of refrigerant R-12 passing through a short tube. However, metastable flow in a capillary tube was not really discovered until the late 1950's.

Cooper et al. (1957) appeared to have been the first capillary tube researchers to witness metastable flow in a glass capillary tube and found out that regardless of inlet pressure loss of the capillary tube, the calculated length of the liquid region was less than the measured length. Their results are shown in Table 1.2.

Table 1.2 Effect of the operating parameters on the length of the metastable flow

Parameters	length of metastable flow
$D_c \downarrow$	$\uparrow$
$L_c \uparrow$	$\uparrow$
$p_0 \uparrow$	$\uparrow$

However, Cooper et al. (1957) did not obtain any correlation and curves on the length of metastable flow, and their calculation for capillary tube length was still based on thermal equilibrium. After this, the existence of metastable flow in the capillary tube was also proved by Dudley (1962).

Mikol and Dudley (1964 and 1963) reported on a detailed experimental study of adiabatic single-phase and two-phase flow in capillary tubes. Their work involved visual studies of refrigerant flow in glass capillary tubes and data collection from instrument copper capillary tubes. Mikol and Dudley (1963) first obtained typical distributions of pressure and temperature along the adiabatic capillary tube, which included the region of metastable flow (Figure 1.4). From these curves, the regions of subcooled liquid flow, metastable flow and two-phase flow could be determined for the experimental case, which made it possible to transit from qualitative analysis to quantitative research for metastable flow. Mikol and Dudley (1964) used photographic means to improve upon the observations of Cooper et al. (1957). In their experiments, the maximum length of the metastable flow was 0.7 m. Their major finding on metastable flow are summarized below:

1. Metastable flow must be considered in capillary tube design, since metastable conditions occurred in all of their visual and data runs in adiabatic capillary tubes;

2. The flow in the capillary tube could be described as a stable mode of subcooled liquid flow, metastable liquid flow, an inception of vaporization that started with vapor bubbles appearing at the tube wall and merging into a vapor core surrounded by liquid.

In their paper, the cavitation index for incipient cavitation was introduced as follows

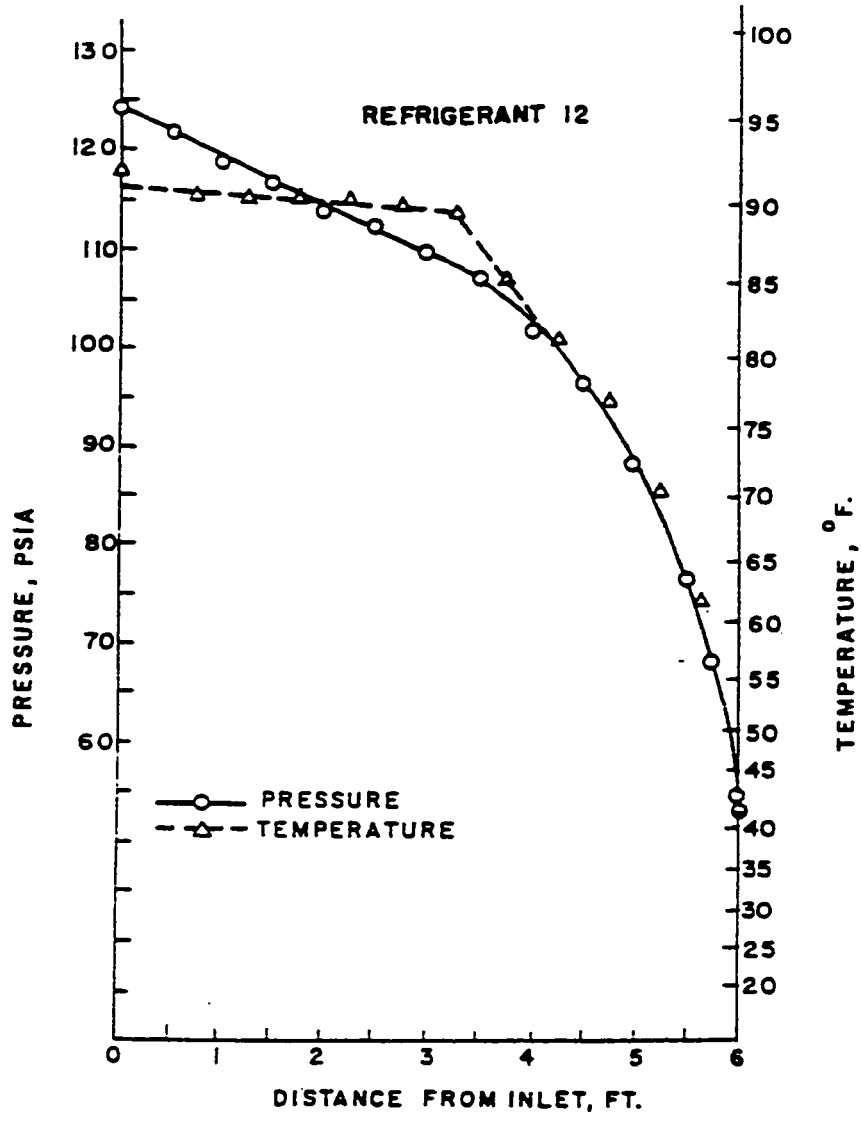

Figure 1.4 Distributions of pressure and temperature along an adiabatic capillary tube (Mikol, 1963)

$$\sigma_i = \frac{p_{sat} - p_v}{\frac{\rho_l V_l^2}{2}} \tag{1.1}$$

The relative curves of the cavitation index σ_i against velocity V_l, Reynolds number Re and Weber number, We ($=\rho_l V_l^2 D_c / \sigma$), were plotted. However, wide scatter of experimental data was observed, and was attributed to experimental instability and discontinuous function of inception of vaporization against macroscopic variables.

Mikol and Dudley's work (1964) was reinforced by Niaz and Davis (1969). Again the metastable region was shown to exist experimentally. Erth (1969) claimed that the metastable flow region "was an anomaly" produced by laboratory conditions despite the findings of Cooper et al. (1957) and Mikol and Dudley (1964).

From the end of the 1970's, research on metastable flow in capillary tubes had attracted more people. Rezk and Awn (1979) also obtained the distribution curves of pressure and temperature along an adiabatic capillary tube by means of experiment, which was similar to Mikol's (1963) work (Figure 1.4). Although the length of metastable flow and the superheated degree (or underpressure of vaporization) for the experimental case could be determined, correlation for the metastable flow was not provided. The distribution curves were only used for qualitative analyses. Their paper did not illustrate the curves for the selection of capillary tube length nor did it mention whether or not they had taken the effect of the metastable flow into account.

The visual flow of Cooper et al. (1957), and Mikol and Dudley (1964) was again observed by Koizumi and Yokoyama (1980). They performed visual and experimental studies using a glass capillary tube and instrumented copper and stainless steel capillary tubes without heat exchange. Some results from their experiment are listed as follows:

1. The superheated degree of vaporization at inception was from 2 to 4 °C; the average length of the metastable flow was 0.39 m; the maximum length was 0.6 m; the measured flow rate in the capillary tube was higher by about 14% than the calculated flow rate for which the metastable flow was not considered.

2. Length of metastable flow decreased with increase of velocity, while, superheated degree of vaporization (or underpressure of vaporization) increased with increase of velocity;

3. Under the given velocity, the length of metastable flow increased with decrease of tube diameter.

Koizumi and Yokoyama (1980) did not provide a correlation of metastable flow length (or underpressure of vaporization). In their formula on pressure and capillary tube length, the metastable flow was not considered.

The effects of the non-equilibrium metastable flow on capillary tube flow were studied by Kuipjers and Janssen (1983). They found out that the maximum increase in mass flow rate in the adiabatic capillary tube was about 10% due to the metastable flow. To correlate underpressure of vaporization, they suggested that the decompression rate and turbulence played important roles in the

magnitude of the underpressure of vaporization, and assumed that the underpressure of vaporization, Δp_{sv}, consisted of two parts: static underpressure $\Delta p_{sv,static}$ and turbulence item, i.e.

$$\Delta p_{sv} = \Delta p_{sv,static} - \psi_{turb} \frac{G_c^2}{2\rho_l} \tag{1.2}$$

where ψ_{turb} was the turbulence factor and G_c was mass flux in the capillary tube. In their paper

$$\psi_{turb} = 9.60$$

From Equation (1.2), it could be seen that the underpressure of vaporization decreased with increase of mass flow rate, which was different from the results obtained by Koizumi and Yokoyama (1980).

Maczek et al. (1983) developed a mathematical model for both single-phase and two-phase flow regions of an adiabatic capillary tube, which was based on a thermal nonequilibrium theory of creation and expansion of a nucleation bubble inside the superheated fluid. However, they only reported a comparison of computational and experimental results of capillary tube length, and did not present the calculated distributions of pressure and temperature along the capillary tube. Maczek et al. (1983) thought that the results of the calculation were not satisfactory, and needed further work.

In the research of critical two-phase flow in an adiabatic capillary tube, Shultz (1987) analyzed the effect of metastable flow on back pressure, and concluded that the effect was weak.

Li et al. (1989 and 1990) and Chen et al. (1990) published the most complete work on metastable flow of refrigerant in adiabatic capillary tubes. From their experiments of the refrigerant CFC-12 through capillary tubes with an inside diameter of 0.66 and 1.17 mm, the relationship of metastable flow with the inlet temperature, inlet pressure, mass flow rate and back pressure, were analyzed, and it was concluded that:

1. The larger the diameter of the capillary tube, the lower the underpressure of vaporization, and the shorter the length of the metastable flow;

2. The underpressure of vaporization increases with an increase in the refrigerant mass flow rate;

3. An increase of the inlet subcooling decreased the underpressure of vaporization;

4. The effect of the change of back pressure on the underpressure of vaporization was small.

Utilizing the classic nucleation theory for the heterogeneous nucleation of refrigerant flowing through capillary tubes and experimental data, a correlation for the determination of the underpressure of vaporization was established (Li, 1989 and Chen et al., 1990).

Although the adiabatic capillary tube tests showed strong evidence of metastable flow, it was not observed in the diabatic capillary tube flow (Pate, 1982 and Pate and Tree, 1984). Pate and Tree (1984) instrumented a capillary tube-suction line heat exchanger for temperature and pressure measurements along the assembly length, and reported that the test did not show any evidence

of metastable flow. Since then, no published literature has addressed the problem.

1.3.2 Theoretical research

Theoretical studies on adiabatic two-phase flows in capillary tubes have been conducted actively along with experimental studies. Some models had been proposed in the past for modeling the flow process inside a capillary tube which had measured boundary conditions (mass flow rate, inlet and outlet parameters etc.) and pressure distribution along the tube. These models predicted the flow rate change under the various parameters, which was described in Chen et al.'s (1988) review article.

Before the 1980s, the models pertained only to describing adiabatic two-phase flows in horizontal capillary tubes with different momentum equations, for instance, Cooper et al. (1957), Erth (1969), Hopkins (1950), Mikol and Dudley (1963) and Whitesel (1957). They differed from each other basically in simplifying assumptions and in the methods used to obtain the numerical solutions. Also they did not take into account the nonequilibrium metastable flow, which affected the accuracy of the calculation to determine the location of the inception of vaporization. After that, the metastable flow was considered in the models, such as those of Koizum and Yokoyama's (1980), Kuijpers and Janssen's (1983), Li et al.'s (1990) and Melo et al.'s (1992). Inception of

vaporization was calculated utilizing the theory of nucleation inside the superheated fluid. As a result, the calculation accuracy increased.

Numerical simulation of two-phase flow in capillary tubes can be carried out by a homogeneous model which assumes a thermodynamic equilibrium between the vapor and liquid phases, or by a non-homogeneous model with a variety of nonequilibrium conditions. The nonequilibrium effects are associated with the relative velocity and temperature difference between the phases. Most of the models of the two-phase flow in capillary tubes were homogeneous models, such as those of Maczek and Krolicki's (1981), Kuehl and Goldschmidt's (1991), and Escanes et al.'s (1995).

Maczek and Krolicki (1981) established a homogeneous model for a diabatic throttling process of CFC-12 in a refrigeration system, and calculated the capillary tube length and the total pressure drop for the given inlet and outlet parameters. They used the Clausius-Clapeyron equation as the evaporating equation. The Runge-Kutta method was used to solve the equations. The deviation of their calculations compared with their experiments was within 8%. In 1983, Maczek et al. developed a new model in which only the bubble flow was considered as the flow regime along a capillary tube, and its computational results deviated less from the experimental data than the homogeneous model results did. However for actual two-phase flow in a capillary tube, the refrigerant will experience a series of changes from a non-homogeneous bubble flow to a mist annular flow at the exit (Li, 1989).

Pate (1982) analyzed his experimental results of a diabatic capillary tube from many aspects of two-phase flow phenomena, such as energy distributions, momentum force distributions, quality, and friction coefficient. Based on these, he established the model to calculate the distributions of pressure and temperature of refrigerant along the capillary tube and suction line. An implicit finite difference method was used to solve the equations. Inception of vaporization was estimated by trial and error. The assumption of linear quality distribution was made, which was based on the fact that the increase of quality in the two-phase region was approximately linear. A correlation of quality replaced the unknown quality variable in the governing differential equations, which was a linear function of the distance in the two-phase flow region. In 1983, Pate utilized a correlation of the non-linear quality instead of that of linear quality. However, in the numerical calculation the correlation of linear quality was used for the first marching steps.

Yan and Wang (1991) established a non-linear quality, homogeneous flow model to simulate real operating conditions of a diabatic capillary tube. However, their results did not compare with any experimental data.

In 1995, Escanes et al. developed a transient homogeneous two-phase flow model for a diabatic capillary tube. The solution had been carried out using an implicit step-by-step numerical scheme. Empirical relations were introduced into the model to match the calculation results with the experimental data of Bolstad and Jordon (1948), and Mikol (1963).

1.3.3 Effect of oil in refrigerant on performance of capillary tube

Bolstad and Jordan (1948) compared the flow rate of refrigerant CFC-12 through a capillary tube of 1.07 mm I. D. and 4.88 m length with and without an oil separator. They found that oil in the refrigerant increased the flow rate by approximately 8%. They also reported that the evaporator pressure in the usual operating range had only a very minor effect on the flow rate. In 1992, Wijaya published his experimental results for capillary tubes of 0.66 mm I.D. and 0.84 mm I.D., and their length ranging between 1.52 m and 3.05 m, which showed that the effect of oil content in refrigerant HFC-134a on flow rate was marginal. The mass flow rate without oil was marginally higher than that with oil. His conclusion was different from that of Bolstad and Jordan (1948). Kuehl and Goldschmidt (1990) did their experiment utilizing 23 combinations of 5 diameters: 1.07 mm, 1.24 mm, 1.37 mm, 1.50 mm, 1.63 mm, and 5 lengths: 0.546 m, 0.80 m, 1.05 m, 1.31 m, 1.56 m. Experimental data were obtained in a closed-loop system (with oil) and showed that the oil content did not appear to have a significant effect on capillary tube flow.

In summary, there are no reports in the experimental evidence of the metastable flow of refrigerant through a diabatic capillary tube. In addition, there are no reports in the literature of any attempts to provide a non-homogeneous two-phase flow model for a diabatic capillary tube.

1.4 Objectives and scope of study

The objectives of this study have been to improve upon the knowledge of the performance of a diabatic capillary tube in the steady state condition through experiments and theoretical modeling.

These objectives were:

1. Analyzing the experimental data to provide conditions for metastable flow in a diabatic capillary tube.
2. Building an experimental facility capable of measuring boundary conditions and the distributions of pressure and temperature along the capillary tube and suction line.
3. Collecting experimental data for a range of operating conditions including adiabatic and diabatic capillary tube conditions, and refrigerant with and without oil.
4. Using nucleation theory and experimental data to derive a correlation of underpressure of vaporization for a diabatic capillary tube.
5. Developing a non-homogeneous two-phase flow model to simulate the performance of refrigerant flowing through a diabatic capillary tube.
6. Analyzing and comparing the calculation results with experimental data.

CHAPTER 2

EXPERIMENT

The purposes of the experiment are to search for evidence of metastable flow in a diabatic capillary tube, and to provide data on capillary tube performance under conditions of adiabatic flow and diabatic flow, as well as with and without oil. The major parameters measured are inlet and outlet conditions and mass flow rate, as well as distributions of temperature and pressure along the capillary tube and suction line.

This Chapter is divided into three parts as follows:

1. experimental setup
2. experimental range of the parameters
3. pressure profiles and metastable flow

2.1 Experimental setup

The experimental setup consists of three parts: the test loop, the insulation and the instrumented capillary tube-suction line.

2.1.1 Test loop

The test loop simulates the actual refrigeration system that normally supplies refrigerant to the capillary tube. The test loop allows the boundary conditions to be easily controlled, allows the mass flow rate in the capillary tube and in the suction line to be regulated. It also allows the refrigerant HFC-134a flow with or without oil in the capillary tube.

Figure 2.1 shows a schematic diagram of the overall test loop. The test loop essentially is divided into a refrigerant flow system and a capillary tube support structure that also insulates the capillary tube from ambient heat losses or gains. The Figures 2.2 and 2.3 are photographs of the overall view of the experimental test loop, and discharge end of the capillary tube, respectively.

The basic system of refrigerant flow consists of a rotary compressor (2), a condenser (4), an evaporator (14) and a test section (11) in which one capillary tube and a suction line are employed as a heat exchanger (Figure 2.1). The capillary tube is connected to the inlet and outlet couplers installed at each end of the tube (Figure 2.4). Two oil separators (3) (Figure 2.5) are installed in the compressor discharge line and can be bypassed when oil performance in the

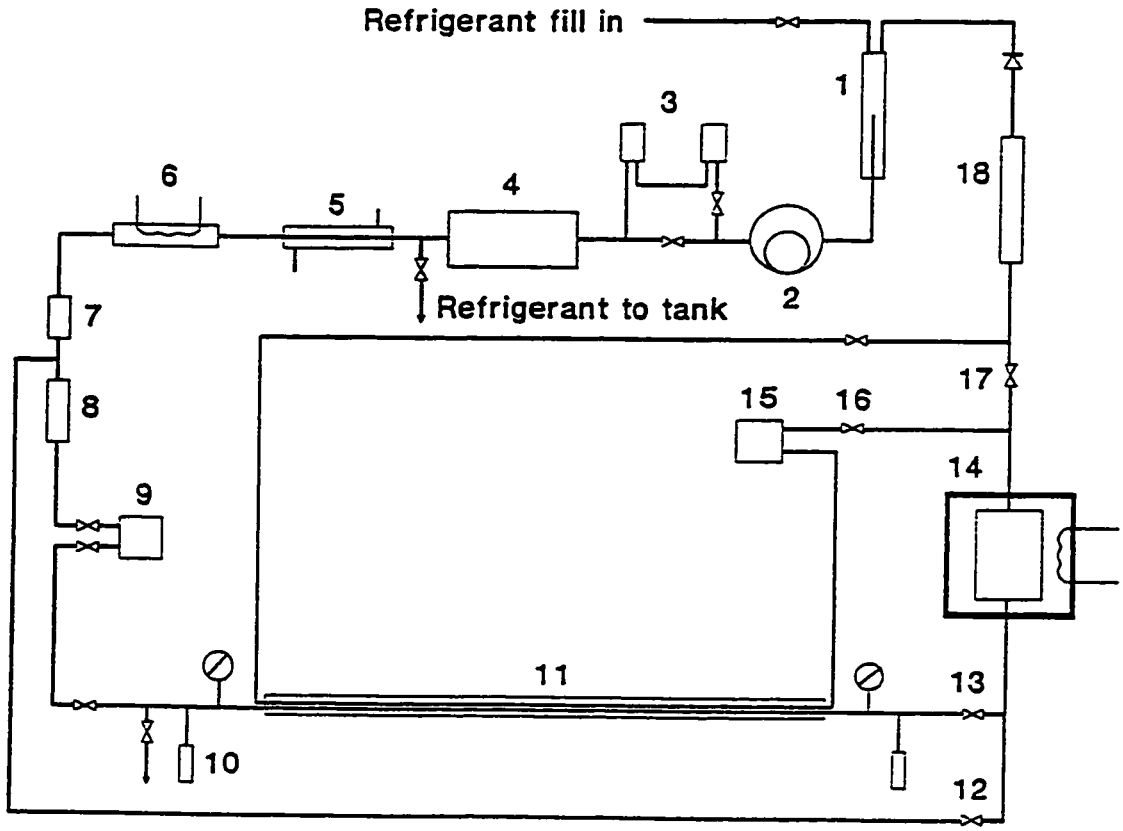

1. Receiver; 2. Rotary compressor; 3. Oil separators; 4. Condenser; 5. Subcooler; 6. Electrical heater; 7. Filter; 8. Vapor-liquid separator; 9. Flow rate meter; 10. Thermocouple; 11. Test section; 12. Hand expansion valve; 13. Hand valve; 14. Evaporator; 15. Flow rate meter; 16, 17. Hand valve; 18. Connector.

Figure 2.1 Schematic diagram of the test loop

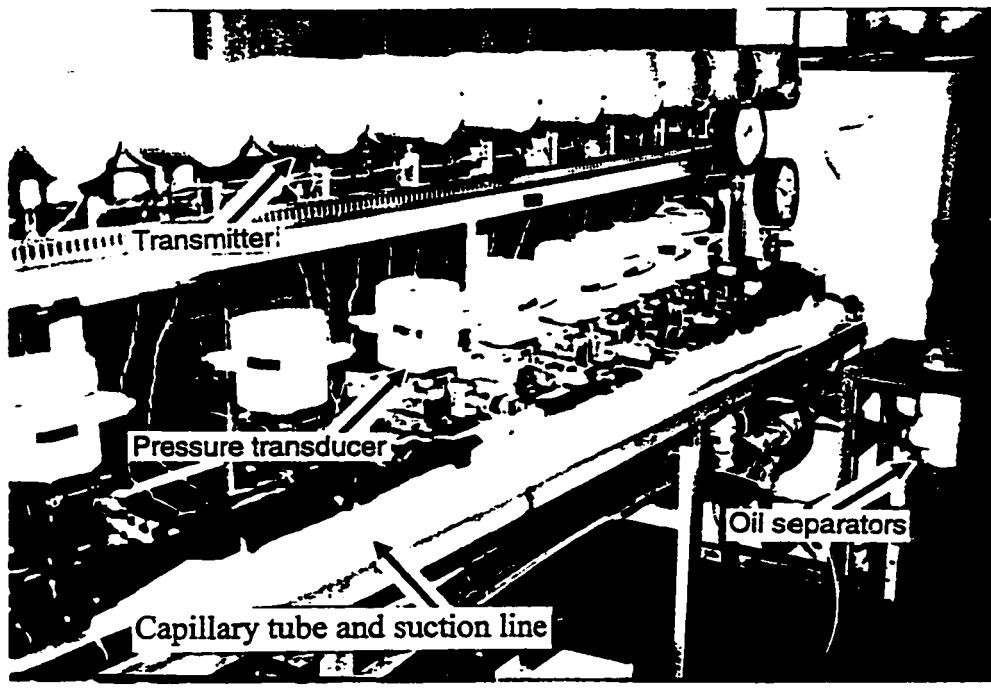

Figure 2.2 Photograph of the test loop

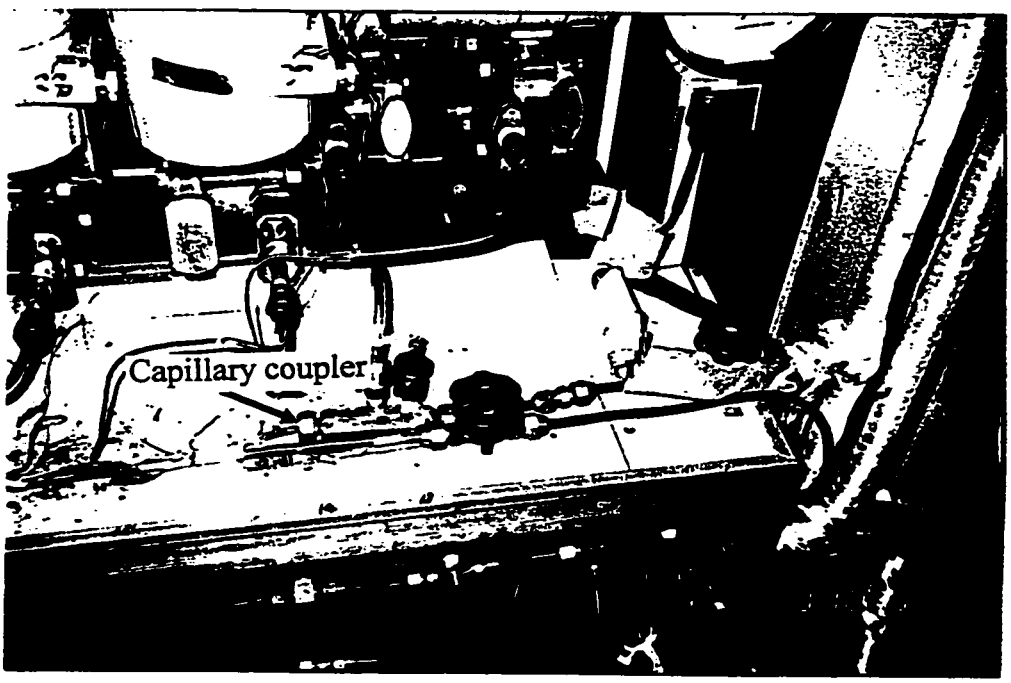

Figure 2.3 Discharge end of the capillary tube

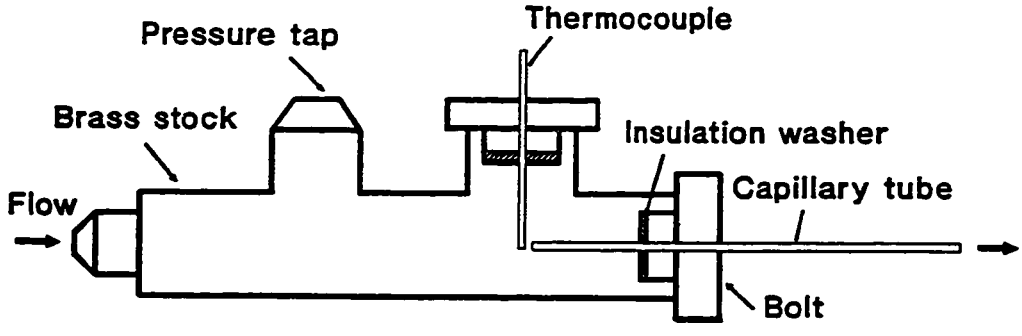

Figure 2.4 Schematic diagram of capillary coupler

Figure 2.5 Oil separators

compressor discharge line and can be bypassed when oil performance in the capillary tube is simulated. Impurities in the refrigerant are removed by a filter (7). In order to control the refrigerant subcooling at the inlet of the capillary tube, a subcooler (5) and an electrical heater (6) are arranged following the condenser (4). The subcooler is cooled by water and the electrical heater is controlled by a rheostat. Once the desired subcooling temperature is set, the refrigerant flow in the test section is adjusted by diverting the excess fluid through a bypass, using a hand expansion valve (12), into the evaporator (14). The discharge pressure is controlled by a hand valve (13). The mass flow rate of the refrigerant is measured by a flow rate meter (9). To reduce fluctuation in measurement of mass flow rate a vapor-liquid separator (8) (Figure 2.6) is connected before flow rate meter (9).

A suction line is soldered to the capillary tube, which forms the heat exchanger. To improve heat transfer, the capillary tube-suction line is wrapped with aluminum foil (Figure 2.7). To simulate the conditions of different heat transfer between the capillary tube and the suction line the mass flow rate of the refrigerant vapor supplied to the suction line from the evaporator (14) is adjusted by the two hand valves (16) and (17), and is measured by the flow rate meter (15). The excess vapor flows through a bypass into the rotary compressor (2). Thermocouples are mounted directly into the suction line flow stream through the tube wall.

The two mass flow meters have an uncertainty of $\pm 2 \times 10^{-5}$ kg/s. All valves are refrigeration valves.

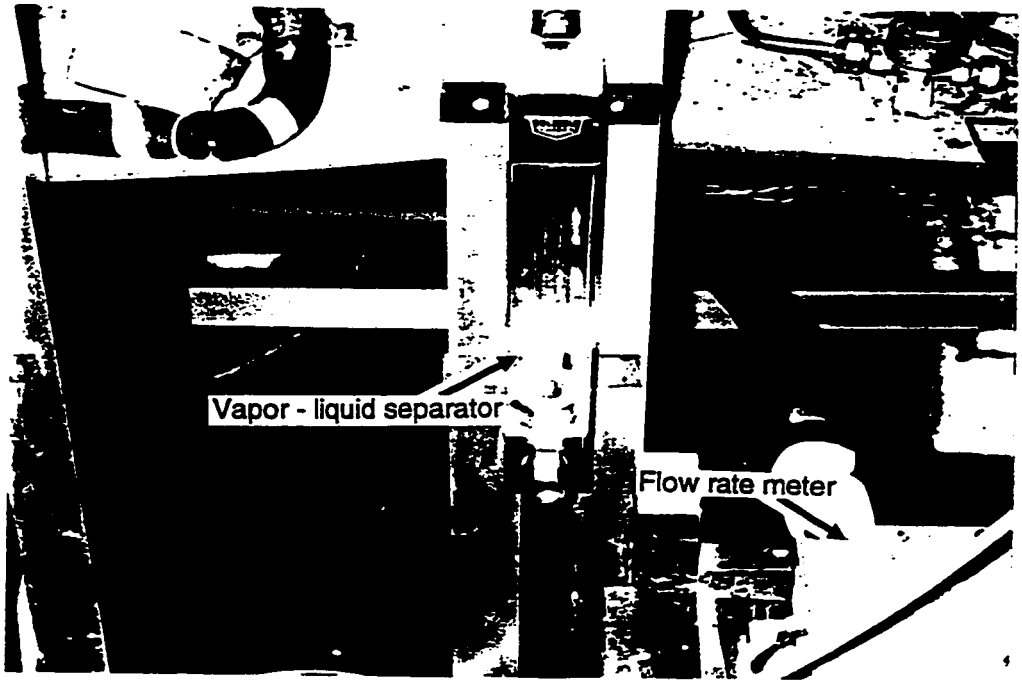

Figure 2.6 Vapor-liquid separator

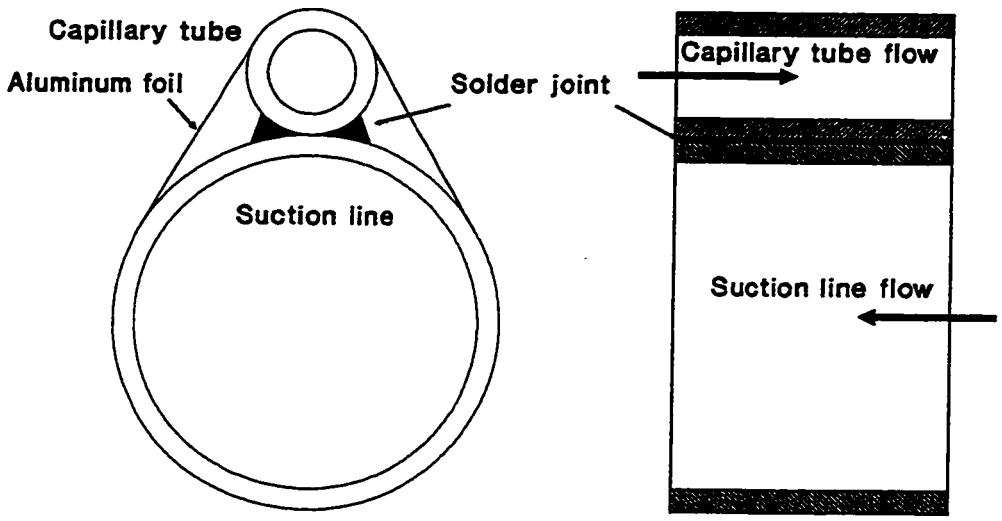

Figure 2.7 Capillary tube and suction line

In preparing the unit, all component parts were disassembled, cleaned, and connected with copper tubing. The system was then evacuated and charged with dry nitrogen several times. It was then charged with refrigerant HFC-134a.

2.1.2 Insulation

Heat losses to ambient are minimized by insulating the capillary tube and suction line with at least 30 mm of styrofoam type insulation. In addition, the insulation acted as a support bed for the capillary tube and suction line. The outside of the insulation assembly is previously shown in the Figure 2.2 photograph.

The temperature of the outside surface of the insulation along the capillary tube and suction line is measured for each experimental case. Figures 2.8 and 2.9 show two of them. It can be seen from the Figures that the temperature distributions of the outside surface of the insulation can be considered as uniform. Heat loss for the insulation can be calculated according to the formula for heat transfer of natural convection because the experiment is carried out in a separated chamber.

The heat loss q_{amb} per unit area of capillary tube and suction line is calculated as follows:

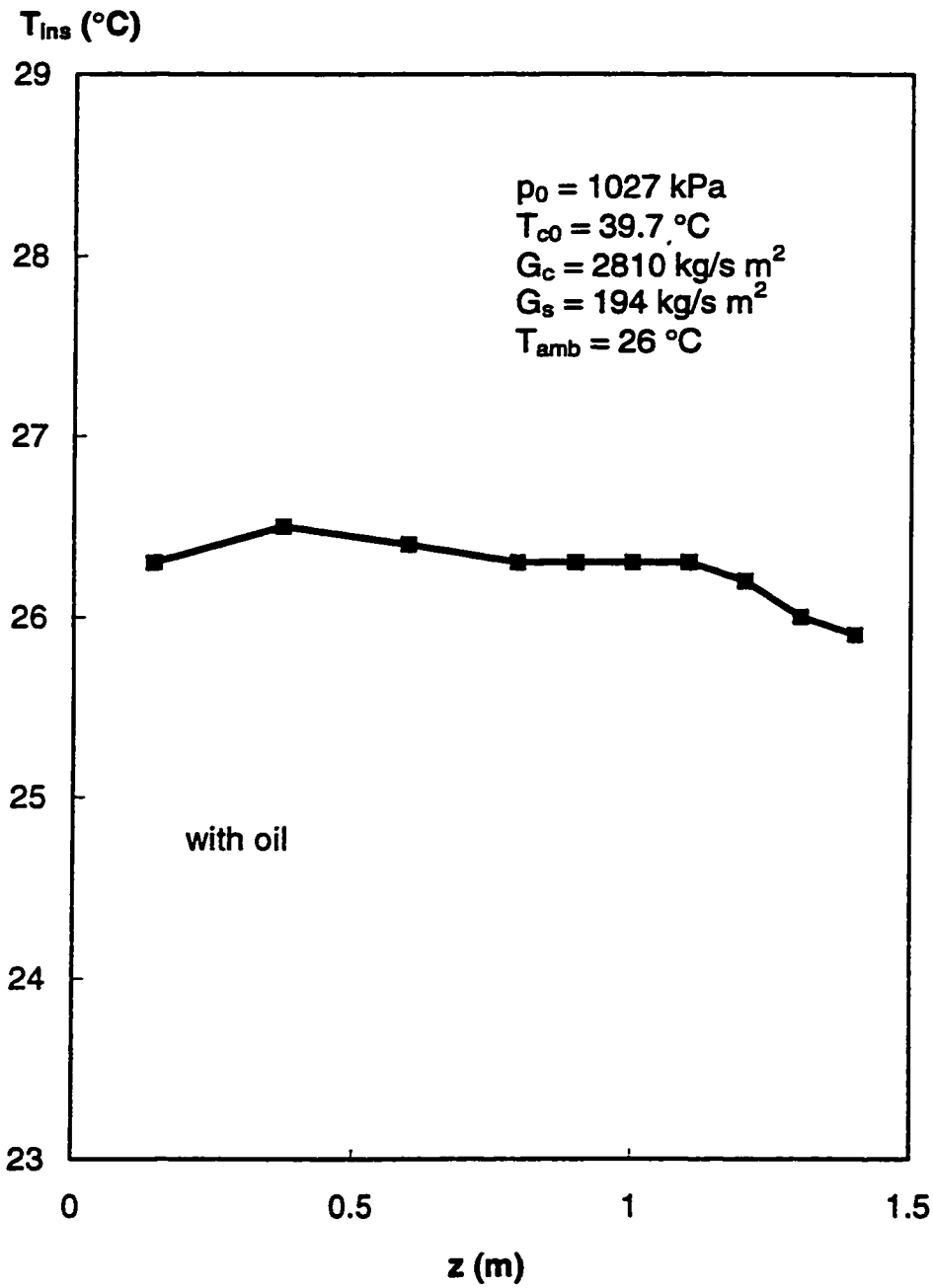

Figure 2.8 Temperature distribution of the outside surface of the insulation at the ambient temperature T_{amb} = 26 °C

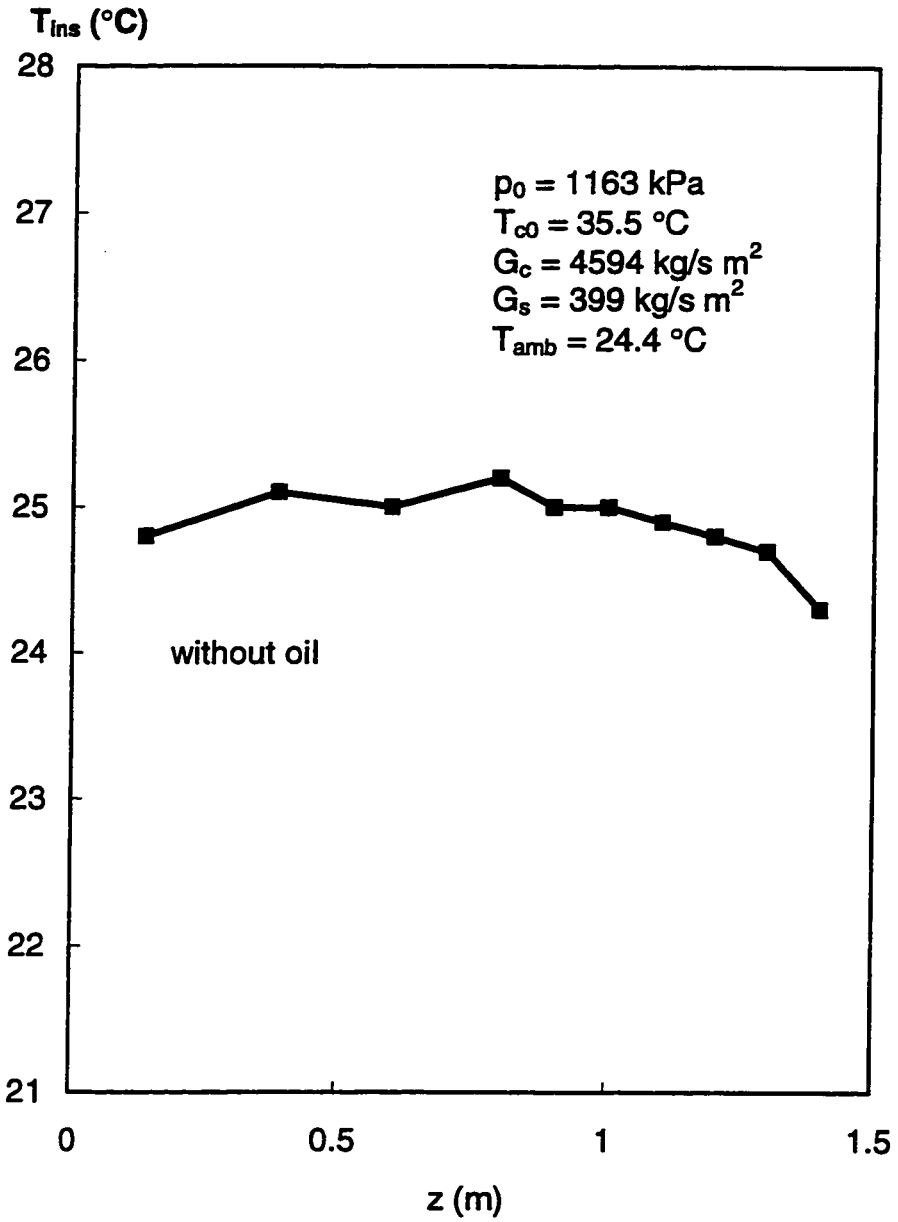

Figure 2.9 Temperature distribution of outside surface of the insulation at the ambient temperature T_{amb} = 24.4 °C

$$q_{amb} = \bar{h}_{amb}(T_{ins} - T_{amb}) \tag{2.1}$$

where T_{ins} and T_{amb} are average temperature of the outside surface of the insulation and ambient temperature, respectively. $\bar{h}_{amb}$ is the heat transfer coefficient and can be determined by (ASHRAE Handbook -- Fundamentals, 1993)

$$Nu_{amb} = 0.56(Gr\ Pr)^{0.25} \qquad 10^4 < Gr\ Pr \le 10^8 \tag{2.2}$$

$$Nu_{amb} = 0.13(Gr\ Pr)^{0.33} \qquad 10^8 < Gr\ Pr < 10^{12} \tag{2.3}$$

where Gr and Pr are Grashof number and Prandtl number, respectively, which are defined as follows

$$Gr = \frac{D_{ins}^3 \rho_{air}^2 \beta g (T_{ins} - T_{amb})}{\mu_{air}^2} \tag{2.4}$$

$$Pr = \frac{\mu_{air} c_{p,air}}{k_{air}} \tag{2.5}$$

where D_{ins} is the outside diameter of insulation, $D_{ins} \approx 70$ mm. β in Equation (2.4) is the coefficient of thermal expansion and can be approximately calculated by (Qian et al., 1984)

$$\beta \approx \frac{1}{273.15 + T} \tag{2.6}$$

where T is the film temperature and is defined as follows

$$T = \frac{T_{ins} + T_{amb}}{2} \tag{2.7}$$

2.1.3 Capillary tube and suction line

The capillary tube and suction line made of copper are used for study. The capillary tube of 0.6 mm I. D. is soldered to a 1.36 m length of 4 m m I. D. suction line (Figure 2.7). The first 0.14 m and the last 0.1 m of the capillary tube are unattached resulting in an overall capillary tube length of 1.5 m. Figure 2.10 illustrates the above dimensions.

The capillary tube and suction line were instrumented for the following:

1. pressure in the capillary tube;
2. temperature of the wall surface of the capillary tube;
3. temperature inside the suction line.

Pressure taps were made in the wall of the capillary tube using a laser beam drilling process. The process produced burr-free holes of diameter of 0.15 mm that did not distort the flow field in the small diameter capillary tube. The pressures along the capillary tube were obtained by 10 pressure transducers, which have a precision of 0.4% of the maximum scale, connected to a computer data acquisition system. The pressure transducers were powered from a constant voltage power supply via a 6 volt AC/DC converter. Figure 2.11 is a photograph of the pressure transducer and its connecting assembly.

Temperatures along the wall of the capillary tube were measured by 10 thermocouples. Suction line vapor temperatures were measured by mounting thermocouples directly into the vapor stream through the tube wall and 30° angle

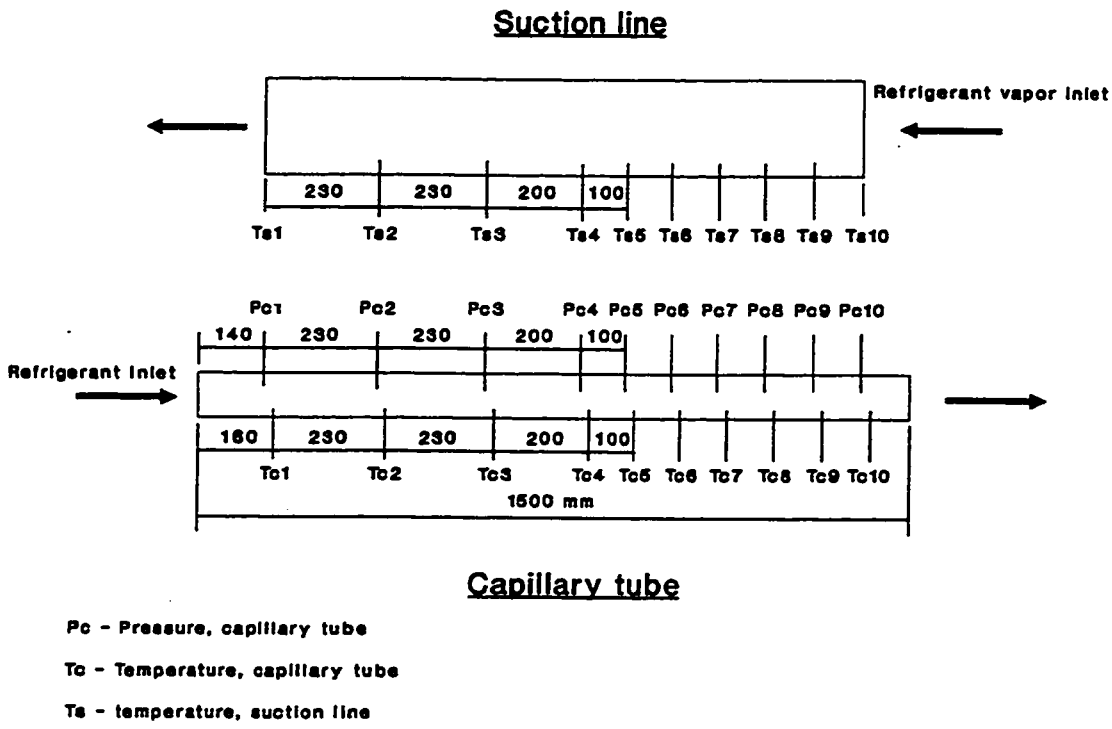

Figure 2.10 Capillary tube - suction line schematic diagram

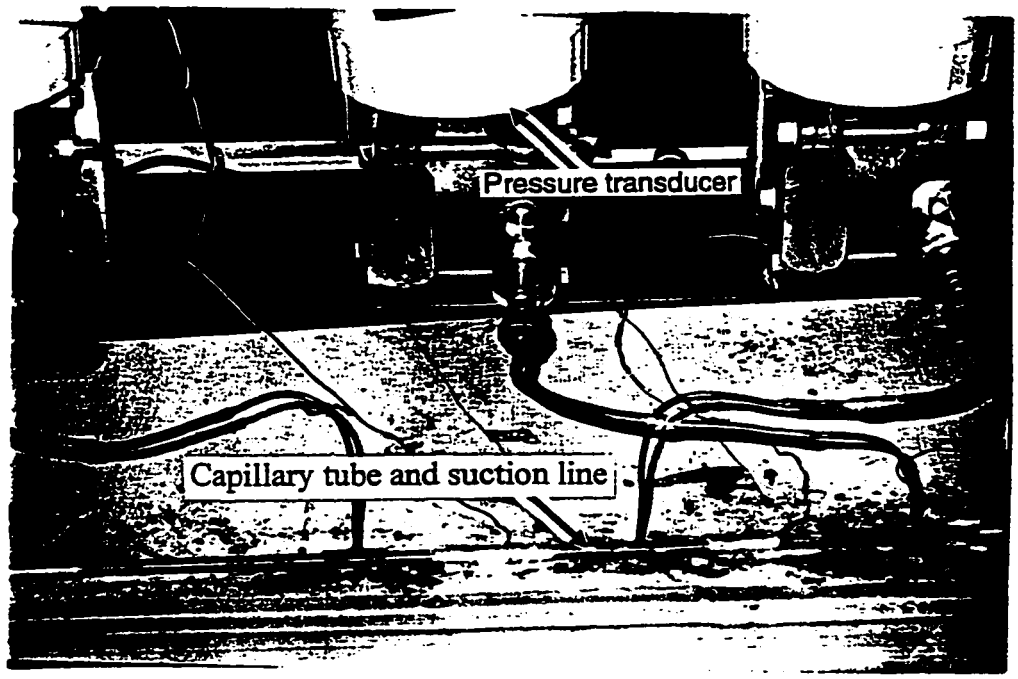

Figure 2.11 Photograph of the instrumentation

of inclination to the center of the flow stream. All thermocouples were copper-constantan with diameter of 0.15 mm with individual ice reference baths and with a maximum uncertainty of ± 0.3 °C. The signal from these thermocouples was connected to the same computer data acquisition system.

The capillary tube and suction line simulated an adiabatic capillary tube when the vapor flow to the suction side was shut off.

The oil effect on the flow performance in the capillary tube was carried out when the oil separators were bypassed. The oil contents in the refrigerant with and without the oil separators were 1.2% and 24.1%, respectively. They were determined by measurements as follows: Samples were taken from the inlet of the capillary tube and put into a sealed bottle and weighed (W_1). Then, the bottle was opened to release the refrigerant for 24 hours and weighed (W_2) again. The ratio of the difference between the two weights to the total weight, $(W_1 - W_2)/ W_1$, was the oil content. For simplicity the item "**with oil**" represents the case without separators, and the item "**without oil**" represents the case with separators.

2.2 Experimental range of the parameters

All experimental tests were conducted by setting the desired capillary tube inlet pressure and temperature. The discharge pressure of the capillary tube was adjusted by a hand-valve. Refrigerant vapor temperature at the inlet of the

suction line was the same as the discharge temperature of the evaporator. The refrigerant vapor flow rates in the suction line were adjusted from zero to full flow rate. Usually, 30 minutes were needed for the system to reach steady state operation.

The ranges of the parameters used in the present investigation are as follows:

inlet temperature	28.2 - 41.1 °C
inlet pressure	9.13 -13.4 bar
inlet subcooling	1.83 -16.8 °C
mass flux in the capillary tube	2550 - 5800 kg/s m^2
mass flux in the suction line	0 - 1200 kg/s m^2

2.3 Pressure profiles and metastable flow

Figure 2.12 shows the typical distributions of the measured pressure p and the saturated pressure p_{sat} corresponding to the measured temperature along the adiabatic capillary tube. From Figure 2.12 it is seen that the flow of the refrigerant in the capillary tube can be divided into four regions:

Region 1: Subcooled, single liquid phase

Region 2: Thermal nonequilibrium, single liquid phase

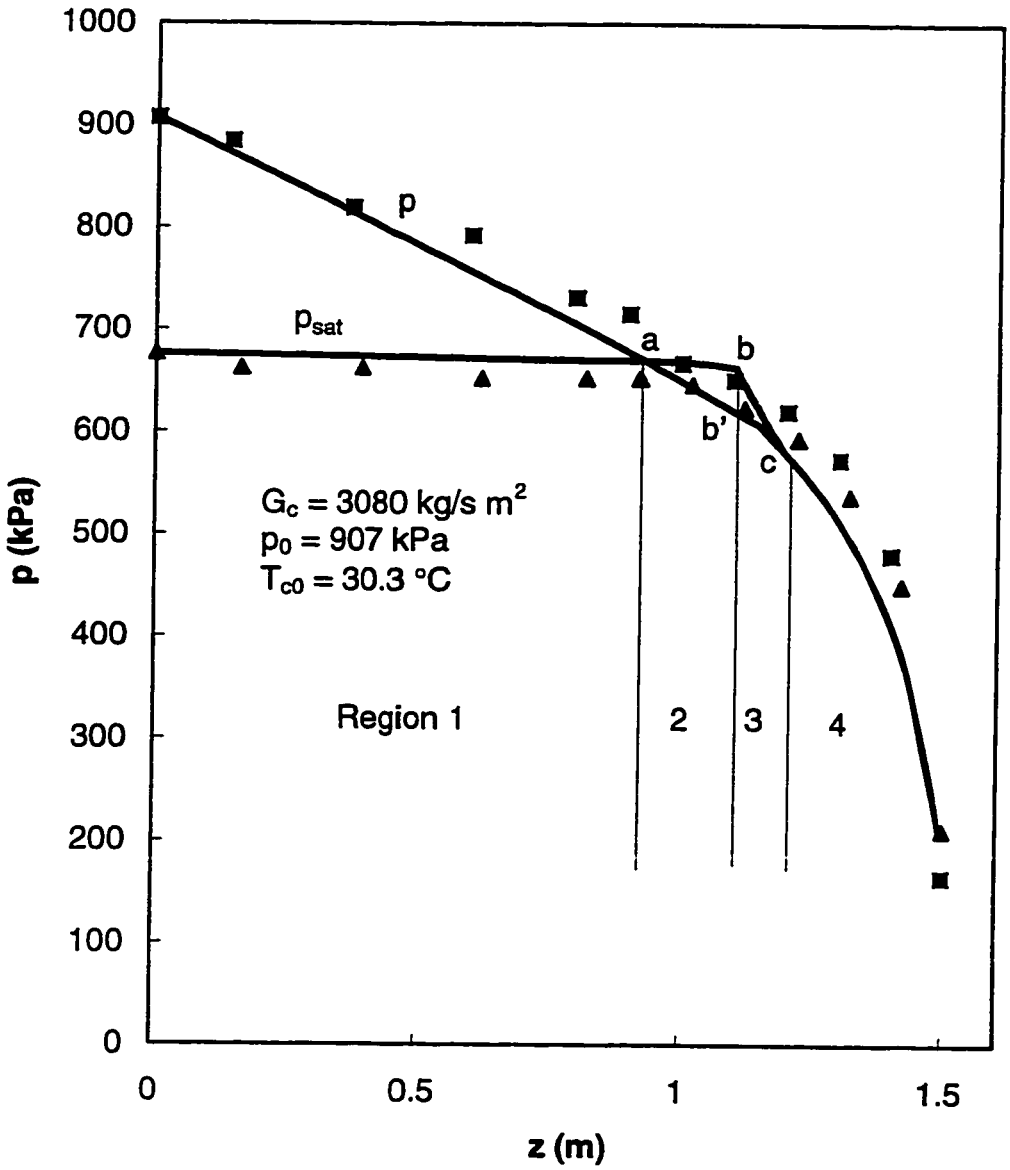

Figure 2.12 Distributions of the pressure, p, and the saturated pressure, p_{sat}, corresponding to the temperature along the adiabatic capillary tube

Region 3: Thermal nonequilibrium, vapor-liquid two phases

Region 4: Thermal equilibrium, vapor-liquid two phases

In Region 1, the measured temperature of the refrigerant is nearly constant, and its corresponding calculated saturated pressure is also constant. However, the measured pressure decreases linearly due to the friction losses. At the intersection point, a, of the two pressure curves, the measured pressure is equal to the saturated pressure; therefore, the refrigerant is at the saturated state at the intersection point. It can be seen that vaporization does not take place at the intersection. After point a in Region 2, both the calculated saturated pressure, p_{sat}, and the measured pressure, p, follow their original respective directions until they reach section b-b' (Figure 2.12). At point b, p_{sat} suddenly drops, which marks the p_{sat} curve an inflexion at this point. The sudden drop in pressure, p_{sat}, is due to the sudden drop in its corresponding temperature, which is caused by vaporization of the refrigerant with absorption of the latent heat of vaporization at this point. After point c in Region 4, the two pressure curves again join together. It indicates that after point c, the measured pressure, p, is equal to the saturated pressure. This means that the thermal equilibrium state is reached after point c. The underpressure of vaporization, which is defined as the difference of the pressures measured at points a and b', is used as the characteristic quantity for the thermal nonequilibrium of the refrigerant flowing through the capillary tube.

Figures 2.13 - 2.15 show the distributions of the measured pressure and the saturated pressure corresponding to the measured temperature along the

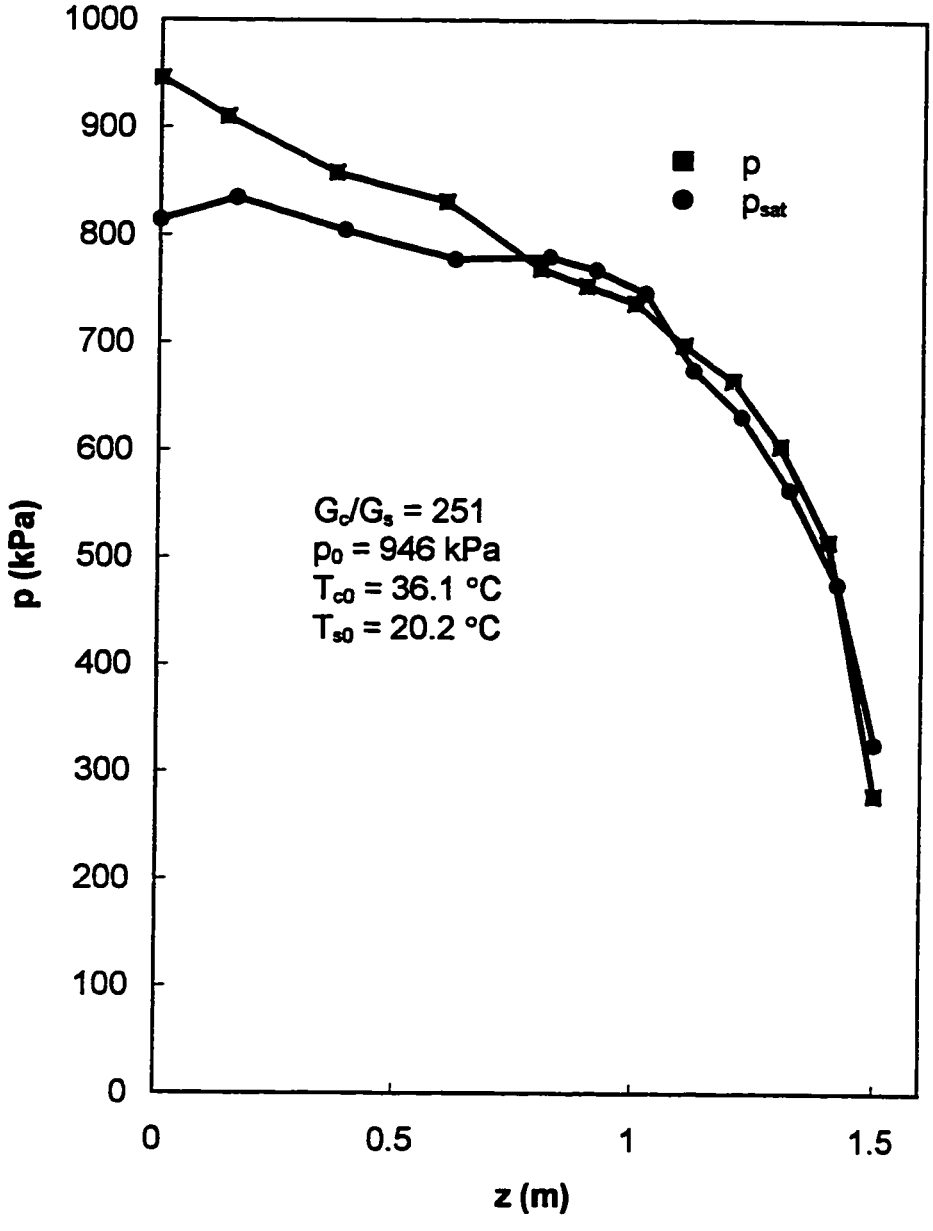

Figure 2.13 Measured pressure, p, and the saturated pressure, p_{sat}, corresponding to the measured temperature along the diabatic capillary tube

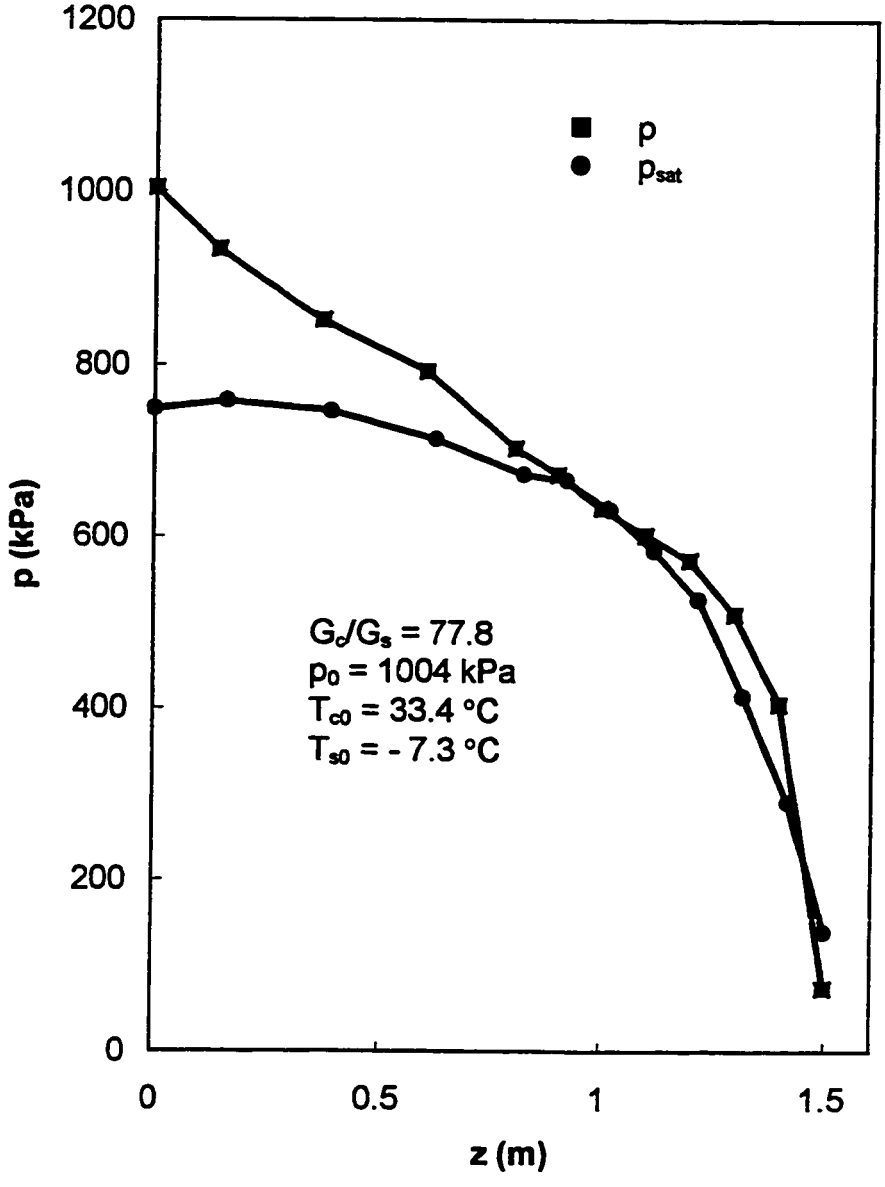

Figure 2.14 Measured pressure, p, and the saturated pressure, p_{sat}, correspondingto the measured temperature along the diabatic capillary tube

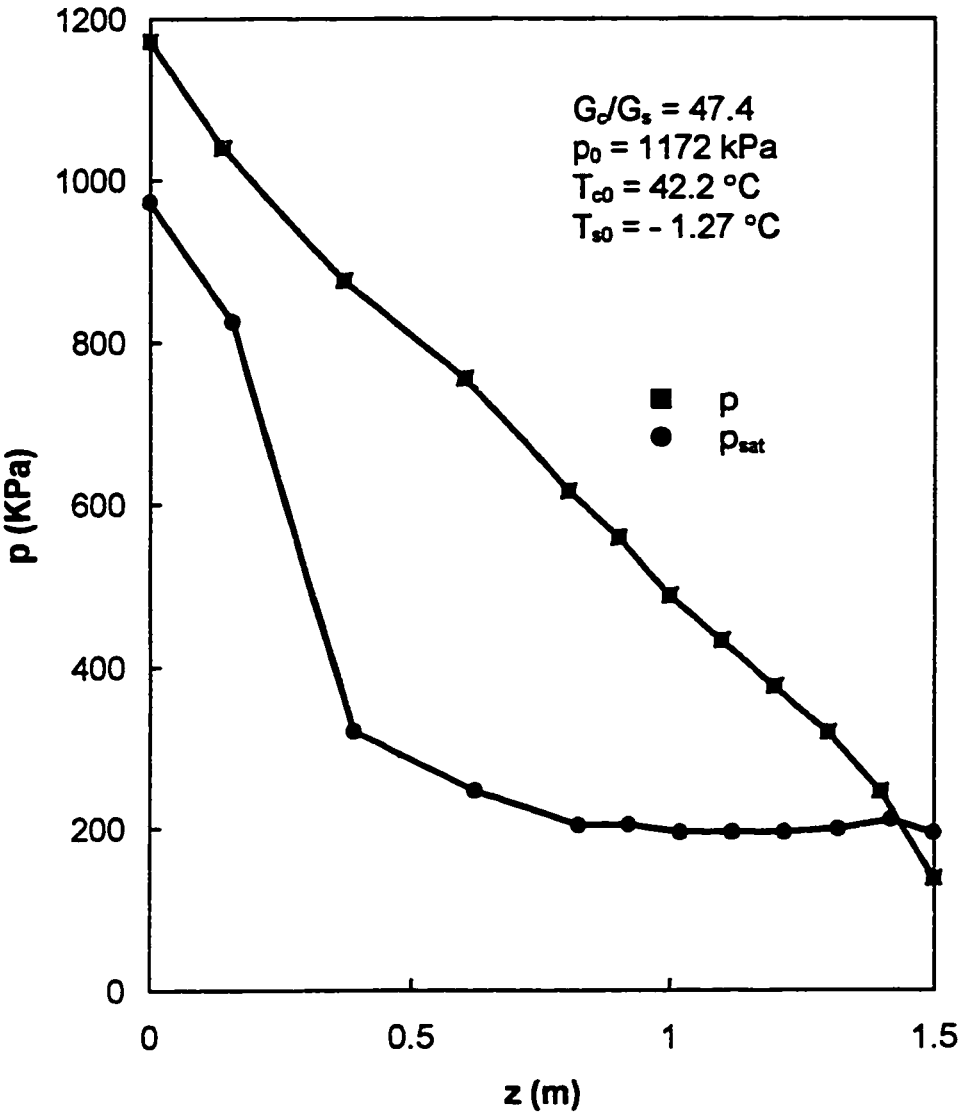

Figure 2.15 Measured pressure, p, and the saturated pressure, p_{sat}, corresponding to the measured temperature along the diabatic capillary tube

diabatic capillary tube for different heat transfer conditions caused by different mass flux ratio in the capillary tube and suction line. The heat transfer is stronger with decrease of mass flux ratio. From these figures some interesting information is revealed as follows:

1. The metastable flow of refrigerant exists in the capillary tube when the heat transfer between the capillary tube and the suction line is weaker, as shown in Figure 2.13.

2. When the heat transfer increases for the case of $G_c/G_s = 77.8$, the measured pressure curve has a point touched to the curve of the saturated pressure corresponding to the measured temperature along the diabatic capillary tube (Figure 2.14). It is expected that the metastable flow will vanish when $G_c/G_s < 77.8$. This ratio of $G_c/G_s = 77.8$ is called the critical ratio of the metastable flow.

3. When the heat transfer between the capillary tube and the suction line is strong, such as the case of $G_c/G_s = 47.4$, the inception of vaporization is located near the exit of the capillary tube, as shown in Figure 2.15. The measured pressure is linear along the whole capillary tube; and the saturated pressure corresponding to the measured temperature first decreases quite rapidly, then is smooth until to the exit.

The diabatic capillary tube tests show that there exists metastable flow, when the heat transfer between the capillary tube and the suction line is weak. In the next Chapter a correlation will be established to estimate the metastable flow in a diabatic capillary tube.

CHAPTER 3

METASTABLE FLOW OF LIQUID REFRIGERANT THROUGH A DIABATIC CAPILLARY TUBE

3.1 Bubble nucleation in a diabatic capillary tube

Nucleation theory began to be developed in the 1920's. The early work is thoroughly reviewed in the book by Frenkel (1955). After then, the work by Katz and Blander (1973) and by Blander and Katz (1975) generalized the theory. A lot of research applied the theory to solve practical problems. Fisher (1948) examined bubble nucleation at a smooth rigid interface, and Moore (1959), Apfer (1971) and Jarvis et al. (1975) studied nucleation at the interface between two liquids. Cole (1974) reviewed nucleation at cracks and crevices. Alamgir and Lienhard (1981) applied nucleation theory to successfully obtain a correlation for

the pressure undershoot during the depressurization of hot water. In 1990, Chen et al. applied the theory to the nucleation of refrigerant flow in adiabatic capillary tubes and established a correlation of underpressure of vaporization. In this Chapter, an attempt is made to apply nucleation theory to predict the pressure difference between the thermodynamic saturated point and the point of inception of vaporization of refrigerant HFC-134a flowing through a diabatic capillary tube.

3.1.1 Analysis

The nucleation process in a liquid can be divided into two types: homogeneous nucleation, in which the liquid is not in contact with a gas phase and in which the liquid has a zero contact angle with all surfaces; and heterogeneous nucleation, in which the nucleation events occur at an interface between the liquid and another phase it contacts. Here the theory based on homogeneous nucleation is used for analysis.

To form a cluster of m molecules within an originally homogeneous liquid phase, the reversible work, W, must be expended. Thus, if φ_l and φ_g are the chemical potential per molecule in the liquid and vapor phases, respectively, we find (Reiss, 1977)

$$W = (\varphi_l - \varphi_g) m_n + f_\alpha m_n^{2/3} \tag{3.1}$$

The first term on the right hand-side of this equation represents the reversible work attending the formation of the cluster, while the second term is the reversible work expended in forming the surface of vapor nuclei. The quantity f_α is given by

$$f_\alpha = 4\pi\left(\frac{3v_m}{4\pi}\right)^{\frac{2}{3}}\sigma \tag{3.2}$$

where v_m is the volume per molecule in the vapor phase. If the liquid is subcooled or saturated,

$$\varphi_g \leq \varphi_l \tag{3.3}$$

so that the first term on the right of Equation (3.1) is positive or zero, and W is a monotone-increasing function of m_n. Thus, an increased expenditure of reversible work is required in the formation of large clusters, and the process is not spontaneous in the thermodynamic sense. As a result, large clusters do not form and the subcooled or saturated liquid appears stable against vaporization.

If the liquid is superheated, then the inequality, Equation (3.3), is reversed and the first term on the right of Equation (3.1) is negative. However, the numerical aspects of the situation are such that, for small values of m_n, the increase in the second term with increase of m_n is faster than that of the first term, so that as m_n increases, so does W at first. W will reach a maximum value when $m_n = m_n^*$ (Figure 3.1). Beyond this point, the first term increases at a faster rate with increase of m_n than that of the second term, and eventually W

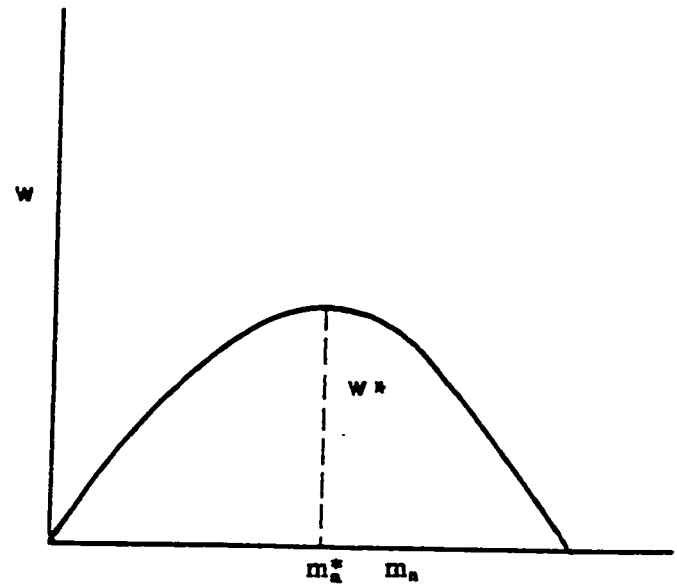

Figure 3.1 Reversible work of formation of a cluster containing m_n molecules

decreases with increasing m_n.The value of m_n corresponding to this maximum W is referred to as a vapor nucleus since it can grow spontaneously. So, the liquid temperature must be superheated for vaporization. The expenditure of reversible work required to reach the nuclear state is denoted by W*, as in Figure 3.1. It marks the size of the reversible work barrier over which the growing cluster must pass in order to complete the process of vaporization.

It is worth noting that the barrier is produced by the positive term $f_\alpha m_n^{2/3}$ so that it is the work of formation of the vapor-liquid interface which supplies the principal obstacle to uninhibited vaporization. The decrease of surface tension with increase of liquid temperature results in a lowering of the barrier.

In the superheated liquid the molecules of which the liquid is composed are considered to have a distribution of energies such that only a very small fraction have energies considerably greater than the average. Such "activated" molecules, their excess energy being called the "energy of activation" are presumed to initiate the process by means of which a vapor bubble is brought into existence. Because of the collision process in the liquid, there is a probability that a sufficient number of the activated molecules can join to form an activated cluster with an equilibrium radius (Hetsroni, 1982 and Cole, 1974).

For homogeneous nucleation, assumptions are as follows (Cole, 1974 and 1979; Li, 1989):

1. Activated clusters of all possible sizes exist;

2. The number of activated clusters of any one size depends on stepwise collision process to particular size.

It is known from statistical thermodynamics that the rate of formation of activated clusters containing m molecules is given by the expression (Kauzmann, 1967 and Waldram, 1985)

$$n = NB\exp\left(-\frac{\Delta A}{KT}\right) \tag{3.4}$$

where n is the rate of formation of activated clusters per unit volume containing m_n molecules, N is the number of molecules per unit volume, B is the collision frequency of molecules (KT/Planck's constant) (Alamgir and Lienhard, 1981) and ΔA is the increase of availability, which can be written as

$$\Delta A = A - A_i \tag{3.5}$$

where A is availability which is a measure of the maximum amount of reversible work, and A_i is initial availability of the system.

The system consists of three parts (Figure 3.2):

1. Activated cluster at uniform temperature T and uniform pressure p*;

2. Liquid phase at uniform temperature T and uniform pressure p;

3. Interface of liquid phase and activated cluster at uniform temperature T and pressure p_σ.

The availability of the system can be expressed as the sum of the contributions from the above three parts. Thus (Cole, 1974 and 1979)

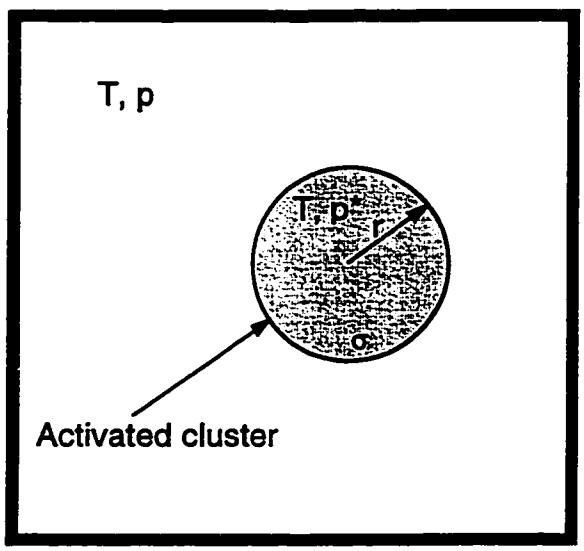

Figure 3.2 Description of system containing a single activated cluster

$$A = A_l + A^* + A_\sigma \tag{3.6}$$

The availability of the liquid phase is

$$A_l = m_l(u_l - Ts_l + pv_l) \tag{3.7}$$

The availability of the activated cluster is

$$A^* = m^*(u^* - Ts^* + pv^*) \tag{3.8}$$

and the availability of the interface may be expressed as

$$A_\sigma = m_\sigma(u_\sigma - Ts_\sigma + pv_\sigma) + 4\pi r^2\sigma \tag{3.9}$$

Substituting Equations (3.7) to (3.9) into (3.6), we get

$$A = [m_l(u_l - Ts_l + pv_l) + m^*(u^* - Ts^* + pv^*) + m_\sigma(u_\sigma - Ts_\sigma + pv_\sigma)] + 4\pi r^2\sigma \tag{3.10}$$

where m_l, m^* and m_σ are the mass of the liquid phase, activated cluster and interface, respectively. Before activation of molecules the initial availability of the system is

$$A_i = m_i(u_l - Ts_l + pv_l) \tag{3.11}$$

Substituting Equations (3.10) and (3.11) into (3.5), we have

$$\Delta A = [m_l(u_l - Ts_l + pv_l) + m^*(u^* - Ts^* + pv^*) + m_\sigma(u_\sigma - Ts_\sigma + pv_\sigma)] + 4\pi r^2\sigma - m_i(u_l - Ts_l + pv_l) \tag{3.12}$$

We introduce the specific Gibbs function which is defined in terms of the temperature and pressure of the system,

$$g_n = u - Ts + pv \tag{3.13}$$

For liquid phase the specific Gibbs function is

$$g_{nl} = u_l - Ts_l + pv_l \tag{3.14}$$

For the activated cluster

$$g_n^* = u^* - Ts^* + p^* v^* \tag{3.15}$$

For the interface

$$g_{n\sigma} = u_\sigma - Ts_\sigma + p_\sigma v_\sigma \tag{3.16}$$

If we define the interface phase boundary so that the surface has properties similar to the liquid phase, then (Model and Roid, 1983)

$$p_\sigma = p \tag{3.17}$$

So, Equation (3.16) becomes

$$g_{n\sigma} = u_\sigma - Ts_\sigma + pv_\sigma \tag{3.18}$$

Substituting Equations (3.14), (3.15) and (3.18) into (3.12), we obtain

$$\Delta A = m_l g_{nl} + m^* \left[g_n^* + (p - p^*) v^* \right] + m_\sigma g_{n\sigma} + 4\pi r^2 \sigma - m_i g_{nl} \tag{3.19}$$

Using the mass conservation

$$m_l = m_l + m^* + m_\sigma \tag{3.20}$$

Equation (3.19) becomes

$$\Delta A = m^* \left(g_n^* - g_{nl} \right) + m_\sigma (g_{n\sigma} - g_{nl}) + 4\pi r^2 \sigma + m^* (p - p^*) v^* \tag{3.21}$$

Assuming that the phase of interface between liquid phase and activated cluster is liquid, and the pressure p* is equal to pressure p (Cole, 1974), i.e.

$$g_{n_\sigma} = g_{nl} \tag{3.23}$$

$$p^* = p \tag{3.24}$$

the increase of the availability of the system is approximated by

$$\Delta A = m^*\left(g_n^* - g_{nl}\right) + 4\pi r^2\sigma \tag{3.25}$$

Expressing the mass of activated cluster as

$$m^* = \frac{4\pi r^3}{3v^*} \tag{3.26}$$

Equation (3.25) becomes

$$\Delta A = \frac{4}{3}\frac{g_n^* - g_{nl}}{v^*}\pi r^3 + 4\pi r^2\sigma \tag{3.27}$$

For a system that can undergo a change of phase, the requirement of thermodynamic equilibrium is that the change in the increase of the availability be zero when the pressure and temperature are kept constant,

$$\left.\frac{\partial(\Delta A)}{\partial r}\right|_{T,p} = 4\pi r^2\frac{g_n^* - g_{nl}}{v^*} + 8\pi r\sigma = 0 \tag{3.28}$$

Thus we have

$$g_n^* - g_{nl} = -\frac{2\sigma v^*}{r_e} \tag{3.29}$$

where r_e is defined as the equilibrium cluster radius for given external temperature T and pressure p.

Substituting Equation (3.29) back into Equation (3.27) gives the expression for the increase of the availability of a cluster of any size

$$\Delta A = 4\pi r^2 \sigma \left[1 - \frac{2}{3}\left(\frac{r}{r_e}\right)\right] \tag{3.30}$$

A plot of ΔA versus the cluster radius r, as shown in Figure 3.3, exhibits a maximum at the equilibrium cluster radius r_e. The activated clusters with a radius less than r_e will collapse, while clusters with a radius greater than r_e will experience spontaneous growth. A cluster with radius r_e is hence called a vapor nucleus.

If $r = r_e$ in Equation (3.30), we can obtain the expression of the maximum increase in availability for an equilibrium cluster (vapor nucleus)

$$\Delta A = \frac{4}{3}\pi r_e^2 \sigma \tag{3.31}$$

Substituting Equation (3.31) into (3.4), the rate of formation of the vapor nucleus per unit volume is

$$n_e = NB \exp\left(-\frac{4\pi r_e^2 \sigma}{3KT}\right) \tag{3.32}$$

If the equilibrium vapor pressure in the vapor nucleus is the saturated pressure, the Laplace-Kelvin Equation at the equilibrium state (Cole, 1979) becomes

$$\left(\frac{\rho_l - \rho_g}{\rho_l}\right)\left(p_{sat} - p\right) = \frac{2\sigma}{r_e} \tag{3.33}$$

Equation (3.32) becomes

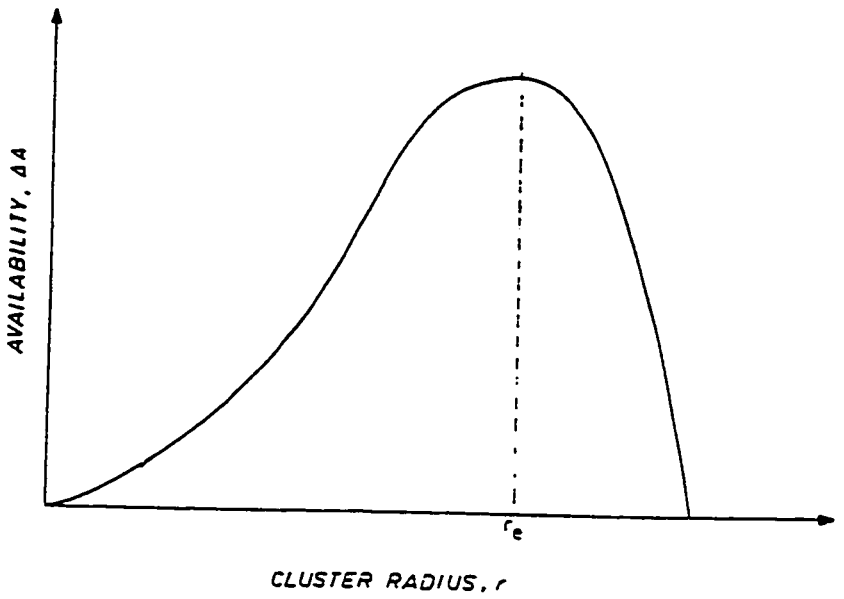

Figure 3.3 Availability of an activated cluster of radius r_e

$$n_e = NB\exp\left[-\frac{16\pi\sigma^3}{3KT\left(1-\frac{\rho_v}{\rho_l}\right)^2(p_{sat}-p)^2}\right] \tag{3.34}$$

When refrigerant HFC-134a flows through a capillary tube, the rate of the formation of the vapor nucleus does not satisfy Equation (3.34), which is derived for the homogeneous nucleation. Usually the nucleation is non-homogeneous, therefore, we introduce a heterogeneous factor ϕ into the exponential term of Equation (3.34). According to the research of Blander and Katz (1975), the density of molecules is now proportional to

$$N = \left(\frac{N_A}{v_l}\right)^{\frac{2}{3}} \tag{3.35}$$

where N_A is Avogadro's number. Thus, Equation (3.34) becomes

$$n_e = B\left(\frac{N_A}{v_l}\right)^{\frac{2}{3}}\exp\left[-\frac{16\pi\sigma^3\phi}{3KT\left(1-\frac{\rho_v}{\rho_l}\right)^2(p_{sat}-p)^2}\right] \tag{3.36}$$

3.1.2 Bubble density in a diabatic capillary tube

The total bubble density N_R in a diabatic capillary tube with respect to time from $\tau = 0$ to $\tau = \tau_v$ is

$$N_R = \int_0^{\tau} n_e d\tau \tag{3.37}$$

We consider refrigerant flowing through a diabatic capillary tube with subcooled inlet condition, as shown in figure 3.4. It is assumed that the thermodynamic saturated position of the measured pressure, p, is located at z_{sat} with its pressure $p = p_{sat}$ and temperature $T_c = T_{csat}$. The inception position of vaporization is located at z_v with its pressure $p = p_v$ and temperature $T_c = T_{cv}$ because the metastable flow process causes the delay of vaporization. The pressure difference, $p_{sat} - p_v$, is the characteristic quantity of the metastable flow, and is defined as the underpressure of vaporization. In order to integrate the Equation (3.37), we observe the refrigerant flowing from the position $z = z_{sat}$ at $\tau = 0$ to the position $z = z_v$ at time $\tau = \tau_v$, and have

$$\tau = 0, \qquad z = z_{sat} \qquad p = p_{sat} \qquad T_c = T_{csat}$$

$$\tau = \tau_v, \qquad z = z_v \qquad p = p_v \qquad T_c = T_{cv}$$

So, the bubble density N_R is obtained by substituting Eq. (3.36) into Eq. (3.37)

$$N_R = \int_0^{\tau_v} B\left(\frac{N_A}{v_l}\right)^{\frac{2}{3}} \exp\left[-\frac{16\pi\sigma^3\phi}{3KT_c\left(1-\frac{\rho_v}{\rho_l}\right)^2 (p_{sat}-p)^2}\right] d\tau \tag{3.38}$$

Because the rate of nucleation at equilibrium state is a function of liquid temperature, T_c, and pressure, p, of the system, the differential of time, τ, can be expressed as:

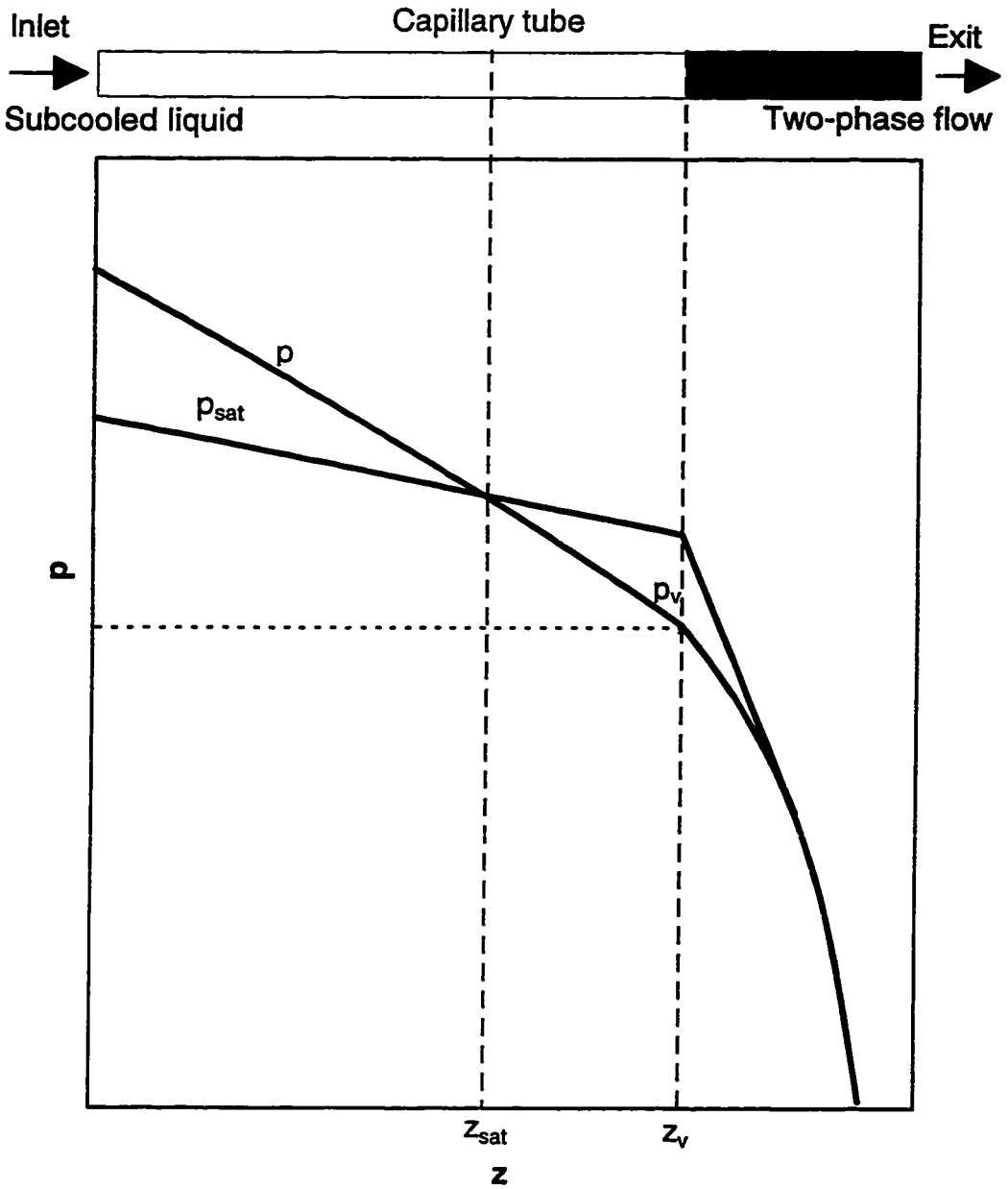

Figure 3.4 Metastable flow of refrigerant through a diabatic capillary tube

$$d\tau = \frac{\partial \tau}{\partial z}\frac{\partial z}{\partial p}\bigg|_{T_c=T_{cv}} dp + \frac{\partial \tau}{\partial z}\frac{\partial z}{\partial T_c}\bigg|_{p=p_v} dT_c \tag{3.39}$$

For the flow before the inception, we have

$$\frac{\partial p}{\partial z} = \left(\frac{\partial p}{\partial z}\right)_f \tag{3.40}$$

$$\frac{\partial z}{\partial \tau} = V_{cl} \tag{3.41}$$

where $\left(\frac{\partial p}{\partial z}\right)_f$ is the pressure drop for flow resistance and V_{cl} is flow velocity.

Thus, Equation (3.39) becomes

$$d\tau = \frac{1}{V_{cl}\left(\frac{\partial p}{\partial z}\right)_f} dp + \frac{1}{V_{cl}}\frac{1}{\left(\frac{\partial T_c}{\partial z}\right)} dT_c \tag{3.42}$$

Substituting the Equation (3.42) into (3.38), we obtain

$$N_R = N_{R1} + N_{R2} \tag{3.43}$$

where

$$N_{R1} = \frac{1}{V_{cl}\left(\frac{\partial p}{\partial z}\right)_f} B\left(\frac{N_A}{v_l}\right)^{\frac{2}{3}} \int_{p_{sat}}^{p_v} \exp\left[-\frac{16\pi\sigma^3\phi}{3KT_{cv}\left(1-\frac{\rho_g}{\rho_l}\right)^2 (p_{sat}-p)^2}\right] dp \tag{3.44}$$

$$N_{R2} = \frac{1}{V_{cl}} B\left(\frac{N_A}{v_l}\right)^{\frac{2}{3}} \int_{T_{cat}}^{T_{cv}} \frac{1}{\frac{\partial T_c}{\partial z}} \exp\left[-\frac{16\pi\sigma^3\phi}{3KT_c\left(1-\frac{\rho_g}{\rho_l}\right)^2 (p_{sat}-p_v)^2}\right] dT_c \tag{3.45}$$

N_{R1} is the bubble density for an approximately adiabatic condition due to pressure drop for flow resistance, and N_{R2} is the additional quantity of bubble density due to heat transfer from the capillary tube to the suction line. We first integrate N_{R1}.

$$N_{R1} = \frac{1}{V_{cl}\left(\frac{\partial p}{\partial z}\right)_f} B\left(\frac{N_A}{v_l}\right)^{\frac{2}{3}} \sqrt{\frac{16\pi\sigma^3\phi}{3KT_{cv}\left(1-\frac{\rho_g}{\rho_l}\right)^2}} \int_{p_{sat}}^{p_v} \exp\left\{-\left[\sqrt{\frac{16\pi\sigma^3\phi}{3KT_{cv}\left(1-\frac{\rho_g}{\rho_l}\right)^2 (p_{sat}-p)^2}}\right]^2\right\} \cdot$$

$$\cdot d\left[\sqrt{\frac{3KT_{cv}\left(1-\frac{\rho_g}{\rho_l}\right)^2 (p_{sat}-p)^2}{16\pi\sigma^3\phi}}\right] \qquad (3.46)$$

Let

$$(\eta\phi)' = \frac{16\pi\sigma^3\phi}{3KT_{cv}\left(1-\frac{\rho_g}{\rho_l}\right)^2 (p_{sat}-p)^2} \qquad (3.47)$$

We have $p = p_v$ $\qquad (\eta\phi)' = (\eta\phi)$

$p = p_{sat}$ $\qquad (\eta\phi)' = \infty$

Thus, Equation (3.46) becomes

$$N_{R1} = \frac{1}{V_{cl}\left(\frac{\partial p}{\partial z}\right)_f} B\left(\frac{N_A}{v_l}\right)^{\frac{2}{3}} \sqrt{\frac{16\pi\sigma^3\phi}{3KT_{cv}\left(1-\frac{\rho_g}{\rho_l}\right)^2}} \int_{\infty}^{(\eta\phi)} \exp\left\{-\left[\sqrt{(\eta\phi)'}\right]^2\right\} d\left[\frac{1}{\sqrt{(\eta\phi)'}}\right] \qquad (3.48)$$

Integrating Equation (3.48), we get (Spiegel, 1968)

$$N_{R1} = \left(\frac{N_A}{v_l}\right)^{\frac{2}{3}} B \frac{p_{sat} - p_v}{V_{cl}\left(\frac{\partial p}{\partial z}\right)_f} \left[\exp(-\eta\phi) - \sqrt{\pi\eta\phi}\, erfc\left(\sqrt{\eta\phi}\right)\right] \tag{3.49}$$

where

$$\eta = \frac{16\pi\sigma^3}{3KT_{cv}\left(1 - \frac{\rho_g}{\rho_l}\right)^2 (p_{sat} - p_v)^2} \tag{3.50}$$

Next we integrate the N_{R2} (Equation 3.45). It is assumed that the wall temperature of the capillary tube and the suction line is uniform. For the capillary tube, the thermal balance for an element dz is shown in Figure 3.5, i.e.

$$dQ = \bar{h}_c \left(T_c - \bar{T}_w\right) dA_{ac} \tag{3.51}$$

For the suction line

$$dQ = \bar{h}_s \left(\bar{T}_w - T_s\right) dA_{as} \tag{3.52}$$

From the above two equations, we get

$$\left(\frac{1}{\bar{h}_c\, dA_{ac}} + \frac{1}{\bar{h}_s\, dA_{as}}\right) dQ = T_c - T_s \tag{3.53}$$

dA_c and dA_s can respectively be expressed as

$$dA_{ac} = \pi D_c dz \tag{3.54}$$

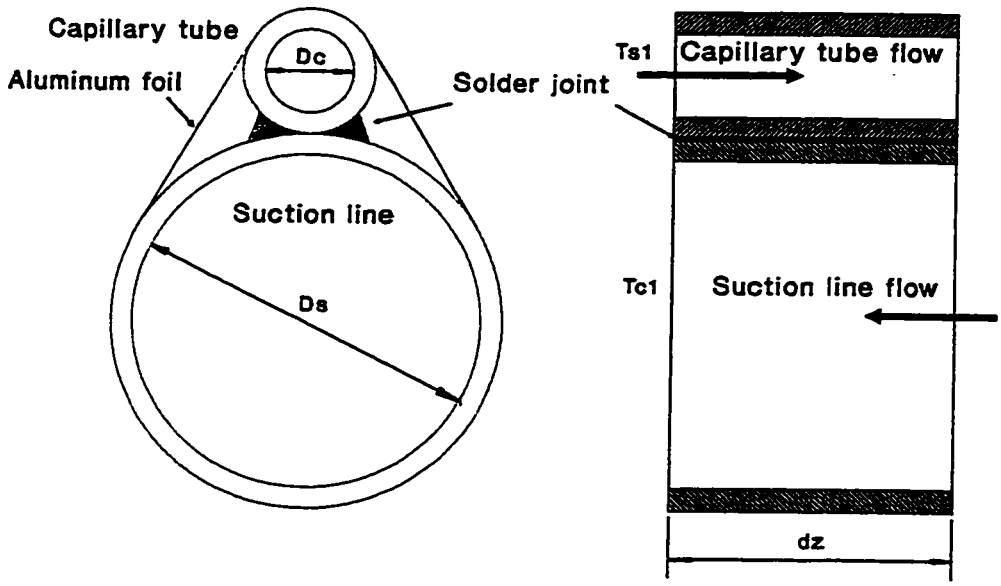

Figure 3.5 Heat transfer between capillary tube and suction line

$$dA_{as} = \pi D_s dz \tag{3.55}$$

Thus Equation (3.53) becomes

$$\left(\frac{1}{\bar{h}_c \pi D_c} + \frac{1}{\bar{h}_s \pi D_s}\right)\frac{dQ}{dz} = T_c - T_s \tag{3.56}$$

For the capillary tube we also have

$$dQ = c_{pc}\,\dot{m}_c\,dT_c \tag{3.57}$$

Substituting into Equation (3.56), we get

$$\frac{dT_c}{dz} = -\frac{\pi}{c_{pc}\,\dot{m}_c\left(1/\bar{h}_c D_c + 1/\bar{h}_s D_s\right)}\left(T_c - T_s\right) \tag{3.58}$$

For the suction line we have

$$dQ = c_{ps}\,\dot{m}_s\,dT_s \tag{3.59}$$

From Equations (3.57) and (3.59), we obtain

$$\frac{dT_s}{dT_c} = -\frac{c_{pc}\,\dot{m}_c}{c_{ps}\,\dot{m}_s} \tag{3.60}$$

Integrating the above we get

$$T_s = -\frac{c_{pc}\,\dot{m}_c}{c_{ps}\,\dot{m}_s}T_c + C \tag{3.61}$$

where C is constant. The temperatures of refrigerant in the capillary tube and suction line at the inlet cross section of the capillary tube can be defined

$T_c = T_{c1}$ $T_s = T_{s1}$

Thus the constant C is

$$C = T_{s1} + \frac{\dot{c}_{pc} \dot{m}_c}{\dot{c}_{ps} \dot{m}_s} T_{c1} \tag{3.62}$$

Then Equation (3.60) becomes

$$C = -\frac{\dot{c}_{pc} \dot{m}_c}{\dot{c}_{ps} \dot{m}_s}(T_c - T_{c1}) + T_{s1} \tag{3.63}$$

Substituting the above into Equation (3.58) we get

$$\frac{dT_c}{dz} = \bar{A} - \bar{B} T_c \tag{3.64}$$

where

$$\bar{A} = \frac{\pi}{\dot{c}_{pc} \dot{m}_c \left(1/\bar{h}_c D_c + 1/\bar{h}_s D_s\right)} \left(T_{s1} + \frac{\dot{c}_{pc} \dot{m}_c}{\dot{c}_{ps} \dot{m}_s} T_{c1} \right) \tag{3.65}$$

$$\bar{B} = \frac{\pi}{\dot{c}_{pc} \dot{m}_c \left(1/\bar{h}_c D_c + 1/\bar{h}_s D_s\right)} \left(\frac{\dot{c}_{pc} \dot{m}_c}{\dot{c}_{ps} \dot{m}_s} + 1 \right) \tag{3.66}$$

Substituting Equations (3.50) and (3.64) into (3.45), we have

$$N_{R2} = \left(\frac{N_A}{v_l} \right)^{\frac{2}{3}} B \frac{1}{V_{cl}} \int_{T_{cm}}^{T_{cr}} \frac{1}{\bar{A} - \bar{B} T_c} \exp\left(-\frac{T_{cv} \eta \phi}{T_c} \right) dT_c \tag{3.67}$$

The total number of vapor nuclei per unit area is

$$N_R = \left(\frac{N_A}{v_l}\right)^{\frac{2}{3}} \frac{B}{V_{cl}} \left\{ \frac{p_{sat} - p_v}{\left(\frac{\partial p}{\partial z}\right)_f} \left[\exp(-\eta\phi) - \sqrt{\pi\eta\phi}\, erfc\left(\sqrt{\eta\phi}\right)\right] + \int_{T_{csat}}^{T_{cv}} \frac{1}{\bar{A} - B\bar{T}_c} \exp\left(-\frac{T_{cv}\eta\phi}{T_c}\right) dT_c \right\} \tag{3.68}$$

3.1.3 heterogeneity factor ϕ

In Equation (3.68), all the external effects on the underpressure of vaporization, p_{sat} - p_v, such as the roughness of the capillary tube wall, the degree of the flow turbulence, the non-uniformity of the nucleus, the distribution of the nucleus and the impurity contained in the refrigerant are considered to be included in the synthetic heterogeneous nucleation factor, ϕ, which can be expressed by

$$\phi = f\,(D_c, G_c, T_{cri}, \Delta T_{csub}, T_{csat}, \sigma, k_l, \mu_l, D_s, G_s, \mu_g, p_{sat0}, p_{sat0} - p_{sat}) \tag{3.69}$$

We divide the factor ϕ into the sum of two parts: ϕ_1 and ϕ_2. The factor ϕ_1 only relates to the condition in an adiabatic capillary tube, and factor ϕ_2 only relates to the condition of heat transfer between the capillary tube and suction line. Thus the factor ϕ becomes

$$\phi = \phi_1 + \phi_2 \tag{3.70}$$

where

$$\phi_1 = f_1\,(D_c, G_c, T_{cri}, \Delta T_{csub}, \sigma, k_l, \mu_l, T_{csat}) \tag{3.71}$$

$$\phi_2 = f_2 (D_s, G_s, \mu_g, p_{sat0}, p_{sat0} - p_{sat}) \quad (3.72)$$

For finding the expression on factor ϕ dimensional analysis is used (Lin, 1992).

The basic dimensions are mass M, length L, time τ and temperature T. The dimensions of the parameters in Equation (3.71) and (3.72) are as follows:

D_c and D_s: L

G_c and G_s: $ML^{-2}\tau^{-1}$

T_{cri}, T_{csat} and ΔT_{csub}: T

σ $M\tau^{-2}$

μ_l and μ_g: $ML^{-1}\tau^{-1}$

k_l: $ML^2\tau^{-2}T^{-1}$

p_{sat} and p_{sat0}: $ML^{-1}\tau^{-2}$

For the factor ϕ_1 we have

Table 3.1 Dimension of parameters related to the factor ϕ_1

	(a)	(b)	(c)	(d)				
	D_c	G_c	T_{crl}	σ	k_l	μ_l	ΔT_{csub}	T_{csat}
M	0	1	0	1	1	1	0	0
L	1	-2	0	0	2	-1	0	0
τ	0	-1	0	-2	-2	-1	0	0
T	0	0	1	0	-1	0	1	1

For the k_i we have from the Table 3.1

M: $b + d + 1 = 0$

L: $a - 2b + 2 = 0$

τ: $-b - 2d - 2 = 0$

T: $c - 1 = 0$

Solving the above Equations we obtain

$a = -2$

$b = 0$

$c = 1$

$d = -1$

Thus, a dimensional group can be written

$$\pi_1^{'} = \frac{D_c}{\sqrt{\frac{k_i T_{cri}}{\sigma}}} \tag{3.73}$$

From the Table 3.1 another dimensional group can be expressed as follows

$$\pi_1^{''} = \frac{T_{cri}}{T_{csat}} \tag{3.74}$$

Substituting Equation (3.74) into (3.73), the first dimensional group is

$$\pi_1 = \frac{D_c}{D'} \tag{3.75}$$

where

$$D' = \sqrt{\frac{k_l T_{csat}}{\sigma}} \tag{3.76}$$

Since the magnitude of D' is small, the following form is suggested by Chen et al. (1990)

$$D' = \sqrt{\frac{k_l T_{csat}}{\sigma}} \times 10^4 \tag{3.77}$$

For the μ_l we have from the Table 3.1

M: $b + d + 1 = 0$

L: $a - 2b - 1 = 0$

τ: $-b - 2d - 1 = 0$

T: $c = 0$

Solving the above Equations we obtain

$a = -1$

$b = -1$

$d = 0$

Thus the second dimensional group can be written

$$\pi_2 = \frac{D_c G_c}{\mu_l} \equiv \mathrm{Re}_c \tag{3.78}$$

The third dimensional group can be easily obtained as:

$$\pi_3 = \frac{\Delta T_{csub}}{T_{cri}} \tag{3.79}$$

From equations (3.75), (3.78) and (3.79), for engineering applications, ϕ_1 may be written as

$$\phi_1 = C_1 \mathrm{Re}_c^{n_1} \left(\frac{\Delta T_{csub}}{T_{cri}} \right)^{n_2} \left(\frac{D_c}{D'} \right)^{n_3} \tag{3.80}$$

For the factor ϕ_2 we have

Table 3.2 Dimension of parameters related to the factor ϕ_2

	(a)	(b)	(c)		
	p_{sat0}	G_s	μ_g	D_s	$p_{sat0} - p_{sat}$
M	1	1	1	0	1
L	- 1	- 2	- 1	1	- 1
τ	- 2	- 1	- 1	0	- 2
T	0	0	0	0	0

For the D_s we have from Table 3.2

M: $b + d + c = 0$

L: $- a - 2b - c = 1$

τ: $- 2a - b - c = 0$

Solving the above Equations we obtain

$a = 0$

$b = -1$

$c = 1$

Thus the first dimensional group can be written

$$\pi_1 = \frac{G_s D_s}{\mu_g} \equiv \mathrm{Re}_s \tag{3.81}$$

For the p_{sat} we have from the Table 3.2

M: $b + d + c = 1$

L: $-a - 2b - c = -1$

τ: $-2a - b - c = -2$

Solving the above Equations we obtain

$a = 1$

$b = 0$

$c = 0$

Thus the second dimensional group can be written

$$\pi_2 = \frac{p_{sat0} - p_{sat}}{p_{sat0}} \tag{3.82}$$

From Equations (3.81) and (3.82), ϕ_2 can be written by

$$\phi_2 = C_2 \, \mathrm{Re}_s^{n_4} \left(1 - \frac{p_{sat}}{p_{sat0}} \right)^{n_5} \tag{3.83}$$

Substituting Equations (3.80) and (3.83) into (3.70), the heterogeneity factor ϕ may be represented in the following dimensionless form as

$$\phi = C_1 \, \mathrm{Re}_c^{n_1} \left(\frac{\Delta T_{csub}}{T_{csat}} \right)^{n_2} \left(\frac{D_c}{D'} \right)^{n_3} + C_2 \, \mathrm{Re}_s^{n_4} \left(1 - \frac{p_{sat}}{p_{sat0}} \right)^{n_5} \tag{3.84}$$

3.2. Underpressure of vaporization

3.2.1 Correlation of the underpressure of vaporization

It is assumed that the vapor nuclei are uniformly distributed on the wall. We know from geometry that the number of vapor nucleus per unit area at the inception of vaporization is in inverse proportional to the square of the critical radius r_e of the vapor nuclei (Figure 3.6), i. e.

$$N_R = \frac{f}{\pi r_e^2} \tag{3.85}$$

where f is a proportionality constant. Substituting the above into Equation (3.68), we obtain

$$\frac{fV_{cl}}{B\pi \left(\frac{N_A}{v_l} \right)^{\frac{2}{3}} r_e^2} = \frac{p_{sat} - p_v}{\left(\frac{\partial p}{\partial z} \right)_f} \left[\exp(-\eta\phi) - \sqrt{\pi\eta\phi}\, erfc\left(\sqrt{\eta\phi} \right) \right] + \int_{T_{csat}}^{T_{cv}} \frac{1}{\bar{A} - \bar{B} T_c} \exp\left(-\frac{T_{cv}\eta\phi}{T_c} \right) dT_c \tag{3.86}$$

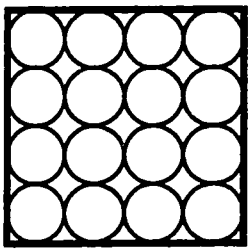

Figure 3.6 Relationship between the number and critical radius of vapor nucleus

Using Laplace-Kelvin Equation (Cole, 1974)

$$r_e = \frac{2\sigma}{\left(1-\frac{\rho_g}{\rho_l}\right)\left(p_{sat}-p_v\right)} \tag{3.87}$$

and considering that the heterogeneous nucleation factor ϕ includes the effect of f and using Equation (3.50), Equation (3.86) can be written as

$$\frac{4\sigma V_{cl}}{3BKT_{cv}\eta\left(\frac{N_A}{v_l}\right)^{\frac{2}{3}}} = \frac{p_{sat}-p_v}{\left(\frac{\partial p}{\partial z}\right)_f}\left[\exp\left(-\eta\phi\right)-\sqrt{\pi\eta\phi}erfc\left(\sqrt{\eta\phi}\right)\right]+\int_{T_{cmt}}^{T_{cv}}\frac{1}{\bar{A}-\bar{B}T_c}\exp\left(-\frac{T_{cv}\eta\phi}{T_c}\right)dT_c \tag{3.88}$$

Because Equation (3.88) contains the complementary error function, $erfc\left(\sqrt{\eta\phi}\right)$, and the integration, they are not convenient for the calculation of the underpressure of vaporization, p_{sat} - p_v. The Gibbs number Gb is introduced as following (Skripov, 1974; Alamgir and Lienhaed, 1981)

$$Gb = \frac{\Delta A}{KT} \tag{3.89}$$

Comparing with Equations (3.4) and (3.36), for the position of vaporization, we obtain

$$Gb = \frac{16\pi\sigma^3}{3KT_{cv}\left(1-\frac{\rho_g}{\rho_l}\right)^2\left(p_{sat}-p_v\right)^2}\phi \tag{3.90}$$

It can be written by

$$\frac{(p_{sat}-p_v)\sqrt{KT_{cv}}}{\sigma^{\frac{3}{2}}}=\sqrt{\frac{16\pi}{3Gb}}\left(\frac{\rho_l}{\rho_l-\rho_g}\right)\phi \tag{3.91}$$

Substituting Equation (3.79) into the above gives the dimensionless form of underpressure of vaporization as

$$\frac{(p_{sat}-p_v)\sqrt{KT_{cv}}}{\sigma^{\frac{3}{2}}}=\sqrt{\frac{16\pi}{3Gb}}\left(\frac{\rho_l}{\rho_l-\rho_g}\right)\left[C_1\,\mathrm{Re}_c^{n_1}\left(\frac{\Delta T_{csub}}{T_{cri}}\right)^{n_2}\left(\frac{D_c}{D'}\right)^{n_3}+C_2\,\mathrm{Re}_s^{n_4}\left(1-\frac{p_{sat}}{p_{sat0}}\right)^{n_5}\right] \tag{3.92}$$

3.2.2 Final form of the underpressure of vaporization

Using the experimental data, we can obtain the values of heterogeneous nucleation factor ϕ corresponding to each experimental condition from Equation (3.86). Then constants Gb, C_1, C_2 and n_1 - n_5 in Equation (3.90) can be determined by a fitting method. As mentioned in Section 1.3, factor ϕ is divided into two parts: ϕ_1 and ϕ_2. Using the results obtained by Chen et al. (1990), the constants in factor ϕ_1 can be determined, because it relates to the condition of an adiabatic capillary tube, i.e.

$C_1 = 1.032$

$n_1 = 0.914$

$n_2 = -0.208$

$n_3 = -3.18$

$Gb = 38.68$

From the experimental data the constants in factor ϕ_2 are

$$C_2 = -0.0122$$

$$n_4 = 0.234$$

$$n_5 = 0.957$$

The final form of the underpressure of vaporization can be written as follows

$$\frac{(p_{sat} - p_v)\sqrt{KT_{cv}}}{\sigma^{\frac{3}{2}}} = 0.658\left(\frac{\rho_l}{\rho_l - \rho_g}\right)\phi \tag{3.93}$$

where

$$\phi = \phi_1 - \phi_2 \tag{3.94}$$

$$\phi = 1.032\,\mathrm{Re}_c^{0.914}\left(\frac{\Delta T_{csub}}{T_{cri}}\right)^{-0.208}\left(\frac{D_c}{D'}\right)^{-3.18} \tag{3.95}$$

$$\phi_2 = 0.0122\,\mathrm{Re}_s^{0.234}\left(1 - \frac{p_{sat}}{p_{sat0}}\right)^{0.957} \tag{3.96}$$

and

$$D' = \sqrt{\frac{k_l T_{csat}}{\sigma}} \times 10^4 \tag{3.97}$$

Equation (3.93) is valid in the experimental region:

$$4640 < \mathrm{Re}_c < 14500$$

$$0 < \mathrm{Re}_s < 29000$$

$$1.83 < \Delta T_{csub} < 16.8 \ ^\circ\mathrm{C}$$

$$28.2 < T_{c0} < 41.1 \ ^\circ\mathrm{C}$$

$$9.13 < p_0 < 13.4 \ \mathrm{bar}$$

$$2550 < G_c < 5340 \text{ kg/s m}^2$$

$$G_s < 1200 \text{ kg/s m}^2$$

For adiabatic capillary tube we have

$$p_{sat} = p_{sat0} \tag{3.98}$$

Equation (3.93) becomes

$$\phi = \phi_1 = 1.032\,\mathrm{Re}_c^{0.914}\left(\frac{\Delta T_{csub}}{T_{cri}}\right)^{-0.208}\left(\frac{D_c}{D'}\right)^{-3.18} \tag{3.99}$$

It is the same as the result obtained by Chen et al. (1990).

For the case of oil in the refrigerant, Equation (3.95) can be written as follows

$$\phi_1 = 1.032\,\mathrm{Re}_c^{0.914}\left(\frac{\Delta T_{csub}}{T_{cri}}\right)^{-0.208}\left(\frac{f_0 D_c}{D'}\right)^{-3.18} \tag{100}$$

where f_0 is the cross-sectional factor of the tube which considers the effect of oil in the refrigerant.

3.3 Discussion and data comparison

The underpressure of vaporization, $p_{sat} - p_v$, is proportional to ϕ (Equation 3.93), and ϕ_2 can be considered as a correction factor for the basic factor ϕ_1. The ϕ as a function of the parameters ΔT_{csub}, D_c and G_c can be obtained from Equation (3.99).

From Equation (3.99) it can be seen that the underpressure of vaporization of the metastable flow in the single-phase liquid decreases with an

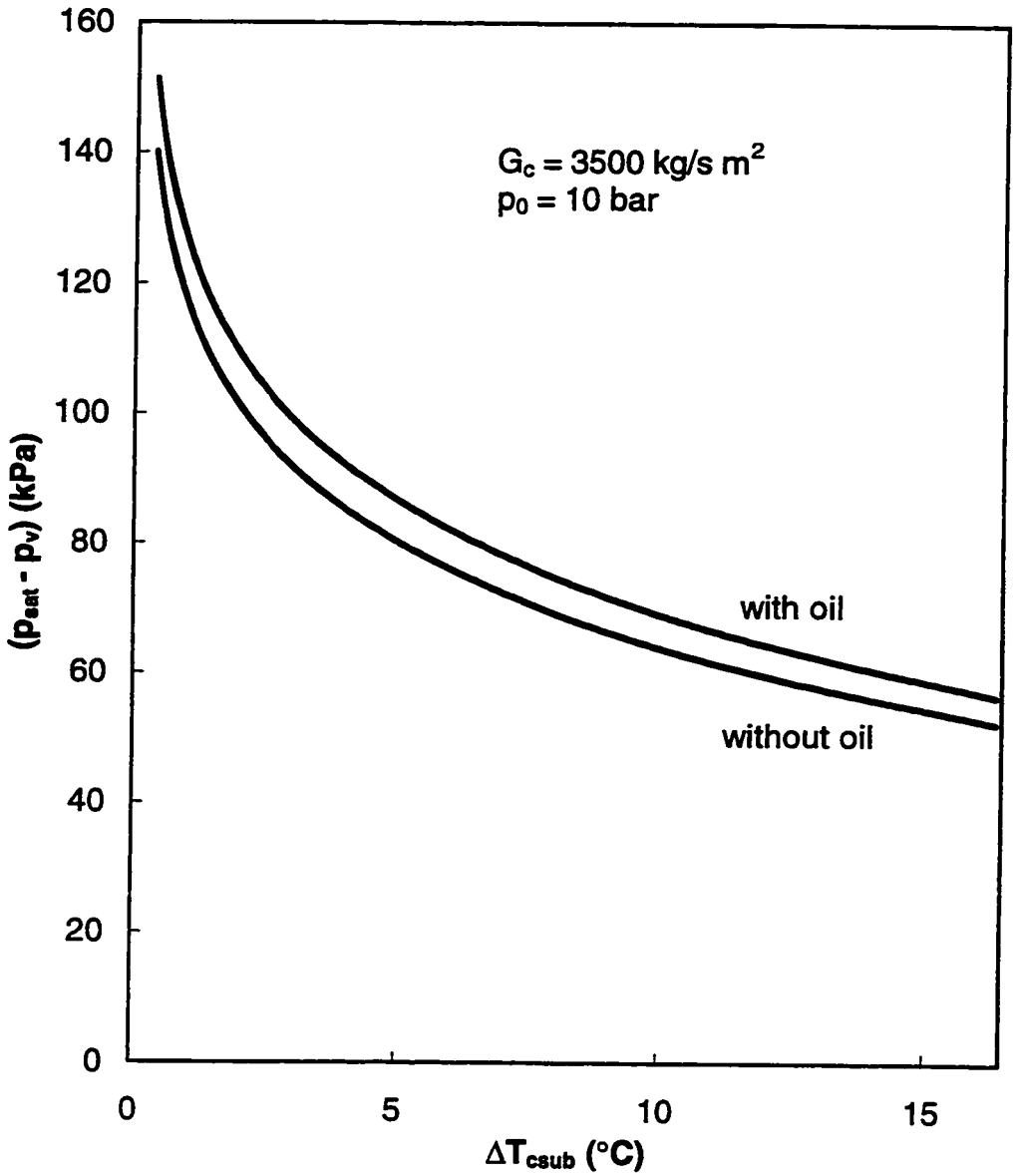

Figure 3.7 Effect of inlet subcooling temperature ΔT_{csub} on underpressure of vaporization, $(p_{sat} - p_v)$

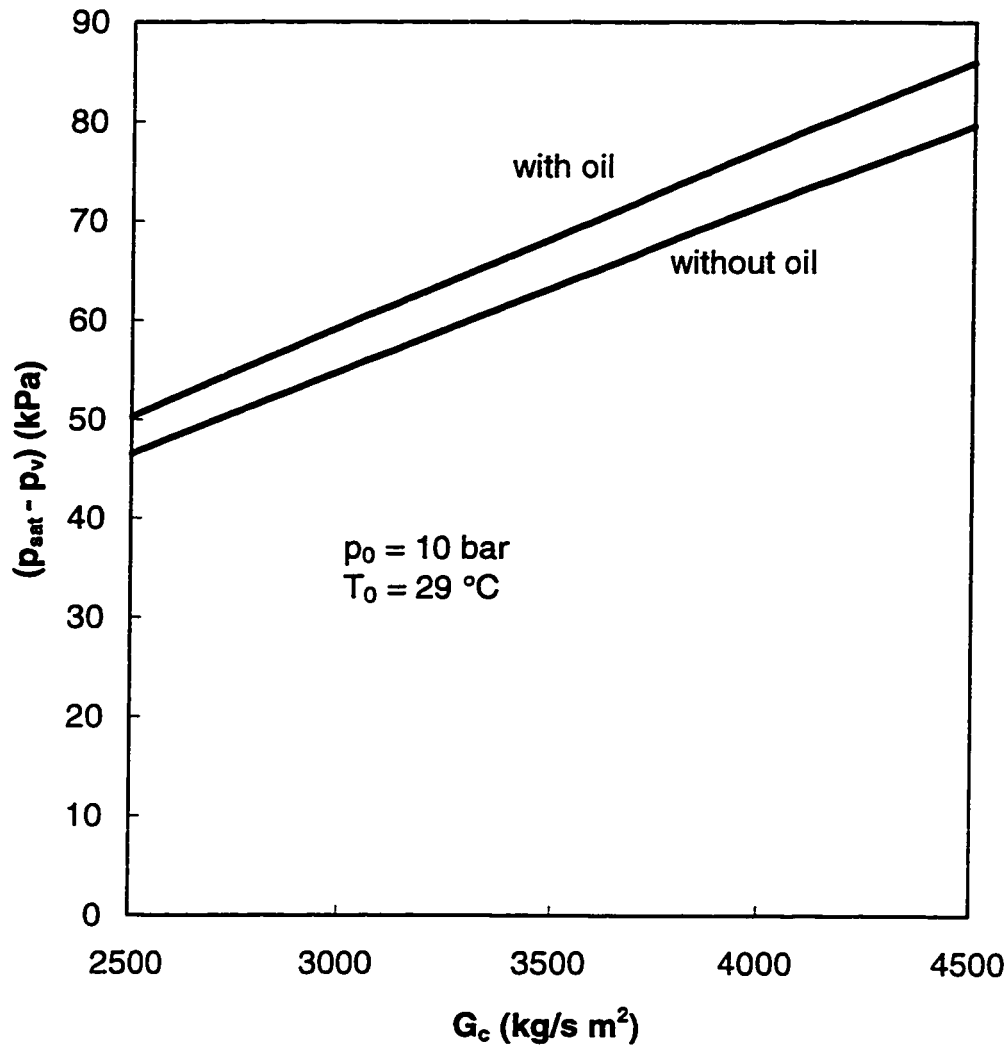

Figure 3.8 Effect of mass flux G_c on underpressure of vaporization, $(p_{sat} - p_v)$

increase in the diameter of the capillary tube. The experiments from both the glass capillary tubes and the copper capillary tubes (Li et al., 1990, Cooper et al., 1957 and Mikol and Dudley, 1964) also confirmed the result. The underpressure of vaporization decreases with an increase of the inlet subcooling and with a decrease of Re_c (or mass flux G_c) of refrigerant in the capillary tube. Figures 3.7 and 3.8 present the effects of the inlet subcooling temperature of the capillary tube, ΔT_{csub}, and the mass flux G_c on the underpressure of vaporization, (p_{sat} - p_v), respectively. Figure 3.7 shows that the underpressure of vaporization decreases non-linearly with an increase of the inlet subcooling temperature ΔT_{csub}. It decreases fast when the inlet subcooling temperature ΔT_{csub} is below 5 °C. Figure 3.8 shows that the underpressure of vaporization increases nearly linearly with the mass flux G_c. The underpressure of vaporization represents the thermal nonequilibrium which increases with a decrease of the inlet subcooling temperature ΔT_{csub}, and with an increase of the mass flux G_c.

It has been observed from the experiment that the underpressure of vaporization decreases with the increase of heat transfer between the capillary tube and suction line, because the enhancement of heat transfer corresponds to an increase of inlet subcooling of the refrigerant. If the mass flux G_c, the inlet pressure p_0 and the inlet temperature T_{c0} in the capillary tube are given, the underpressure of vaporization decreases with the increase of Nusselt number Nu_g of the vapor refrigerant in the suction line until the underpressure of vaporization is equal to zero (Figure 3.9).

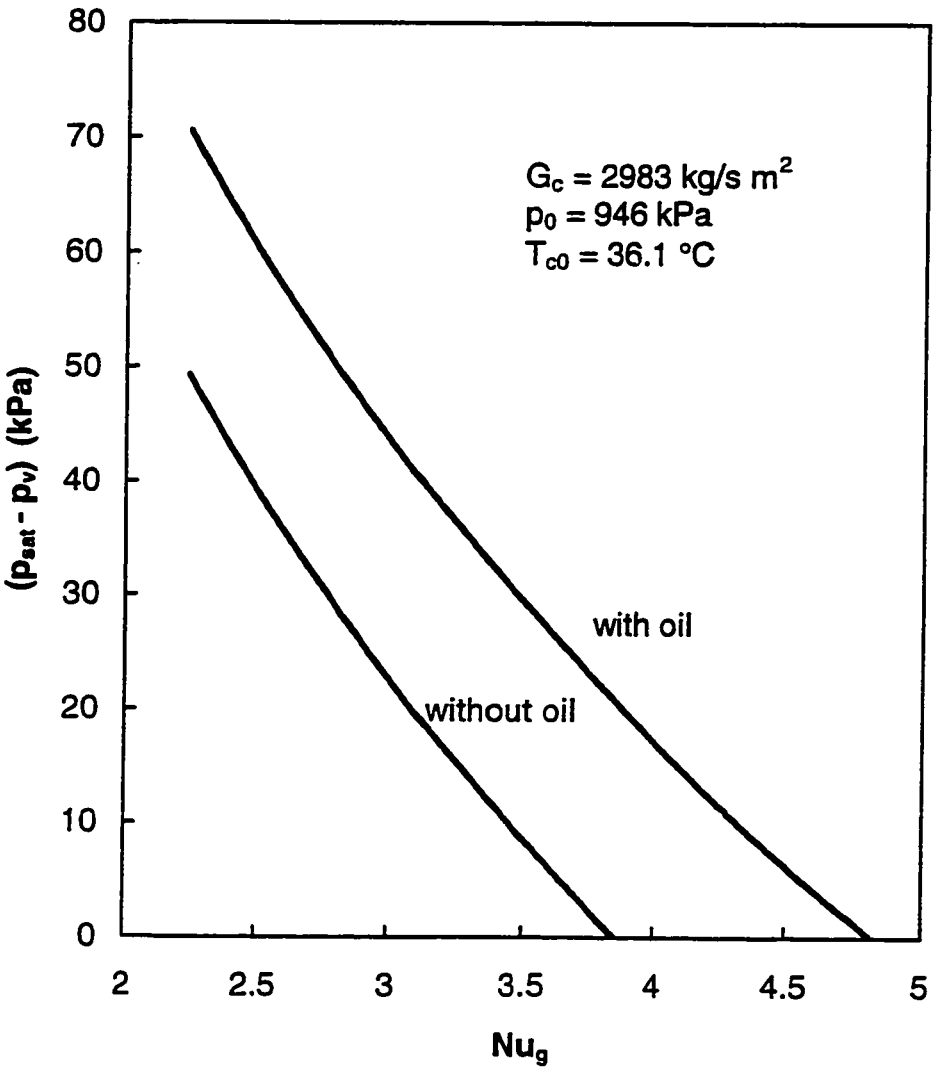

Figure 3.9 Effect of Nusselt number Nu_g of vapor refrigerant in the suction line on the underpressure of vaporization

When a refrigerant with oil flows through a capillary tube, it is expected that a thin oil film is formed on the capillary tube wall. The oil film decreases the real diameter of the capillary tube. The effect of oil in the refrigerant on the metastable flow in the capillary tube increases the underpressure of vaporization (Figures 3.7, 3.8 and 3.9).

The effects of the operating parameters on the underpressure of vaporization ($p_{sat} - p_v$) are summarized in Table (3.3).

Table 3.3 Effect of the operating parameters on the underpressure of vaporization

Parameters	underpressure of vaporization, ($p_{sat} - p_v$)
$G_c \uparrow$	$\uparrow$
$\Delta T_{csub} \uparrow$	$\downarrow$
$Nu_g \uparrow$	$\downarrow$
$D_c \uparrow$	$\downarrow$
with oil	$\uparrow$

Figure 3.10 compares the results predicted by Equation (3.93) with the experimental data. The relative standard error involved in Equation (3.93) is about 28%. The error is caused mainly by fluctuation and instability of the position of the inception of vaporization.

From Equations (3.93) and (3.94), we can see that the underpressure of vaporization is equal to zero when

$$\frac{\phi_1}{\phi_2} = 1 \tag{3.101}$$

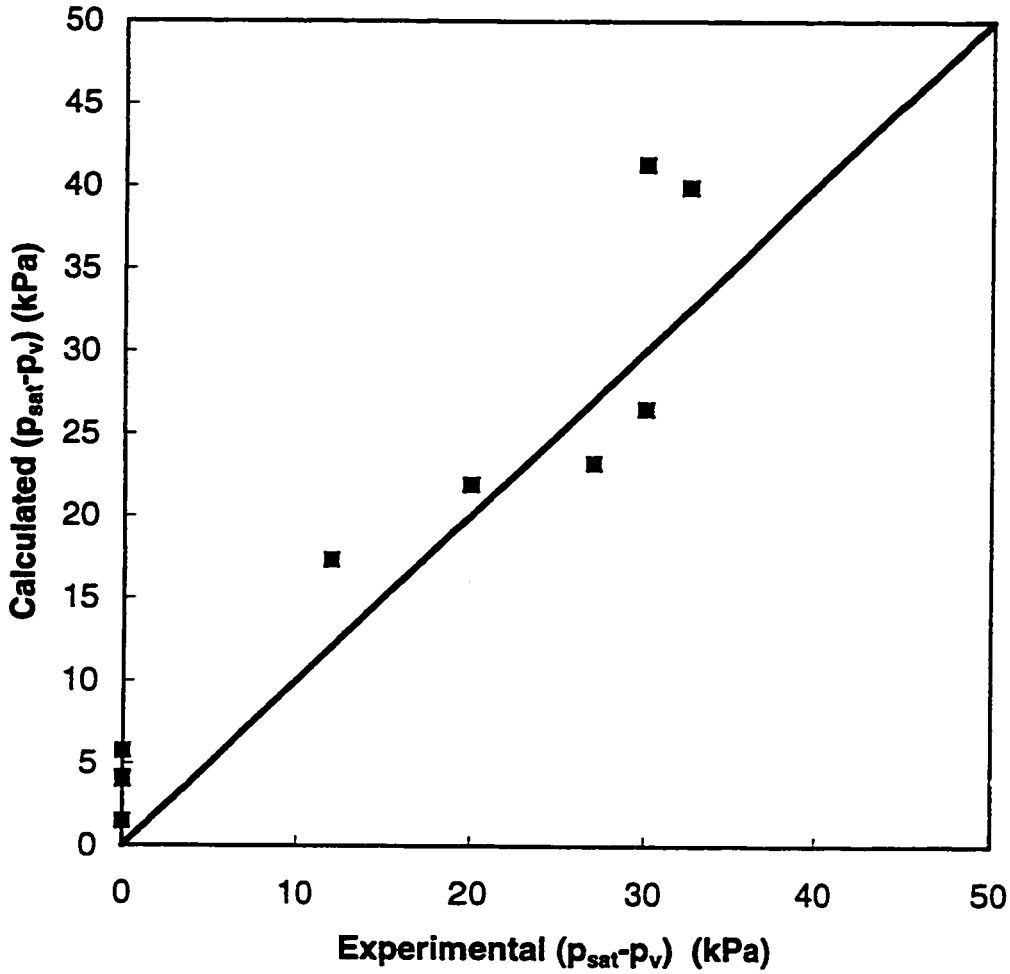

Figure 3.10 Comparison of experimental and calculated values for underpressure of vaporization

CHAPTER 4

NUMERICAL MODEL OF REFRIGERANT HFC-134a FLOW THROUGH A CAPILLARY TUBE

The objective of the numerical model is to model the liquid single-phase flow region and vapor-liquid two-phase flow region in a diabatic capillary tube. Using the model, variables such as pressure (p), temperature (T_c, T_w, T_s), velocity (V_{cg} and V_{cl}), quality (x) and void fraction (α) can be calculated over the length of the capillary tube. This requires that conditions be given at the inlet side of the capillary tube for the liquid single-phase flow region, and starting point for the vapor-liquid two-phase flow region. To calculate the pressure and temperature of the refrigerant in the capillary tube and suction line, and other unknowns, four governing differential equations for the liquid single-phase flow region, eight governing differential equations for the vapor-liquid two-phase flow region and various constitutive equations must be solved over the capillary tube length. It is important to note that this procedure is essentially an initial value and propagation problem since the model marches or propagates the solution from an initial position.

The numerical model consists of two parts: liquid single-phase flow numerical model and vapor-liquid two-phase flow numerical model, because the flow regions in the capillary tube are from subcooled liquid region to two-phase flow region (Figure 3.4). This Chapter is presented in three parts. The first part concerns the liquid single-phase flow numerical model, the second part is the vapor-liquid two-phase flow numerical model, and third part concerns a comparison of the numerical model results with experimental data and discussion.

4.1 The liquid single-phase flow numerical model

The liquid single-phase flow numerical model is presented in four parts as follows:

1. Assumptions;
2. Conservation equations;
3. Constitutive equations;
4. Solution procedure.

4.1.1 Assumptions

The liquid single-phase flow numerical model assumptions are based on the model that accurately simulates experimental tests. The following

assumptions are made for the liquid single-phase flow in a horizontal capillary tube-suction line:

1. Incompressible flow in the capillary tube and suction line, which is based on all liquid refrigerant flowing through the capillary tube and less than 300 Pa total pressure drop for HFC-134a vapor over the length of the suction line.

2. One dimensional steady state conditions, which is based on steady temperature and flow conditions in the capillary tube and suction line during experiments.

3. Uniform temperature of tube walls of capillary tube and suction line at any cross section. This assumption is based on the experimental setup. The setup was constructed such that the copper capillary tube and suction line were soldered together and wrapped in aluminum foil to ensure uniform temperature (Figure 2.7).

4.1.2 Conservation equations

For one dimensional steady state liquid single-phase flow in a capillary tube and refrigerant vapor flow in a suction line the conservation equations presented as follows (Fox and McDonald, 1985, and Pate, 1982):

i. Momentum equation for a capillary tube

The conservation equation of momentum can be expressed as:

$$\frac{d}{dz}(\rho_c V_{cl}^2) = -\frac{dp}{dz} - F_{wl} \tag{4.1}$$

where

$$\rho_l = \rho_l(T_c)$$

The term F_{wl} is the force due to the frictional pressure drop of liquid at the wall. F_{wl} can be expressed as (Li et al, 1990)

$$F_{wl} = -\frac{\lambda_l}{2}\frac{G_c^2}{2\rho_l f_0 D_c} \tag{4.2}$$

where f_0 is the cross-sectional factor of the tube which considers the effect of oil in the refrigerant. For the flow without oil, $f_0 = 1$; for the flow with oil, $f_0 < 1$. λ_l is the liquid frictional pressure drop coefficient.

ii. Energy equation for a capillary tube

For the liquid single-phase flow in a diabatic capillary tube the energy equation of the refrigerant can be written as:

$$\frac{d}{dz}(\rho_l V_{cl} h_l) = V_{cl}\frac{dp}{dz} - q \tag{4.3}$$

Where

$$h_l = h_l(T_c)$$

q is the energy convected to the wall, i.e.

$$q = \frac{4}{f_0 D_c}\bar{h}_l(T_c - T_w) \tag{4.4}$$

where $\bar{h}_l$ is the average convective heat transfer coefficient of refrigerant liquid in the capillary tube.

iii. Heat balance equation in suction line

The heat transfer between the refrigerant vapor and suction line wall is evaluated by the equation:

$$\frac{dT_s}{dz} = \frac{\bar{h}_g \pi D_s}{c_{ps} M_s}\left(T_w - T_s\right) \tag{4.5}$$

where $\bar{h}_g$ is the average convective heat transfer coefficient of refrigerant vapor in the suction line.

iv. Heat balance equation between capillary tube and suction line

The heat transfer between capillary tube and suction line can be described by the following equation

$$\bar{h}_l \pi D_c\left(\frac{dT_c}{dz} - \frac{dT_w}{dz}\right) - \bar{h}_g \pi D_s\left(\frac{dT_w}{dz} - \frac{dT_s}{dz}\right) - q_{amb} = 0 \tag{4.6}$$

where q_{amb} is the heat loss per unit length of the capillary tube and suction line which can be calculated by Equation (2.1).

The system of Equations (4.1), (4.3), (4.5) and (4.6) represents the liquid single-phase flow in a diabatic capillary tube, which has to be solved for the four unknowns: T_c, T_s, T_w and p. However, the values of λ_l, $\bar{h}_l$ and $\bar{h}_g$ are also unknown. These have to be solved through the constitutive equations. The thermodynamic properties ρ_l (T) and h_l (T) can be determined from the ASHRAE Handbook -- fundamentals.

For an adiabatic capillary tube there is no heat transfer from the capillary tube to suction line. The system of the above equations can be simplified as follows

$$\frac{d}{dz}\left(\rho_l V_{cl}^2\right) = -\frac{dp}{dz} - F_{wl} \tag{4.7}$$

$$\frac{d}{dz}\left(\rho_l V_{cl} h_l\right) = V_{cl}\frac{dp}{dz} \tag{4.8}$$

4.1.3 Constitutive equations

i. Liquid frictional pressure drop coefficient λ_l in Equation (4.2)

A capillary tube can not be considered smooth for friction factor considerations because of its small diameter (0.6 mm for this study). As such, the wall roughness must be accounted for. Lin et al. (1991) from their experiment recommended Churchill's equation (1977) for the determination of the coefficient of frictional pressure drop, i.e.

$$\lambda_l = 8\left[\left(\frac{8}{\mathrm{Re}_l}\right)^{12} + \frac{1}{\left(A_l + B_l\right)^{2/3}}\right]^{1/12} \tag{4.9}$$

In the above equation,

$$A_l = \left\{2.457 \ln\left[\frac{1}{\left(7/\mathrm{Re}_l\right)^{0.9} + 0.27\varepsilon / f_0 D_c}\right]\right\}^{16} \tag{4.10}$$

$$B_l = \left(\frac{37530}{\mathrm{Re}_l}\right)^{16} \tag{4.11}$$

and

$$\mathrm{Re}_l = \frac{f_0 D_c G_c}{\mu_l} \tag{4.12}$$

where ε is the roughness of the wall, D_c is the diameter of the capillary tube and μ_l is the viscosity of the refrigerant liquid.

ii. Average convective heat transfer coefficient of refrigerant liquid in the capillary tube, $\bar{h}_l$, in equation (4.4 and 4.6)

The convective heat transfer coefficient of refrigerant liquid in a capillary tube was not verified experimentally. Pate (1982) recommended the Dittus-Boelter (1930) relation to define the convective heat transfer. Even though it was originally derived for smooth tubes, it has been frequently applied to a variety of tube wall conditions. It is:

$$Nu_l = 0.023\,\mathrm{Re}_l^{0.8}\,\mathrm{Pr}_l^{0.3} \tag{4.13}$$

where

$$\mathrm{Nu}_l = \frac{f_0 D_c \bar{h}_l}{k_l} \tag{4.14}$$

iii. Average convective heat transfer coefficient of refrigerant vapor in the suction line, $\bar{h}_g$, in equation (4.5 and 4.6)

After comparing with the experimental data (Pate, 1982), the Colburn (1933) equation for convective heat transfer which is based on the Reynolds

analogy between heat transfer and a smooth friction factor is used in the suction line as follows:

$$Nu_g = 0.0395 \mathrm{Re}_g^{0.8} \mathrm{Pr}_g^{0.333} \tag{4.15}$$

where

$$\mathrm{Nu_g} = \frac{\mathrm{D_s}\,\bar{\mathrm{h}}_\mathrm{g}}{\mathrm{k_g}} \tag{4.16}$$

4.1.4 Solution procedure

The system of equations describing the liquid single-phase flow in a capillary tube can be written in the following form

$$\begin{pmatrix} A_{11} & \cdots & \cdots & A_{14} \\ \vdots & \ddots & & \vdots \\ \vdots & & \ddots & \vdots \\ A_{41} & \cdots & \cdots & A_{44} \end{pmatrix} \begin{pmatrix} dT_c / dz \\ dp / dz \\ dT_s / dz \\ dT_w / dz \end{pmatrix} = \begin{pmatrix} B_1 \\ B_2 \\ B_3 \\ B_4 \end{pmatrix} \tag{4.17}$$

where A_{ij} and B_i (i, j = 1, 2, 3, 4) are the coefficients of the matrix and vector, i.e.,

$$A_{11} = V_{cl} \frac{d\rho_l}{dT_c}$$

$A_{12} = 1$

$A_{13} = A_{14} = 0$

$$A_{21} = V_{cl}\left(h_l \frac{d\rho_l}{dT_c} + \rho_l \frac{dh_l}{dT_c} \right)$$

$A_{22} = - V_{cl}$

$A_{23} = A_{24} = 0$

$A_{31} = A_{32} = A_{34} = 0$

$A_{33} = 1$

$$A_{41} = \pi \bar{h}_l f_0 D_c$$

$A_{42} = 0$

$$A_{43} = \pi \bar{h}_g D_s$$

$$A_{44} = -\pi\left(\bar{h}_l f_0 D_c + \bar{h}_g D_s\right)$$

$$B_1 = -\frac{\lambda_1}{2}\frac{G_c^2}{2\rho_l f_0 D_c}$$

$$B_2 = -\frac{4}{f_0 D_c}\bar{h}_l\left(T_c - T_w\right)$$

$$B_3 = \frac{\bar{h}_g \pi D_s}{c_{ps} M_s}\left(T_w - T_s\right)$$

$B_4 = q_{amb}$

The solution of the decision variables, dT_c/dz, dp/dz, dT_s/dz and dT_w/dz, can be solved by utilizing the initial conditions at the inlet side of the capillary tube and the mass fluxes in the capillary tube and suction line, G_c and G_s. Then the numerical integration is accomplished by the Runge-Kutta method,

4.2 Vapor-liquid two-phase flow numerical model

The vapor-liquid two-phase flow numerical model is presented in six parts:

1. Assumptions;

2. Conservation equations;

3. Constitutive equations;

4. Position of the inception of vaporization;

5. Initial conditions;

6. Solution procedure.

4.2.1 Assumptions

All of the assumptions, except for one, listed in Section 4.1.1 of the liquid single-phase flow numerical model are applicable to the vapor-liquid two-phase flow region. The one exception is incompressible flow assumption in the capillary tube.

Several new assumptions that are applicable to the vapor-liquid two-phase flow region only are also introduced as follows:

1. In each phase and at any cross section of a capillary tube the velocities are uniform;

2. At any cross section of the tube the pressure is uniform.

With these assumptions, the model can be presented by the following sections.

4.2.2 Conservation equations

For one dimensional steady-state vapor-liquid two-phase flow in a capillary tube and suction line the conservation equations presented follow the

works of Chen and Lin (1996), Elias and Lellouche (1994 and 1984), Li et al. (1990), Ewan and Moodie (1990), Dobran (1987), Richter (1983) and Pate (1982).

i. Continuity equations for a capillary tube:

The conservation equations of mass can be expressed as:

For the vapor phase,

$$\rho_g V_{cg} \frac{d\alpha}{dz} + \alpha V_{cg} \frac{d\rho_g}{az} + \alpha \rho_g \frac{dV_{cg}}{dz} - G_c \frac{dx}{dz} = 0 \qquad (4.18)$$

where

$$\rho_g = \rho_g(p)$$

For the liquid phase,

$$-\rho_l V_{cl} \frac{d\alpha}{dz} + (1-\alpha) V_{cl} \frac{d\rho_l}{dz} + (1-\alpha)\rho_l \frac{dV_{cl}}{dz} + G_c \frac{dx}{dz} \qquad (4.19)$$

where

$$\rho_l = \rho_l(T_c)$$

ii. Momentum equations for the capillary tube:

The conservation equations of momentum are written in the following form:

For the vapor phase,

$$xG_c\frac{dV_{cg}}{dz}=-\alpha\frac{dp}{dz}-F_{gl}-F_{wg}-\eta(V_{cg}-V_{cl})G_c\frac{dx}{dz} \tag{4.20}$$

For the liquid phase,

$$(1-x)G_c\frac{dV_{cl}}{dz}=-(1-\alpha)\frac{dp}{dz}+F_{gl}-F_{wl}-(1-\eta)(V_{cg}-V_{cl})G_c\frac{dx}{dz} \tag{4.21}$$

The terms F_{wg} and F_{wl} are the forces due to the frictional pressure drops of vapor and liquid at the wall, respectively. In this study it is assumed that only the liquid phase contacts with the wall and F_{wg} may be neglected. F_{wl} can then be expressed as (Li et al., 1990)

$$F_{wl}=-\frac{\lambda_t}{2}\frac{G_c^2}{2\rho_l f_0 D_c} \tag{4.22}$$

where λ_t is the two-phase frictional pressure drop coefficient.

In equations (4.20) and (4.21) the coefficient η evaluates the momentum exchange caused by the mass transfer (evaporation). The value of the coefficient $\eta\approx0.5$ is used in the present paper following the work of Richter (1983).

iii. Energy equation of mixture for a capillary tube:

For the vapor-liquid two-phase flow in a diabatic capillary tube the energy equation of the mixture can be written as:

$$G_c[h_{gl}+\frac{1}{2}(V_{cg}^2-V_{cl}^2)]\frac{dx}{dz}+xG_c(\frac{dh_g}{dz}+V_{cg}\frac{dV_{cg}}{dz})+(1-x)G_c(\frac{dh_l}{dz}+V_{cl}\frac{dV_{cl}}{dz})=-q \tag{4.23}$$

where

$$h_g=h_g(p)$$

$$h_l=h_l(T_c)$$

and

$$h_{gl}=h_g-h_l \tag{4.24}$$

The q is the energy convected to the wall which can be determined by following Equation:

$$q=\frac{4}{f_0 D_c}\bar{h}_t(T_c-T_w) \tag{4.25}$$

where $\bar{h}_t$ is the average convective heat transfer coefficient of vapor-liquid two-phase flow in the capillary tube.

iv. Heat balance equation between the liquid and vapor phases:

The heat transfer between the liquid and vapor phases due to evaporation is evaluated by the equation:

$$G_c[h_{gl}+\frac{1}{2}(V_{cg}^2-V_{cl}^2)]\frac{dx}{dz}=\bar{h}_{inter}\,a[T_c-T_{csat}(p)] \tag{4.26}$$

where $\bar{h}_{inter}$ is the average interfacial heat transfer coefficient.

v. Heat transfer equation in suction line

The heat transfer between the refrigerant vapor and suction line wall is evaluated by the equation:

$$\frac{dT_s}{dz} = \frac{\bar{h}_g \pi D_s}{c_{ps} M_s}(T_w - T_s) \tag{4.27}$$

vi. Heat balance equation in capillary tube - suction line

The heat transfer between capillary tube and suction line can be described by the following equation

$$\bar{h}_t \pi D_c\left(\frac{dT_c}{dz} - \frac{dT_w}{dz}\right) - \bar{h}_g \pi D_s\left(\frac{dT_w}{dz} - \frac{dT_s}{dz}\right) - q_{amb} = 0 \tag{4.28}$$

The system of Equations (4.18) - (4.21), (4.23) and (4.26) - (4.28) represents the vapor-liquid two-phase flow in a diabatic capillary tube, which has to be solved for the eight unknowns: α, x, V_{cg}, V_{cl}, p, T_c, T_s and T_w. However, the values of F_{gl}, λ_t, $\bar{h}_{inter}$ and $\bar{h}_t$ are also unknown. These have to be solved by the constitutive equations. The thermodynamic properties ρ_g (p), ρ_l (T), h_g (p) and h_l (T) can be also determined from the ASHRAE Handbook -- Fundamentals (1993).

For an adiabatic capillary tube the system equations of above can be simplified as follows

$$\rho_g V_{cg}\frac{d\alpha}{dz}+\alpha V_{cg}\frac{d\rho_g}{dz}+\alpha\rho_g\frac{dV_{cg}}{dz}-G_c\frac{dx}{dz}=0 \tag{4.29}$$

$$-\rho_l V_{cl}\frac{d\alpha}{dz}+(1-\alpha)V_{cl}\frac{d\rho_l}{dz}+(1-\alpha)\rho_l\frac{dV_{cl}}{dz}+G_c\frac{dx}{dz} \tag{4.30}$$

$$xG_c\frac{dV_{cg}}{dz}=-\alpha\frac{dp}{dz}-F_{gl}-F_{wg}-\eta(V_{cg}-V_{cl})G_c\frac{dx}{dz} \tag{4.31}$$

$$(1-x)G_c\frac{dV_{cl}}{dz}=-(1-\alpha)\frac{dp}{dz}+F_{gl}-F_{wl}-(1-\eta)(V_{cg}-V_{cl})G_c\frac{dx}{dz} \tag{4.32}$$

$$[h_{gl}+\frac{1}{2}(V_{cg}^2-V_{cl}^2)]\frac{dx}{dz}+x(\frac{dh_g}{dz}+V_{cg}\frac{dV_{cg}}{dz})+(1-x)(\frac{dh_l}{dz}+V_{cl}\frac{dV_{cl}}{dz})=0 \tag{4.33}$$

$$G_c[h_{gl}+\frac{1}{2}(V_{cg}^2-V_{cl}^2)]\frac{dx}{dz}=\bar{h}_{interface}[T_c-T_{csat}(p)] \tag{4.34}$$

4.2.3 Constitutive equations

Constitutive equations are dependent on the flow regimes and their transition taking place in a capillary tube. The flow regimes may be simplified as: bubble, churn-turbulence and annular flows (Barnea et al., 1983). In the present study it is estimated by comparison of numerical results with experimental data that the transition from bubble to churn-turbulence occurs at α = 0.05, and the transition from churn-turbulence to annular at α = 0.75. The following are the constitutive equations.

i. Interfacial drag force F_{gl} in Equations (4.20) and (4.21):

The interfacial drag force F_{gl} is well known for the bubble and annular flow regimes. For the churn-turbulent flow it can be interpolated linearly with the void fraction α between the bubble flow regime and the annular flow regime. The general equation for the interfacial drag force can be expressed by (Richter, 1983 and Dagan, 1993)

$$F_{gl} = \frac{2Cf}{f_0 D_c}\sqrt{\alpha}\rho_g (V_{cg} - V_{cl})\left|V_{cg} - V_{cl}\right| + C\alpha\rho_l V_{cg}\frac{d}{dz}(V_{cg} - V_{cl}) \qquad (4.35)$$

where the constant C = 0.5 is used in this model (Richter, 1983). Cf is the interfacial friction coefficient and is given as follows

$$Cf = C_D\sqrt{\alpha}(1-\alpha)^{-1.7}\frac{\rho_l}{\rho_g}\frac{f_0 D_c}{d} \qquad 0<\alpha\le 0.05 \qquad (4.36)$$

$$Cf = Cf_{\alpha=0.05} - \left(\frac{Cf_{\alpha=0.05} - Cf_{\alpha=0.75}}{0.7}\right)(\alpha - 0.05) \qquad 0.05<\alpha<0.75 \qquad (4.37)$$

$$Cf = 0.005[1 + 75(1-\alpha)] \qquad 0.75\le\alpha<1 \qquad (4.38)$$

where C_D is the drag coefficient for a bubble and is determined by

$$C_D = \frac{24}{\mathrm{Re}}(1 + 0.15\mathrm{Re}^{0.687}) \qquad \mathrm{Re}\le 1000 \qquad (4.39)$$

$$C_D = 0.44 \qquad \mathrm{Re} > 1000 \qquad (4.40)$$

The Reynolds number Re is defined as follows

$$\mathrm{Re} = \frac{\rho_l d(1-\alpha)\left|V_{cg} - V_{cl}\right|}{\mu_l}$$

where d is the average bubble diameter, which can be determined from the interfacial area, a, per unit volume, i.e.,

$$d = \frac{6\alpha}{a} \tag{4.41}$$

The interfacial area, a, can be calculated for the different flow regimes (Dobran, 1987)

$$a = N_R \pi \left(\frac{6\alpha}{N_R \pi}\right)^{2/3} \qquad 0 < \alpha \le 0.05 \tag{4.42}$$

$$a = a_{\alpha=0.05} - \left(\frac{a_{\alpha=0.05} - a_{\alpha=0.75}}{0.7}\right)(\alpha - 0.05) \qquad 0.05 < \alpha < 0.75 \tag{4.43}$$

$$a = \frac{4}{f_0 D_c}\sqrt{\alpha} \qquad 0.75 \le \alpha < 1 \tag{4.44}$$

where N_R is the bubble density which can be obtained by the Equation (3.68):

$$N_R = \left(\frac{N_A}{v_l}\right)^{\frac{2}{3}} \frac{B}{V_{cl}} \left\{ \frac{p_{sat} - p_v}{\left(\frac{\partial p}{\partial z}\right)_f} \left[\exp(-\eta\phi) - \sqrt{\pi\eta\phi}\, erfc\left(\sqrt{\eta\phi}\right)\right] + \int_{T_{csat}}^{T_\infty} \frac{1}{\bar{A} - \bar{B}T_c} \exp\left(-\frac{T_{cv}\eta\phi}{T_c}\right) dT_c \right\} \tag{4.45}$$

where the factor (p_{sat} - p_v) represents the underpressure of vaporization, which can be determined by the Equations (3.93) to (3.96):

$$\frac{(p_{sat} - p_v)\sqrt{KT_{cv}}}{\sigma^{\frac{3}{2}}} = 0.658\left(\frac{\rho_l}{\rho_l - \rho_g}\right)\phi \tag{4.46}$$

where

$$\phi = \phi_1 - \phi_2 \tag{4.47}$$

$$\phi_1 = 1.032\,\mathrm{Re}_c^{0.914}\left(\frac{\Delta T_{csub}}{T_{cri}}\right)^{-0.208}\left(\frac{f_0 D_c}{D'}\right)^{-3.18} \tag{4.48}$$

$$\phi_2 = 0.0122\,\mathrm{Re}_s^{0.234}\left(1-\frac{p_{sat}}{p_{sat0}}\right)^{0.957} \tag{4.49}$$

where ΔT_{csub} is the inlet subcooling of the capillary tube, and D' is a reference length which is defined as:

$$D' = \sqrt{\frac{k_l T_{csat}}{\sigma}} \times 10^4 \tag{4.50}$$

ii. Two-phase frictional pressure drop coefficient λ_t in Equation (4.22):

From the research of Lin et al (1990), it is known that for the vapor-liquid two-phase flow of refrigerant passing through capillary tubes, the frictional pressure drop coefficient, λ_t, is dependent on the relative roughness, ε/D_c, the Reynolds number, Re_t, and the quality, x, which can be expressed by

$$\lambda_t = \lambda_l \phi_{lo}^2 \tag{4.51}$$

where λ_l is the liquid frictional pressure drop coefficient which can be calculated from Equation (4.9). ϕ_{lo}^2 is the multiplier for the two-phase flow which can be expressed by

$$\phi_{l0}^2 = \left(\frac{A_l + B_l}{A_t + B_t}\right)^{1/8}\left[1 + x\left(\frac{\rho_l}{\rho_g} - 1\right)\right] \tag{4.52}$$

where

$$A_t = \left\{ 2.457 \ln \left[\frac{1}{(7/\mathrm{Re}_t)^{0.9} + 0.27\varepsilon / f_0 D_c} \right] \right\}^{16} \tag{4.53}$$

$$B_t = \left(\frac{37530}{\mathrm{Re}_t} \right)^{16} \tag{4.54}$$

$$\mathrm{Re}_t = \frac{f_0 D_c G_c}{\mu_t} \tag{4.55}$$

and

$$\mu_t = \frac{\mu_l \mu_g}{\mu_g + x^{1.4}(\mu_l - \mu_g)} \tag{4.56}$$

In Equation (4.56), x is the local quality value.

iii. Interfacial heat transfer coefficient $\bar{h}_{inter}$ in Equation (4.26):

The interfacial heat transfer coefficient $\bar{h}_{inter}$ is modeled as follows (Dobran, 1987)

$$\mathrm{Nu}_{inter} = \frac{\bar{h}_{inter}\, d}{k_l} = 2 + 0.6\, \mathrm{Re}_b^{1/2}\, \mathrm{Pr}_l^{1/3} \qquad 0 < \alpha \le 0.05 \tag{4.57}$$

$$\bar{h}_{inter} = \bar{h}_{inter,\alpha=0.05} - \frac{\bar{h}_{inter,\alpha=0.05} - \bar{h}_{inter,\alpha=0.75}}{0.7}(\alpha - 0.05)$$

$$0.05 < \alpha < 0.75 \tag{4.58}$$

$$Nu_{inter} = \frac{\bar{h}_{inter} f_0 D_c \sqrt{\alpha}}{k_g} = 0.023 Re_g^{0.8} Pr_g^{0.4} \qquad 0.75 \le \alpha < 1 \qquad (4.59)$$

The Reynolds numbers in the above are given as

$$Re_b = \frac{\rho_l d |V_{cg} - V_{cl}|}{\mu_l} \qquad (4.60)$$

$$Re_g = \frac{\rho_g f_0 D_c \sqrt{\alpha}}{\mu_g} |V_{cg} - V_{cl}| \qquad (4.61)$$

iv. Average convective heat transfer coefficient of vapor-liquid two-phase flow, $\bar{h}_t$ (in Equation 4.25 and 4.28):

Based on an extension of a concept which states that in two-component bubbly flow the heat transfer is determined by the liquid phase and the only effect of the vapor phase is to increase the liquid velocity (Collier, 1972), the following relation is used in the model (Pate, 1982 and Cui et al, 1993)

$$Nu_t = 0.023 Re_l^{0.8} Pr_l^{0.3} \left(\frac{1-x}{1-\alpha} \right)^{0.8} \qquad (4.62)$$

where

$$Nu_t = \frac{f_0 D_c \bar{h}_t}{k_l} \qquad (4.63)$$

4.2.4 Position of the inception of vaporization

If vaporization of a refrigerant in a capillary tube is in the thermodynamic equilibrium condition, the position of inception can be determined at the saturated flow condition. However, due to the presence of metastable flow, the location of the inception of vaporization has to take account of metastable flow length.

The position of the inception, z_v, is presented by

$$z_v = z_{sat} + \Delta z_{sv} \tag{4.64}$$

Where z_{sat} is the position of the liquid refrigerant at the thermodynamic equilibrium saturated state and Δz_{sv} is the length of the metastable flow. According to the expression for the liquid frictional pressure drop (Equation 4.2), z_{sat} and Δz_{sv} can be expressed as

$$z_{sat} = \frac{2 f_o D_c (p_0 - p_{sat})}{\lambda_l \rho_l V_{cl}^2} \tag{4.65}$$

$$\Delta z_{sv} = \frac{2 f_o D_c (p_{sat} - p_v)}{\lambda_l \rho_l V_{cl}^2} \tag{4.66}$$

Substituting the above into Equation (4.64) yields

$$z_v = \frac{2 f_0 D_c}{\lambda_l \rho_l V_{cl}^2} \left[(p_0 - p_{sat}) + (p_{sat} - p_v) \right] \tag{4.67}$$

The pressure difference between the inlet of the capillary tube and the saturated point, (p_0 - p_{sat}), can be calculated using the liquid single-phase flow model. The pressure difference between the saturated point and the inception, (p_{sat} - p_v), can be determined by Equation (4.46).

4.2.5. Initial conditions

The flashing problem in the capillary tube starts from z_v. It is considered that conditions at z_v are the initial conditions for the vapor-liquid two-phase flow model which include the void fraction α_i, the quality x_i, the liquid-phase velocity V_{cli}, the vapor-phase velocity V_{cgi}, the pressure in the capillary tube, p, the temperature of refrigerant in the capillary tube, T_c, the temperature of the refrigerant vapor in the suction line, T_s and the wall temperature T_w. Among them, V_{cli}, p, T_c, T_s and T_w are determined from the liquid single-phase flow model.

1. Initial void fraction α_i

In the nucleation region, if the same velocities of liquid and vapor phases are assumed, the initial void fraction is (Dobran, 1987)

$$\alpha_i = \frac{\pi}{6} N_R d_i^3 \tag{4.68}$$

where the bubble density N_R is given by Equation (4.45), and the initial diameter of nucleation, d_i, can be determined by the Laplace equation (Cole, 1974)

$$d_i = \frac{4\sigma}{p_{sat} - p_v} \tag{4.69}$$

2. Initial quality x_i from the definition of quality

$$x_i = \frac{\alpha \rho_{gi} V_{cgi}}{G_c} \tag{4.70}$$

3. Initial vapor-phase velocity V_{cgi}:

It is assumed that at the position, $z = z_v$, the vapor velocity V_{cgi} is equal to the liquid velocity V_{cli}.

$$V_{cgi} = V_{cli} \tag{4.71}$$

4.2.6 Solution procedure

The system of equations (Equations 4.18-4.21, 4.23 and 4.26-4.28) describing the vapor-liquid two-phase flow in a diabatic capillary tube can be written in the following form

$$\begin{pmatrix} A_{11} & A_{12} & \cdots & \cdots & \cdots & \cdots & \cdots & A_{18} \\ A_{21} & \ddots & & & & & & \vdots \\ \vdots & & \ddots & & & & & \vdots \\ \vdots & & & \ddots & & & & \vdots \\ \vdots & & & & \ddots & & & \vdots \\ \vdots & & & & & \ddots & & \vdots \\ \vdots & & & & & & \ddots & \vdots \\ A_{81} & \cdots & \cdots & \cdots & \cdots & \cdots & \cdots & A_{88} \end{pmatrix} \begin{pmatrix} dT_c / dz \\ dp / dz \\ dT_s / dz \\ dT_w / dz \\ dV_{cl} / dz \\ dV_{cg} / dz \\ d\alpha / dz \\ dx / dz \end{pmatrix} = \begin{pmatrix} B_1 \\ B_2 \\ B_3 \\ B_4 \\ B_5 \\ B_6 \\ B_7 \\ B_8 \end{pmatrix} \tag{4.72}$$

where A_{ij} and B_i (I, j = 1, 2, ..., 8) are the coefficients of the matrix and vector, i.e.,

$$A_{11} = A_{13} = A_{14} = A_{15} = 0$$

$$A_{12} = \alpha V_{cg} \frac{d\rho_g}{dp}$$

$$A_{16} = \alpha\rho_g$$

$$A_{17} = \rho_g V_{cg}$$

$$A_{18} = - G_c$$

$$A_{21} = (1-\alpha) V_{cl} \frac{d\rho_l}{dT_c}$$

$$A_{22} = A_{23} = A_{24} = A_{26} = 0$$

$$A_{25} = (1 - \alpha)\rho_l$$

$$A_{27} = - \rho_l V_{cl}$$

$$A_{28} = G_c$$

$$A_{31} = A_{33} = A_{34} = A_{37} = 0$$

$$A_{32} = \alpha$$

$$A_{35} = - C\alpha\rho_l V_{cg}$$

$$A_{36} = xG_c + C\alpha\rho_l V_{cg}$$

$$A_{38} = \eta(V_{cg} - V_{cl})G_c$$

$$A_{41} = A_{43} = A_{44} = A_{47} = 0$$

$$A_{42} = 1 - \alpha$$

$A_{45} = G_c(1 - x) + C\alpha\rho_l V_{cg}$

$A_{46} = - C\alpha\rho_l V_{cg}$

$A_{48} = (1 - \eta)(V_{cg} - V_{cl})G_c$

$$A_{51} = (1-x)G_c \frac{dh_l}{dT_c}$$

$$A_{52} = xG_c \frac{dh_g}{dp}$$

$A_{53} = A_{54} = A_{57} = 0$

$A_{55} = (1 - x)G_c V_{cl}$

$A_{56} = xG_c V_{cg}$

$$A_{56} = G_c[h_{gl} + \frac{1}{2}(V_{cg}^2 - V_{cl}^2)]$$

$A_{61} = A_{62} = A_{63} = A_{64} = A_{65} = A_{66} = A_{67} = 0$

$$A_{68} = G_c[h_{gl} + \frac{1}{2}(V_{cg}^2 - V_{cl}^2)]$$

$A_{71} = A_{72} = A_{74} = A_{75} = A_{76} = A_{77} = A_{78} = 0$

$A_{73} = 1$

$$A_{81} = \pi\, \bar{h}_t\, f_0 D_c$$

$A_{82} = A_{85} = A_{86} = A_{87} = A_{88} = 0$

$$A_{83} = \bar{h}_g\, \pi D_s$$

$$A_{84} = -\pi\left(\bar{h}_t\, f_0 D_c + \bar{h}_g\, D_s\right)$$

$B_1 = B_2 = 0$

$$B_3 = -\frac{2Cf}{f_0 D_c}\sqrt{\alpha}\,\rho_g (V_{cg} - V_{cl})\left|V_{cg} - V_{cl}\right|$$

$$B_4 = -\frac{2Cf}{f_0 D_c}\sqrt{\alpha}\,\rho_g (V_{cg} - V_{cl})\left|V_{cg} - V_{cl}\right| - F_{wl}$$

$B_5 = -q$

$$B_6 = \bar{h}_{inter}\, a[T_c - T_{sat}(p)]$$

$$B_7 = \frac{\bar{h}_g}{c_{ps}\pi D_s G_s}(T_w - T_s)$$

$B_8 = q_{amb}$

The solution of the decision variables, dT_c/dz, dp/dz, dT_s/dz, dT_w/dz, dV_{cl}/dz, dV_{cg}/dz, $d\alpha/dz$ and dx/dz can be solved by utilizing the initial conditions the mass fluxes, G_c and G_c, and the calculated results at z_v from the subcooled liquid model. Then the numerical integration is accomplished by the Runge-Kutta method.

4.3 Numerical results and discussion

4.3.1 Numerical results and discussion for the diabatic capillary tube

Figures 4.1, 4.2 and 4.3 show the comparisons of experimental and numerical results on the distributions of the measured pressure and saturated pressure corresponding to the measured temperature of the refrigerant along the capillary tube for three different inlet conditions which may be classified by weak heat transfer between the capillary tube and the suction line for $G_c/G_s = 251$ and 77.8, and strong heat transfer between them for $G_c/G_s = 47.7$. It can be seen from the figures that the vapor-liquid two-phase flow of the refrigerant in the capillary tube can be satisfactorily modeled. The curves of the saturated pressure at the first 0.14 m in the figures are nearly constant because there is an adiabatic section of the capillary tube.

Figures 4.1, 4.2 and 4.3 show that the lengths of heat exchange in the liquid single-phase regions range from about 1.0 m for weak heat transfer to near 1.5 m for strong heat transfer between the capillary tube and suction line. For strong heat transfer the pressure drop in the capillary tube is linear (Figure 4.3), and it means that no vaporization in the capillary tube occurs.

Pate (1982) did his experiment of a capillary tube-suction line exchanger in an opened-loop system, in which refrigerant CFC-12 flowed through the capillary tube and air through the suction line. The calculated results from the present model, as show in Figure 4.4, are good agreement with the experimental data obtained by Pate's test. The error appears to increase near the exit of the capillary tube, which may be caused by the expansion at the exit.

Experimental and numerical observations show that the temperatures of the capillary tube wall and the refrigerant in the capillary tube, T_w and T_c, are very

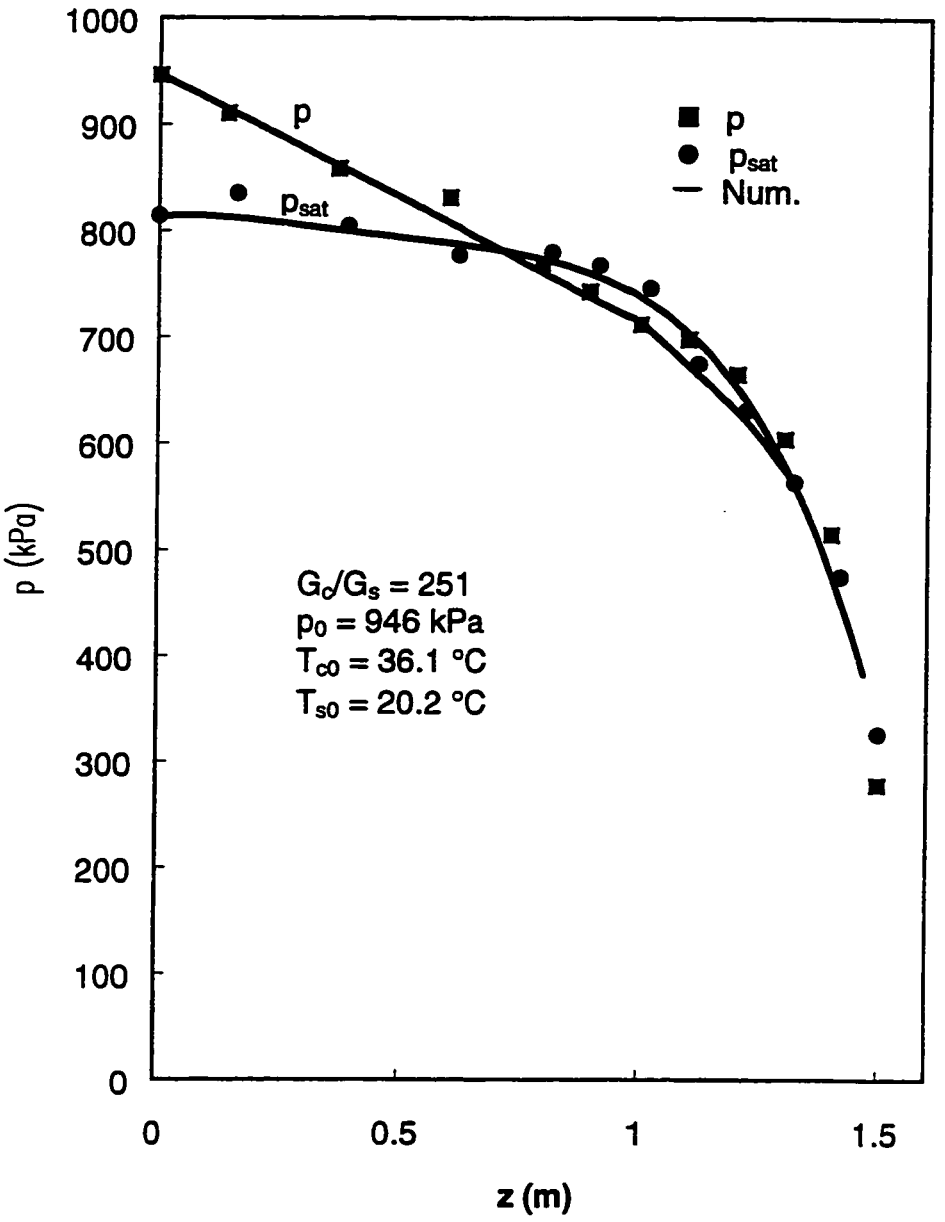

Figure 4.1 Numerical results of distributions in comparison with experimental data for $G_c/G_s = 251$, $p_0 = 946$ kPa, $T_{c0} = 36.1$ °C and $T_{s0} = 20.2$ °C

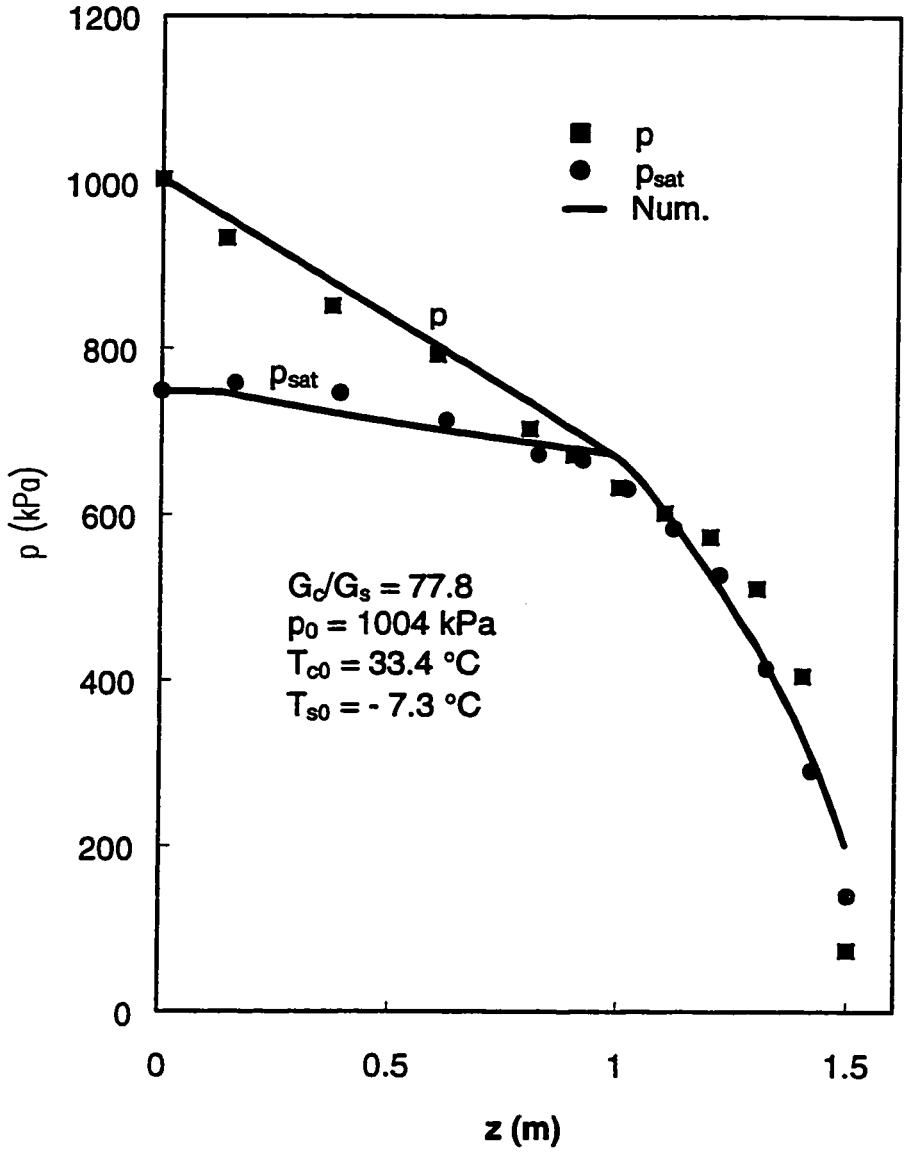

Figure 4.2 Numerical results of distributions in comparison with experimental data for $G_c/G_s = 77.8$, $p_0 = 1004$ kPa, $T_{c0} = 33.4$ °C and $T_{s0} = -7.3$ °C

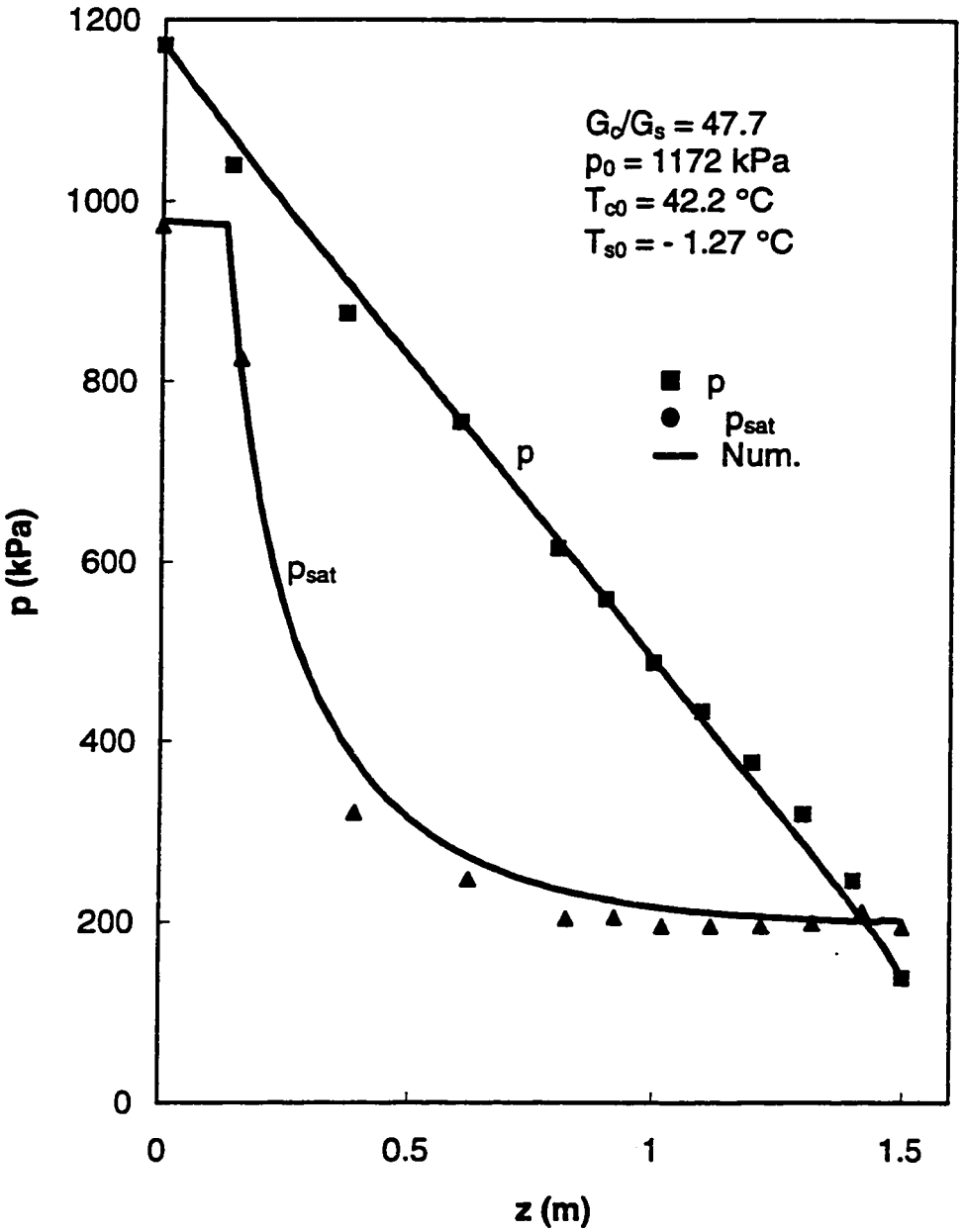

Figure 4.3 Numerical results of distributions in comparison with experimental data for $G_c/G_s = 47.7$, $p_0 = 1172$ kPa, $T_{c0} = 42.2$ °C and $T_{s0} = -1.27$ °C

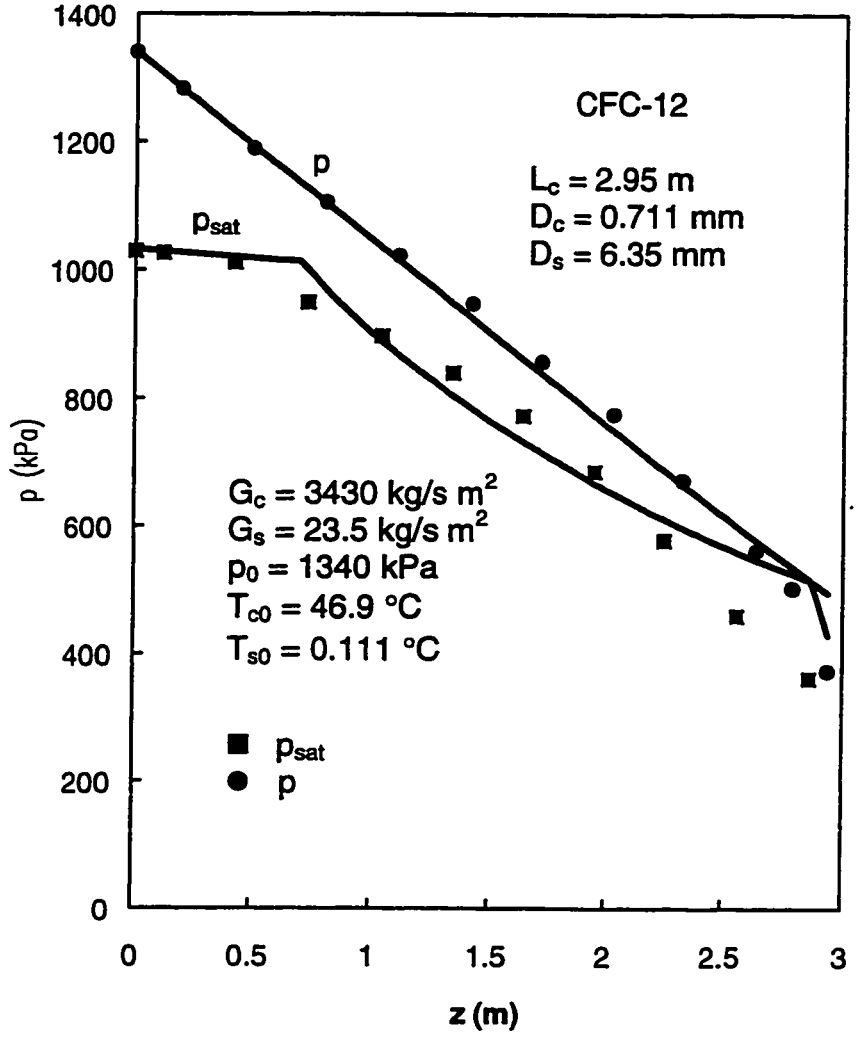

Figure 4.4 Comparison of the calculated results with the experimental data obtained by Pate (1982)

close, as shown in Figures 4.5 and 4.6 and Figure 4.7. This means that the refrigerant temperature in the capillary tube may be evaluated by means of the measurement of the wall temperature of the capillary tube with an error of about 1%. This result was also indicated in the experimental work of Chen et al. (1990).

The differences of the temperatures between the refrigerant in the capillary tube and that in the section line for the three cases studied are also presented in Figures 4.5, 4.6 and 4.7. Of special significance, for the weak heat transfer cases, G_c/G_s = 251 and 77.8 as shown in Figure 4.5 and 4.6, the heat transferred from the capillary tube to the suction line takes place mainly in the vapor-liquid two-phase flow region. However, for strong heat transfer case, G_c/G_s = 47.7 as shown in Figure 4.7, the refrigerant temperature in the capillary tube drops quickly first, then smoothly, and the refrigerant temperature in the suction line is linear. The quick decrease of the temperature in the capillary tube causes the quick decrease of the refrigerant saturated pressure (Figure 4.2), so, the inception of the vaporization moves toward the exit of the capillary tube. The temperature difference causing the heat transfer is large at the inlet of the capillary tube and decreases along the tube (Figure 4.7).

Differences that exist between the numerical and experimental results shown in these figures can be mainly attributed to one of the following reasons:

1. Errors exist in the experimental measurement of the temperatures and pressures of capillary tube and suction line.

2. Errors in the constitutive equations selected for the single-phase and

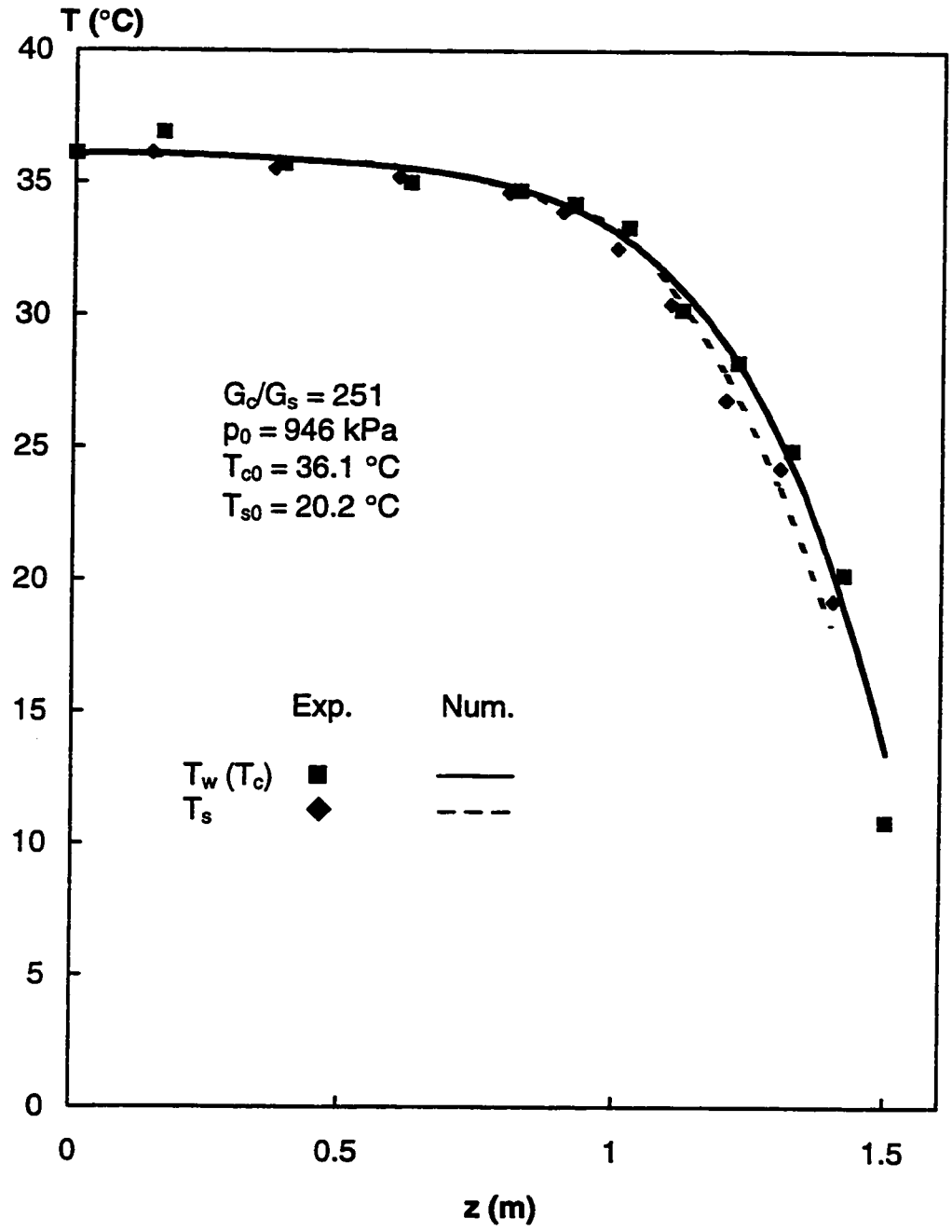

Figure 4.5 Temperature profile for numerical model results and experimental data comparison

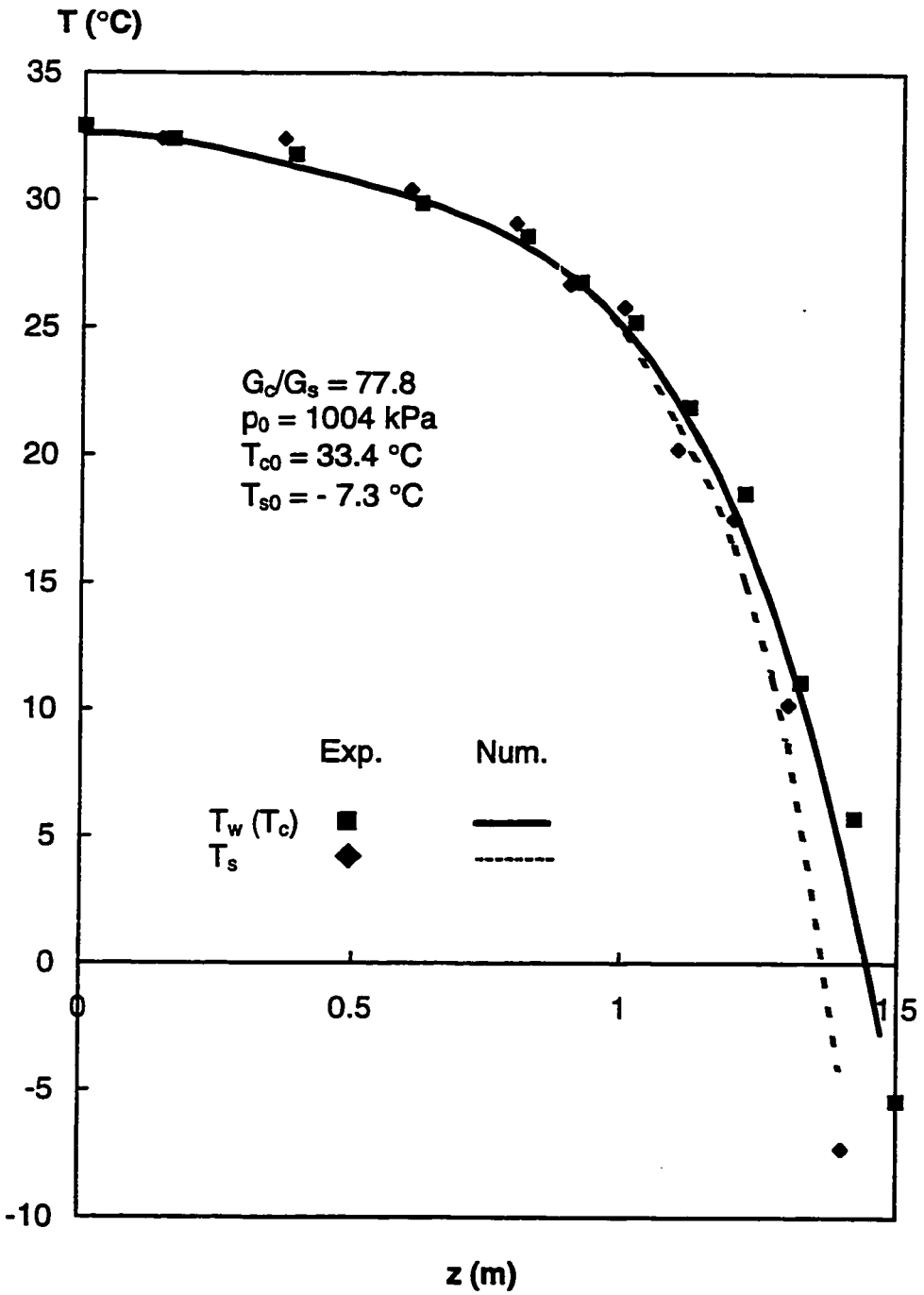

Figure 4.6 Temperature profile for numerical model results and experimental data comparison

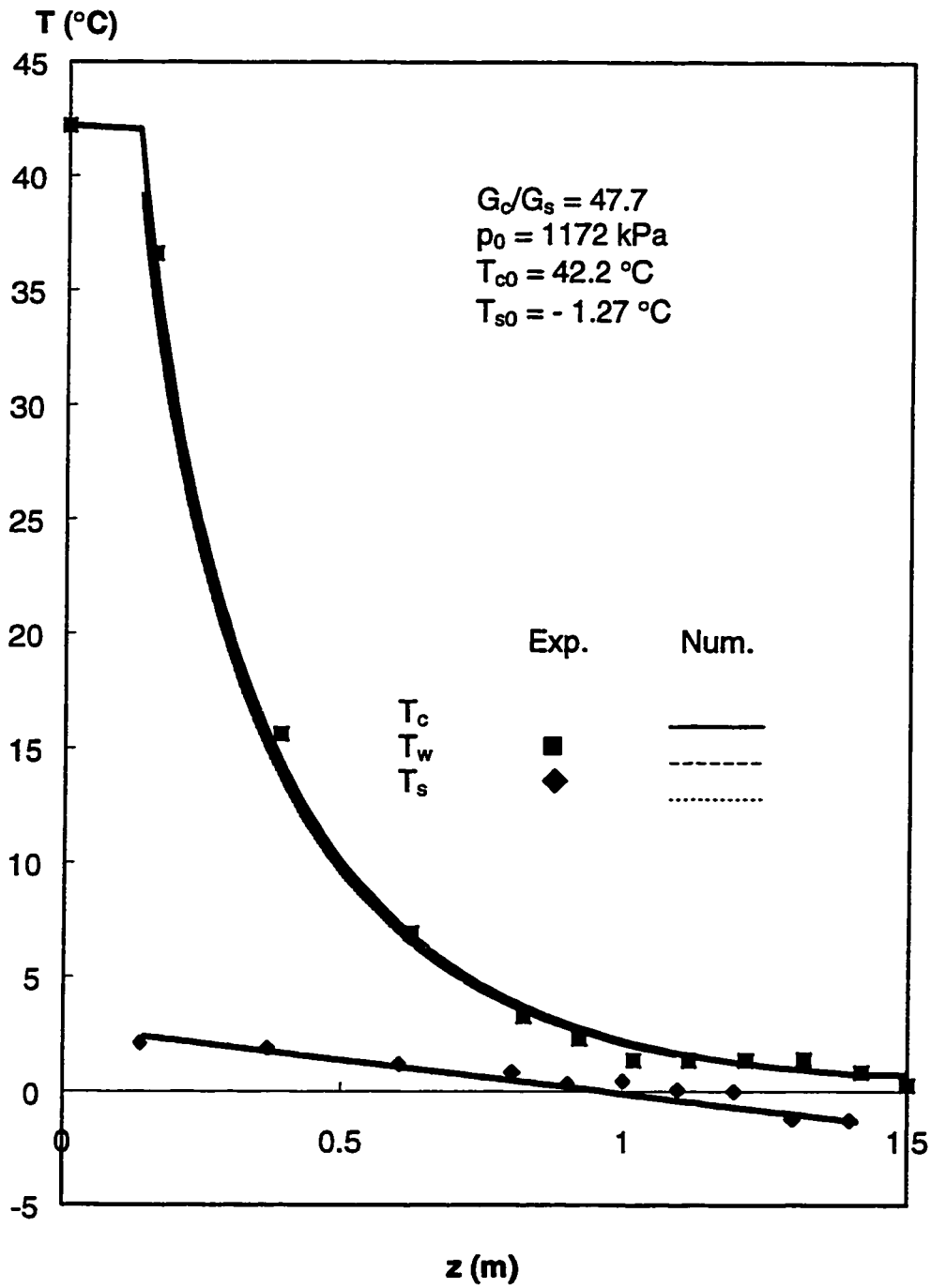

Figure 4.7 Temperature profile for numerical model results and experimental data comparison

two-phase flow regions exist.

The calculated velocities of the vapor and liquid phases along the capillary tube are shown in Figure 4.8 for the first case studied, $G_o/G_s = 251$. The vapor velocity is higher than the liquid velocity and the velocity difference increases towards the end of the capillary tube. The vapor velocity at the exit of the capillary tube is about 7.3% higher than the liquid velocity. Therefore, the vapor-liquid two-phase flow of refrigerant in capillary tubes can be considered as homogeneous flow without having a significant error (Li et al., 1990).

Figure 4.9 shows the numerical variation of the void fraction α of refrigerant HFC-134a along the capillary tube for the first case studied, $G_o/G_s = 251$. The variation of the void fraction α is not linear -- the void fraction α increases relatively fast at the beginning of vaporization and then slows down until the exit of the capillary tube. The void fraction α approaches 0.45 near the exit of the capillary tube.

Figure 4.10 indicates the numerical variation of the quality x along the capillary tube for the same case presented in Figure 4.9. The trend of the quality x is similar to the void fraction α. The quality at the exit of the capillary tube is only 0.013.

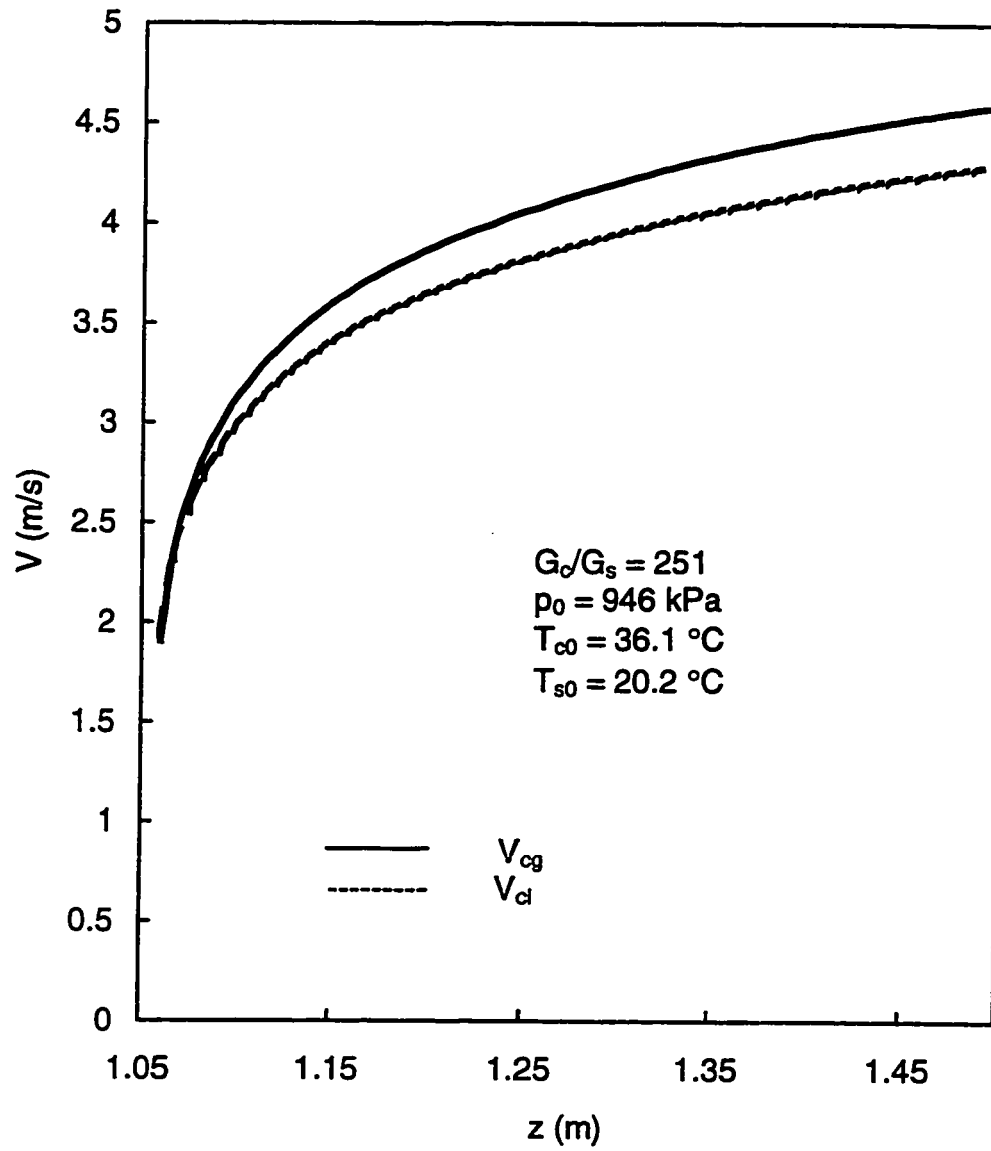

Figure 4.8 Numerical result of velocities, $z_v = 1.06$ m

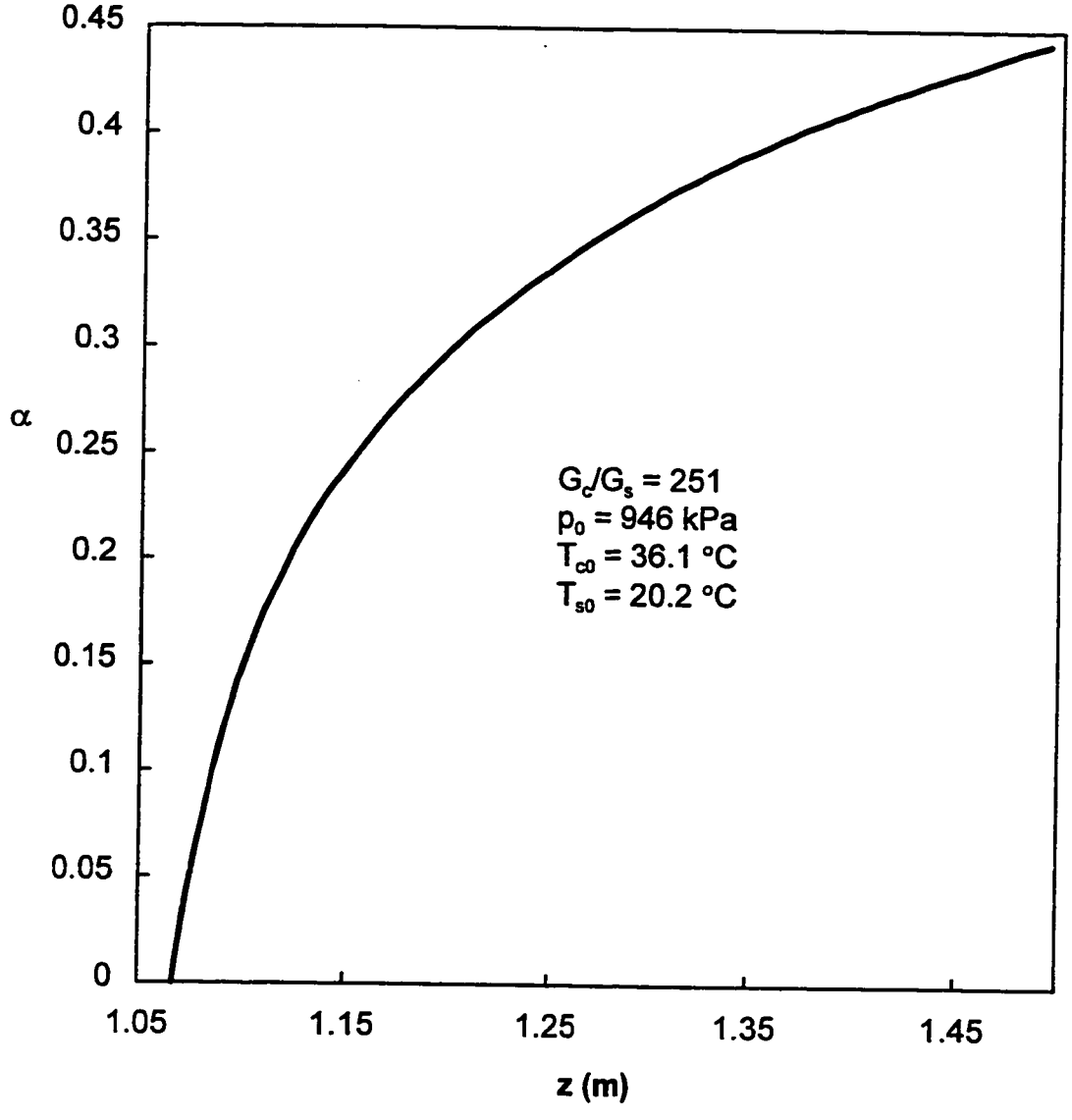

Figure 4.9 Numerical result of void fraction α, z_v = 1.06 m

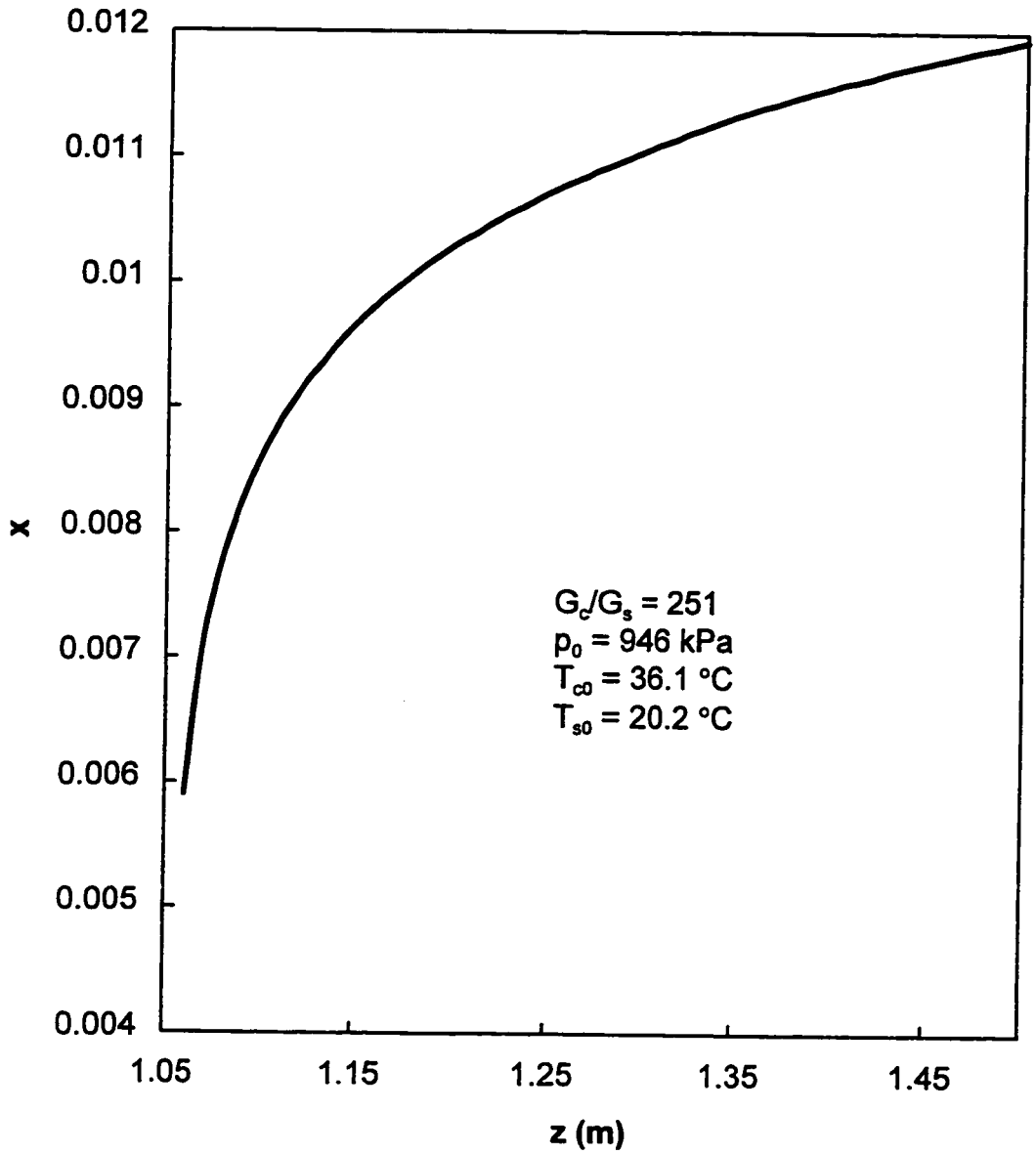

Figure 4.10 Numerical result of quality x, z_v = 1.06

4.3.2 Effect of oil in the refrigerant on the performance of an adiabatic capillary tube

In this section, the effect of oil in the refrigerant on the flowing performance in an adiabatic capillary tube is discussed. The numerical results obtained by the liquid single-phase and the vapor-liquid two-phase flow models are presented and compared with the experimental data with and without oil.

The distributions of the experimental pressure and the saturated pressure corresponding to the temperature measured along the adiabatic capillary tube with numerical results are shown in Figures 4.11 to 4.14. Figures 4.11 and 4.12 show the comparison with oil, while Figures 4.13 and 4.14 show the comparison without oil. It can be seen from the figures that the predicted distributions of the pressure and saturated pressure along the adiabatic capillary tube are in good agreement with the experimental data.

Li (1989) did his experiment of adiabatic capillary tubes in a clossed-loop system of refrigerant CFC-12. Figure 4.15 shows a good agreement of the calculated results from the present model with the experimental data obtained by Li.

Figures 4.16 illustrates the numerical results of the void fraction distributions along the capillary tube with and without oil. The void fraction α of the flow with oil is higher than that without oil. The reason is that the bubble density N_R for the case with oil is higher than that for the case without oil since

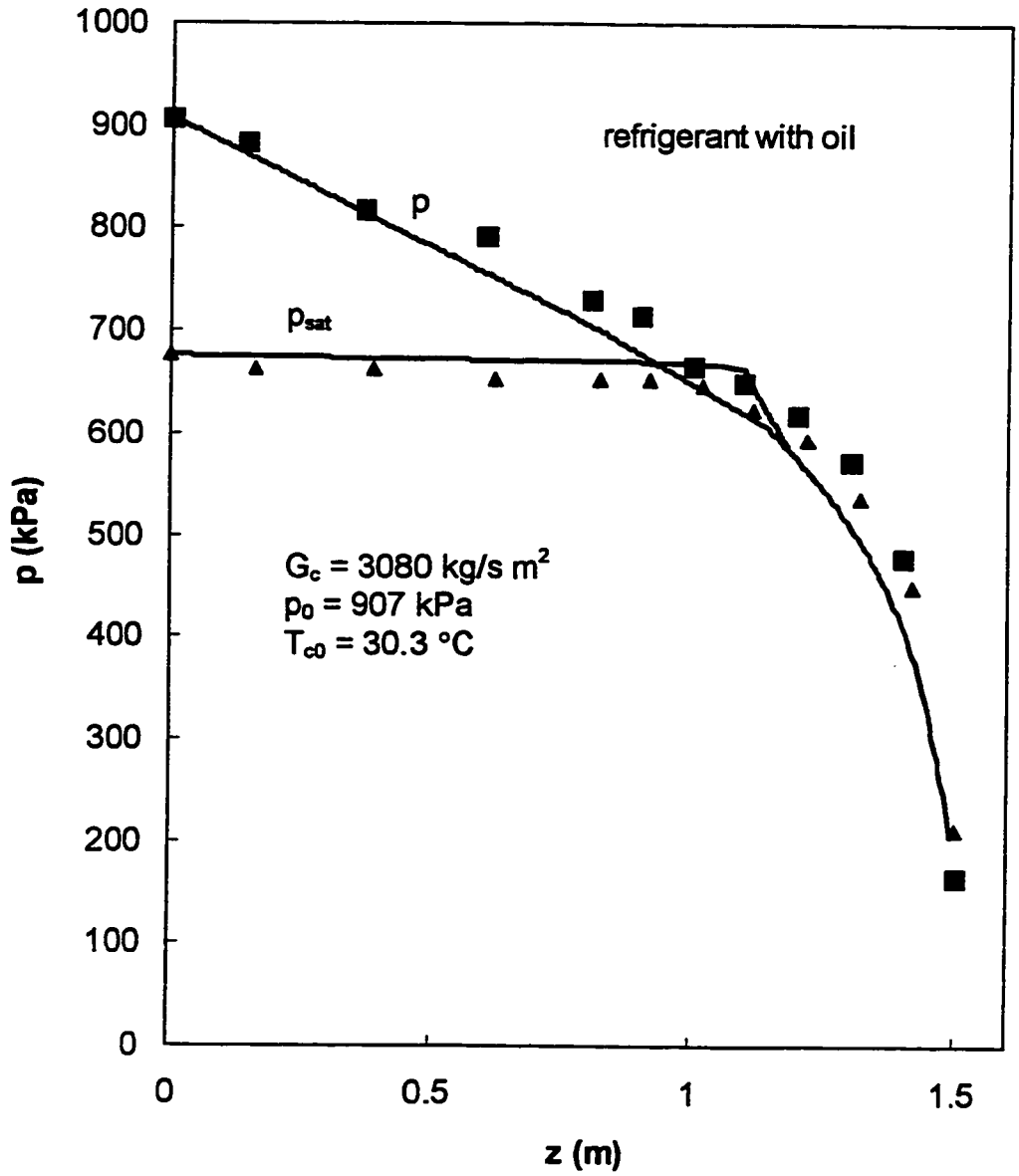

Figure 4.11 Comparison of the predicted distributions of the pressure, p, and the saturated pressure, p_{sat}, corresponding to the temperature along the tube with the experimental data of ΔT_{csub} = 5.51 °C, G_c = 3080 kg/s m^2, p_0 = 907 kPa and T_{c0} = 30.3 °C

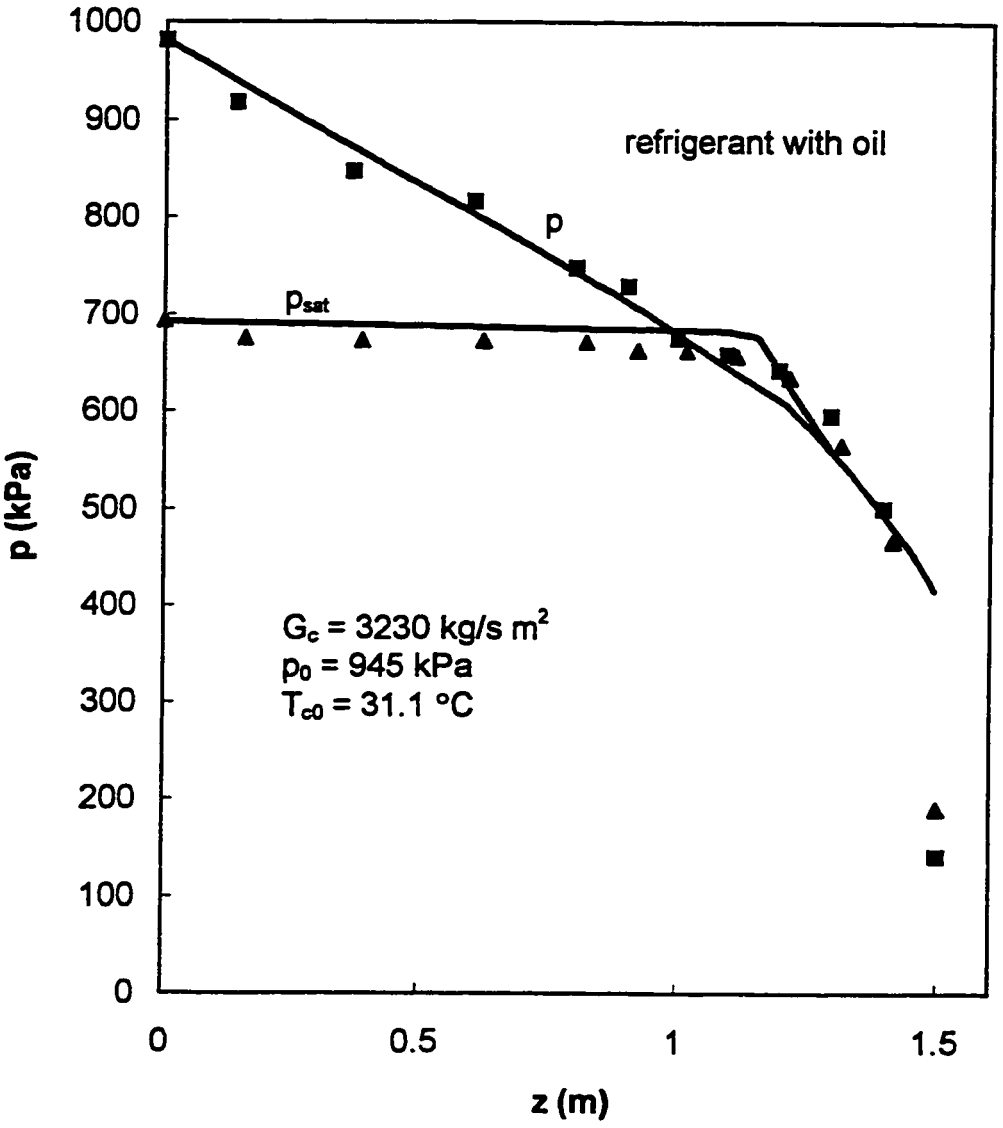

Figure 4.12 Comparison of the predicted distributions of pressure, p, and the saturated pressure, p_{sat}, corresponding to temperature along the tube with the experimental data of ΔT_{csub} = 6.2 °C, G_c = 3230 kg/s m^2, p_0 = 945 kPa and T_{c0} = 31.1 °C

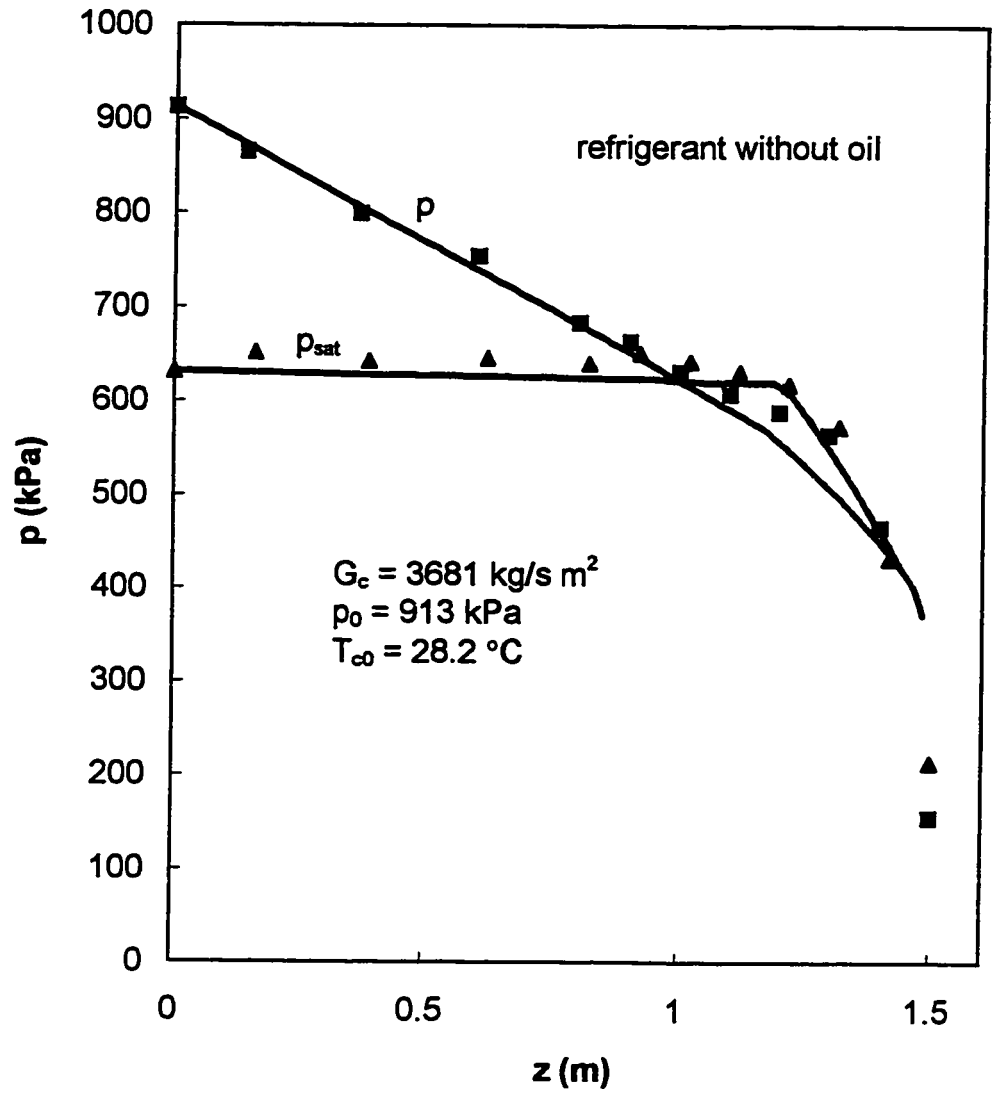

Figure 4.13 Comparison of the predicted distributions of pressure, p, and the saturated pressure, p_{sat}, corresponding to temperature along the tube with the experimental data of ΔT_{csub} = 7.85 °C, G_c = 3681 kg/s m^2, p_0 = 913 kPa and T_{c0} = 28.2 °C

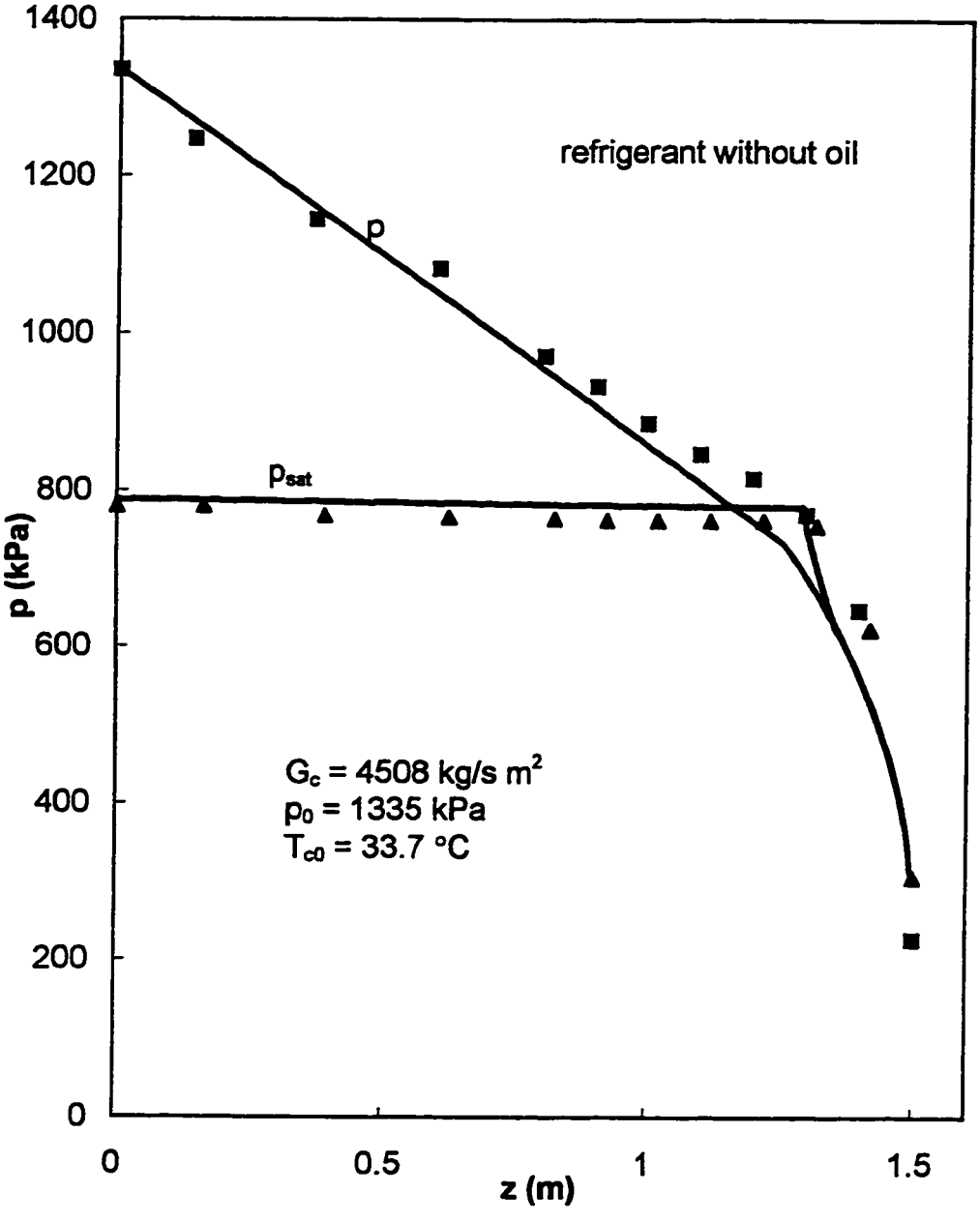

Figure 4.14 Comparison of the predicted distributions of pressure, p, and the saturated pressure, p_{sat}, corresponding to temperature along the tube with the experimental data of ΔT_{csub} = 16.8 °C, G_c = 4508 kg/s m^2, p_0 = 1335 kPa and T_{c0} = 33.7 °C

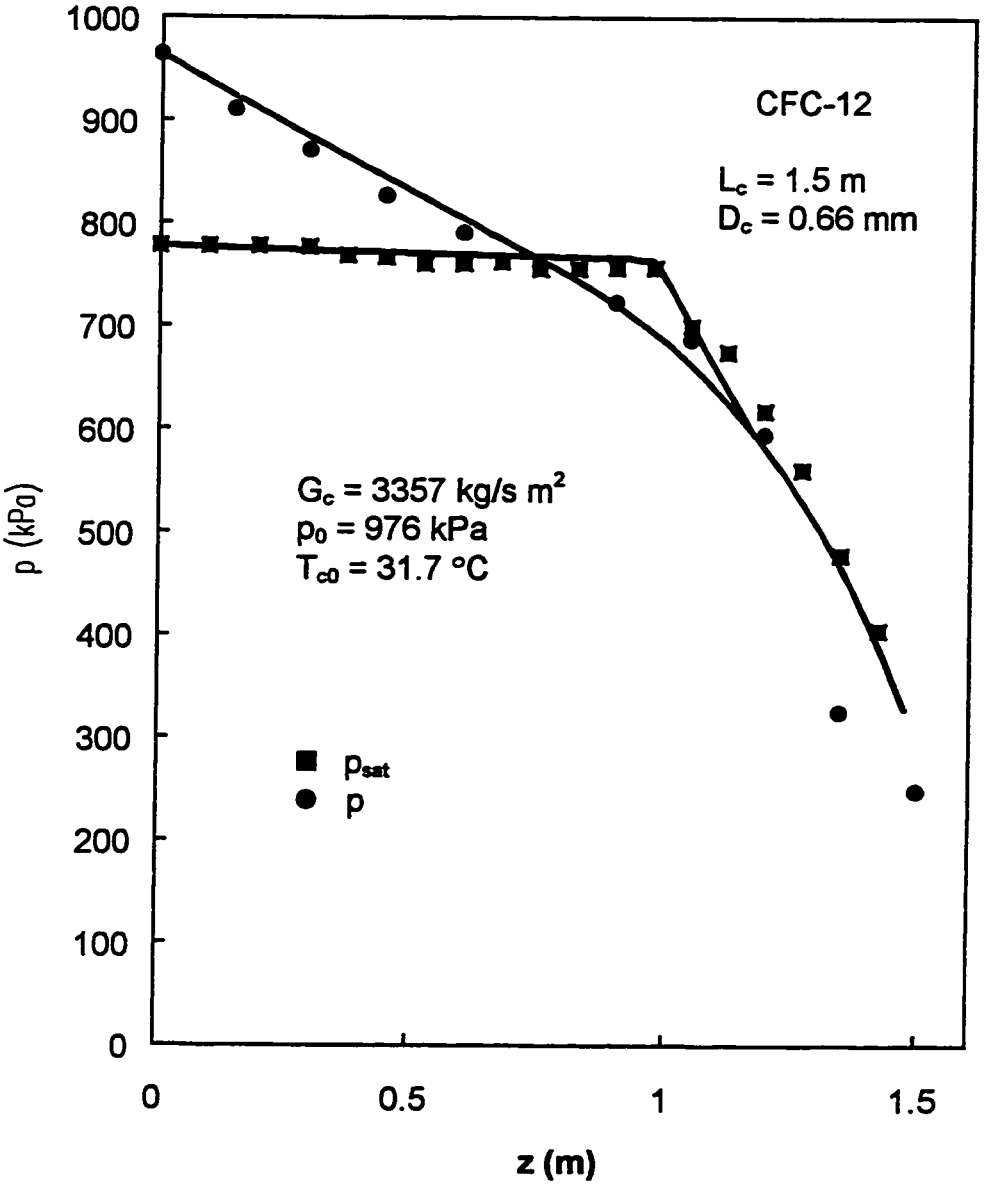

Figure 4.15 Comparison of the calculation results with the experimental data obtained by Li (1989)

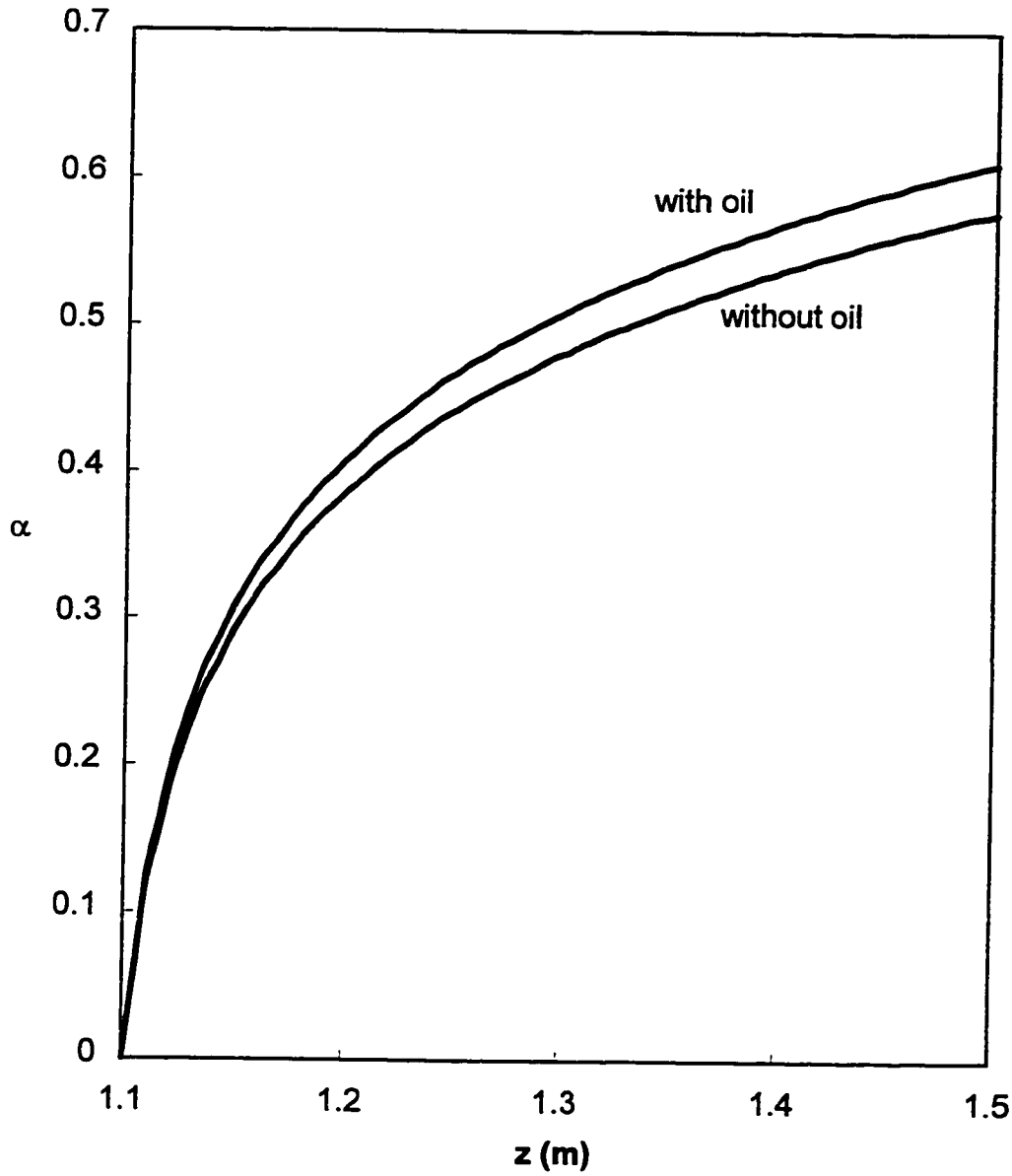

Figure 4.16 Numerical results of void fraction α, z_v = 1.10 m

the underpressure of vaporization for the case with oil is higher than that for the case without oil (Figures 3.7 to 3.9, Equation 4.45). The higher the value of α, the higher the friction resistance of the two-phase flow in the capillary tube, and the lower the mass flux of the flow. Therefore, it is expected that the mass flux of the flow in the capillary tube for the case without oil is higher than that for the case with oil, as shown in Figure 4.18.

Figure 4.17 shows that the predicted and experimental results of the mass flux, G_c, with oil at p_0 = 10 bar and p_{exit} = 0.255 bar is a function of the inlet subcooling, ΔT_{csub}. The predicted results of the mass flux agree with the experimental data, which have an average tolerance of ± 12.7%, and show that the mass flux G_c increases with an increase of the inlet subcooling temperature ΔT_{csub}. The predicted results of the mass flux G_c for different inlet pressures, p_0 = 10 and 13 bar, with and without oil are shown in Figure 4.18. It can be seen that an increase in the inlet pressure p_0 results in an increase in the mass flux. The numerical results indicate that the mass flux without oil is about 2.2% higher than that with oil. This result agrees with Wijaya's (1992) experimental results, however it is different from those obtained by Bolstad and Jordan (1948). If the effects of different refrigerants and different oils on the mass flux in the capillary tube are not considered, the difference of their results can be explained as follows (Chen et al., 1995). When refrigerant with oil flows through a capillary tube, it is expected that a thin oil film is formed on the capillary tube wall. The oil film decreases the wall roughness, and at the same time reduces

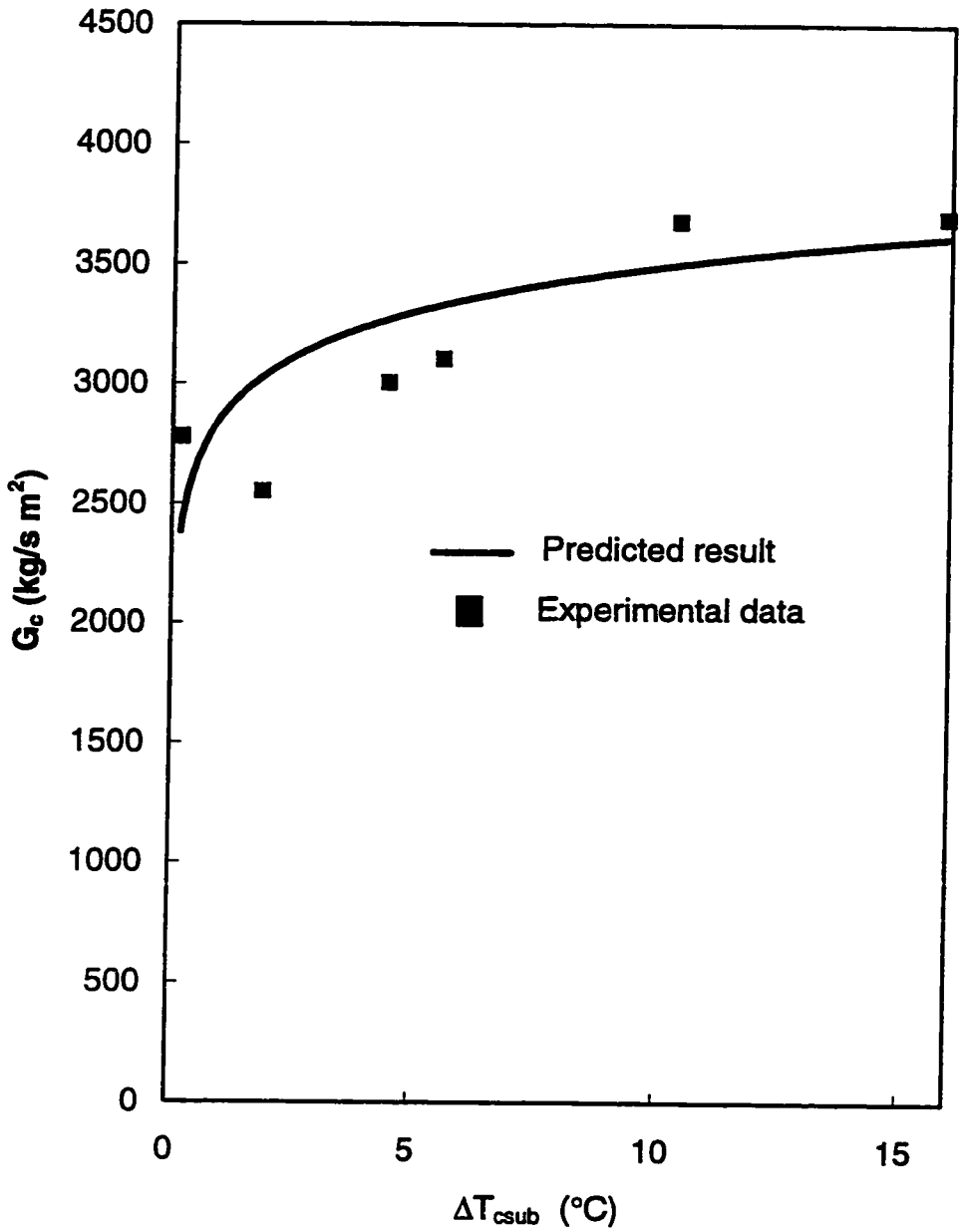

Figure 4.17 The mass flux G_c as a function of subcooling temperature ΔT_{csub} for the case with oil for $p_0 = 10$ bar and $p_{exit} = 0.255$ bar

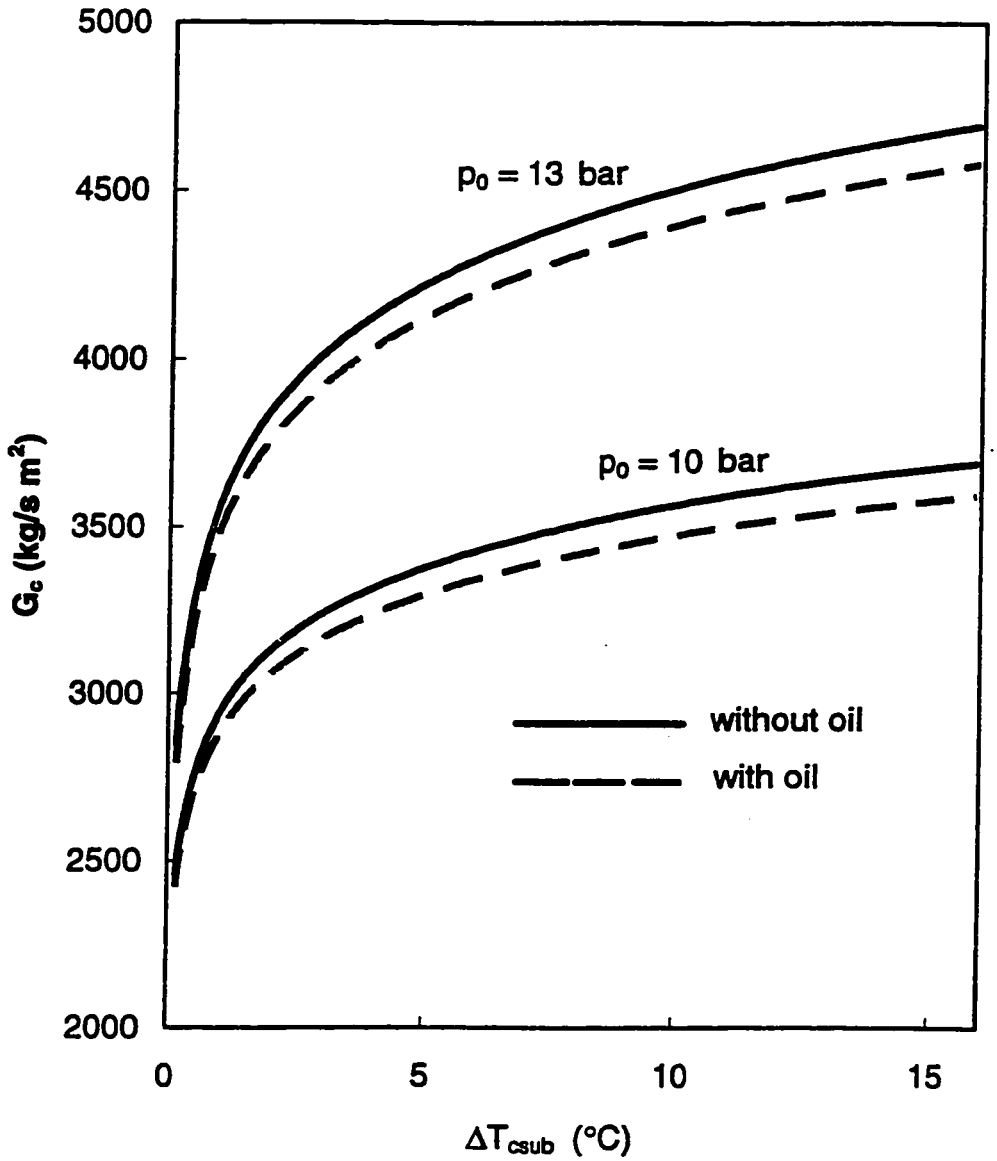

Figure 4.18 Numerical prediction of the mass flux, G_c, as function of the subcooling temperature ΔT_{csub} for p_0 = 10 and 13 bar and p_{exit} = 0.387 bar with and without oil

the flow cross-sectional area (or real diameter). A decrease of the wall roughness increases the mass flux, while a decrease in diameter results in a decrease of the mass flux. In the report of Bolstas and Jordan (1948) the presence of oil in refrigerant increased the mass flux because the factor of the decrease of the wall roughness caused by the oil film dominated the factor of reducing the flow cross-sectional area and because the capillary tube had a large diameter of 1.07 mm. In Wijaya's (1992) work (D_c = 0.66 and 0.84 mm) and the present experiment (D_c = 0.6 mm), the mass flux of refrigerant with oil decreased because the decrease in diameters becomes the dominant factor for the capillary tubes with small diameters of 0.6 mm, 0.66 mm and 0.84 mm.

CHAPTER 5

CONCLUSIONS AND RECOMMENDATIONS

The contributions and conclusions resulting from this study can be divided into two separate categories as follows:

1. Metastable flow of refrigerant in a diabatic capillary tube

A correlation of the underpressure of vaporization for a diabatic capillary tube based on the homogeneous nucleation theory is developed.

The major contribution from the experimental tests is that the distributions of pressure and temperature of refrigerant HFC-134a are measured along a diabatic capillary tube, thus it is verified for the first time that metastable flow of refrigerant through a diabatic capillary tube occurs. Experimental data is used to determine the underpressure of vaporization for a diabatic capillary tube, and verifies the numerical model. Experimental data has been obtained for the following conditions:

1. subcooled inlet

2. diabatic and adiabatic capillary tubes

3. refrigerant HFC-134a with and without oil

The following conclusions based on interpreting the experimental data and the correlation have been contributed:

1. Metastable flow of refrigerant in a diabatic capillary tube exists when heat transfer between the capillary tube and suction line is weak (G_c/G_s > 77.8).

2. When heat transfer increases (G_c/G_s = 77.8), the measured pressure curve has a point touched to the curve of saturated pressure corresponding to the measured temperature along the diabatic capillary tube. The metastable flow will vanish when G_c/G_s < 77.8 in the experiment.

3. The underpressure of vaporization increases with an increase of mass flux, G_c, and with a decrease of diameter of capillary tube. The effect of oil in the refrigerant on the metastable flow in the capillary tube increases the underpressure of vaporization.

2. Numerical model

The nonequilibrium two-fluid vapor-liquid two-phase flow models developed in Chapter 4 can be summarized and concluded as follows:

1. The model may very well describe the flashing flow of the refrigerant through the capillary tube.

2. For strong heat transfer, vaporization in the diabatic capillary tube takes place near the exit of the capillary tube.

3. Refrigerant temperature in the capillary tube can be evaluated by means of measurement of its wall temperature. The error is about 1%.

4. The void fraction of the flow in the capillary tube for the case with oil is higher than that for the case without oil.

5. The mass flux without oil is about 2.2% higher than that with oil.

Future study

The following recommendations for future study and action are based on the results of this study:

1. Develop a correlation of vapor-liquid two-phase flow convective heat transfer coefficient for flashing and cooling flow in a diabatic capillary tube.

2. Investigate the effects of refrigerant with various percentages of oil content on the performance in a capillary tube.

3. Investigate further the relationship between heat transfer and metastable flow in a diabatic capillary tube.

LIST OF REFERENCES

Alamgir, M. D. and J. H. Lienhard, (1981) Correlation of pressure undershoot during hot-water depressurization, J. Heat Transfer, Trans. ASME, Vol. 103, pp. 52-55;

Apfer, R. E., (1971) Vapor nucleation at a liquid - liquid interface, J. Chem. Phys., Vol. 54, pp. 62;

ASHRAE Handbook, (1993) Fundamentals, SI Edition, American Society of Heating, Refrigerating, and Air-Conditioning Engineerings, Inc., Atlanta, pp. 17.28-17.31;

ASHRAE Handbook, (1983) Equipment, American Society of Heating, Refrigerating, and Air-Conditioning Engineerings, Inc., Atlanta, pp. 20 - 28;

Barnea, D., Y. Luninski and Y. Taitel, (1983) Flow pattern in horizontal and vertical two phase flow in small diameter pipes, The Canadian Journal of Chemical Engineering, Vol. 61, October, pp. 617 - 620;

Blander, M and J. L. Katz, (1975) Bubble nucleation in liquids, AIChE J., Vol. 21, pp. 833 - 848;

Bolstad, M. M. and R. C. Jordan, (1949) Theory and use of the capillary tube expansion device, Part II, Nonadiabatic flow, Refrigerating Engineering, June, pp. 577-583;

Bolstad, M. M. and R. C. Jordan, (1948) Theory and use of the capillary tube expansion device, Refrigerating Engineering, Vol. 56, pp. 519-523;

Buchanan, L. B. M., (1938) Refrigerating apparatus, U. S. Patent, 2, 123, 179;

Chen, D. K. and S. Lin, (1996) Flashing flow of oil-HFC134a mixture in a capillary tube: numerical simulation and experiment, Submitted to International Journal of Refrigeration;

Chen, D. K., S. Lin and H. L. Yu, (1995) An experimental study of the effect of oil on mass flux of refrigerant flowing through an adiabatic capillary tube, Proceedings of the International Conference on Energy and Environment, Shanghai, China, pp. 387 - 391;

Chen, Y., Z. Y. Chen and Z. H. Chen, (1988) The status and development of the research on refrigerant two-phase flow in diabetic capillary tubes, J. Shanghai Institute of Mechanical Engineering, Vol. 10, No. 1, pp. 55-64;

Chen, Z. H., R. Y. Li, S. Lin and Z. Y. Chen, (1990) A correlation for metastable flow of refrigerant R12 through capillary tubes, ASHRAE Transaction, Vol. 96, Part 1, pp. 550 - 554;

Churchill, S. W., (1977) Frictional equation spans all fluid flow regimes, Chem. Engng, Vol. 84, 91-92;

Colburn, A. P., (1933) A method of correlating forced convection heat transfer data and a comparison with fluid friction, Trans. AIChE, Vol. 29, p. 174;

Cole, R., (1979) Homogeneous and heterogeneous nucleation, in Boiling Phenomena, Vol. 1, Hemisphere, pp. 71 - 88;

Cole, R., (1974) Boiling nucleation, Advances in heat transfer, Vol. 10, Academic Press, Inc., New York;

Collier, J. G., (1972) Convective boiling and condensation, McGraw-Hill Book Company, UK;

Cooper, L., C. K. Chu and W. R. Brisken, (1957) Simple selection method for capillary derived from physical flow conditions, Refrigerating Engineering, Vol. 65, No. 7, pp. 37-41, 88, 92-104, 107;

Cui, X. H., R. Y. Li and D. K. Chen, (1993) Vapor-liquid two-phase Convective heat transfer coefficient of refrigerant flowing through a diabatic capillary tube, Report of Shanghai Institute of Mechanical Engineering;

Dagan, R., E. Elias, E. Wacholder and S. Olek, (1993) A two-fluid model for critical flashing flows in pipes, Int. J. Multiphase Flow, Vol. 19, No. 1, pp 15-25;

Dittus, F. W. and L. M. K. Boelter, (1930) Univ. Calif., Berkeley, Publ. Eng., vol. 2, p. 443;

Dobran, F., (1987) Nonequilibrium modeling of two-phase critical flow in tubes, ASME Journal of Heat Transfer, Vol. 109, Aug., pp. 731-738;

Dudley, J. C., (1962) A photographic study of the two-phase flow of Freon in small bore tube, Master Thesis, Department of Mechanical Engineering, University of Wisconsin;

Elias, E. and G. S. Lellouche, (1994) Two-phase critical flow, Int. J. Multiphase flow, Vol. 20, Annual Reviews in Multiphase Flow 1994, pp. 91 - 128;

Elias, E. and P. L. Chambre, (1984) A mechanical non-equilibrium model for two-phase critical flow, Int. J. Multiphase flow, Vol. 10, No. 1, pp. 21 - 40;

Erth, R. A., (1969) Two phase flow in refrigerant capillary tubes: analysis and prediction, Ph. D. thesis, Purdue University;

Escanes, F., C.D. Perez-Segarra and A. Oliva, (1995) Numerical simulation of capillary-tube expansion devices, Int. J. Refrig., Vol. 18, No. 2, pp. 113-122;

Ewan B. C. R. and K. Moodie, (1990) Evaluation of a numerical critical pipe flow model with wall nucleation, Int. J. Multiphase Flow, Vol. 16, No. 5, pp. 751 - 759;

Fisher, J., (1948) The fracture of liquids, J. Appl. Phys., Vol. 19, pp. 1062;

Frenkel, J., (1955) Kinetic theory of liquids, Chapter VII, Dover Publications, New York;

Fox, R. W. and A. T. McDonald, (1985) Introduction to fluid mechanics, 3rd Edition, John Wiley & Sons, New York;

Goldstein, S. D., (1981) A computer simulation method for describing two - phase flashing flow in small diameter tubes, ASHRAE trans., Vol. 87, Pt. 2, pp. 51-60;

Hetsroni, G., (1982) Handbook of multiphase systems, Hemisphere, New York, pp. 6.5 - 26;

Hopkins, N. E., (1950) Rating the restrictor tube-method of determining flow capacities for freon-12 and freon-22, Refrigerating Engineering, Vol. 58, No. 11, pp. 1087-1095;

Jarvis, T. J., M. D. Donohue and J. L. Katz, (1975) Bubble nucleation mechanisms of liquid droplets superheated in other liquids, J. colloid Interf. Sci., Vol. 50, pp. 359;

Jones, O. C., (1980) Flashing inception in flowing liquids, ASME Journal of Heat Transfer, Vol. 102, Aug., pp. 439-444;

Katz, D. L. and M. Blander, (1973) Condensation and boiling: corrections homogeneous nucleation theory for nonideal gases, J. Colloid Interf. Sci., Vol. 42, pp. 496;

Koizumi, H. and K. Yokoyama, (1980) Characteristics of refrigerant flow in a capillary tube, ASHRAE trans., Vol. 86, part 2, pp. 19-27;

Kuehl, S. J. and V. W. Goldschmidt, (1990) Steady flow of R-22 through capillary tubes: test data, ASHRAE trans., Vol. 96, Pt. 1, pp. 719-728;

Kuehl, S. J. and V. W. Goldschmidt, (1991) Modeling of steady flows of R-22 through capillary tubes, ASHRAE trans., Vol. 97, Pt. 1, pp. 139-148;

Kuipjers, L. J. M. and M. J. P. Janssen, (1983) Influence of thermal non-equilibrium on capillary tube mass flow, Proceedings of XVIth International Congress of Refrigeration, Commission B2, Paris, pp. 307 - 315;

Li, R. Y., S. Lin and Z. H. Chen, (1990) Numerical modeling of thermodynamic non-equilibrium flow of refrigerant through capillary tubes, ASHRAE Trans., V. 96, Pt. 1;

Li, R. Y., S. Lin, Z. Y. Chen and Z. H. Chen, (1990) Metastable flow of R12 through capillary tubes, Int. J. Refrig., Vol. 13, May, pp. 181 - 186;

Li, R. Y., (1989) Research on thermodynamic nonequilibrium two-phase flow of refrigerant through capillary tubes, Ph.D. Thesis, East China University of Technology;

Lin, S., (1992) Similarity and modeling in engineering systems, Lecture Notes, Concordia University;

Lin, S., C. C. K. Kwok, R. Y. Li, Z. H. Chen and Z. Y. Chen, (1990) Local frictional pressure drop during vaporization of R-12 through capillary tubes, Int. J. Multiphase flow, Vol. 17, No. 1, pp. 95-102;

Maczek, K., Z. Krolicki and E. Sochanecka, (1983) Model of throttling capillary tube with metastable process, Proceedings of the XVIth International Congress of Refrigeration, commission B2, Paris, pp. 154-161;

Maczek, K. and Z. Krolicki, (1981) Non-adiabatic process in throttling capillary tubes used in packaged units, Proc. of the IIR-Meeting, comm. B2, Essen, FRG;

McCloy, G. S., (1939) Refrigeration apparatus, U. S. Patent, 2, 181, 856;

Melo, C., R. T. S. Ferreira and R. H. Pereira, (1992) Modeling adiabatic capillary tubes: a critical analysis, Proceedings of the 1992 Int. Con. energy Efficiency and New Ref., Vol. I, Indiana, USA, pp. 113-122;

Mikol, E. P. and J. C. Dudley, (1964) A visual and photographic study of the inception of vaporization in adiabatic flow, J. Basic Engineering, Trans. ASME, June, pp. 257 - 264;

Mikol, E. P. and J. C. Dudley, (1963) Adiabatic single and two-phase flow in small bore tubes, ASHRAE Journal, Vol. 5, No. 11, pp. 75-86;

Modell, M. and R. C. Reid, (1983) Thermodynamics and its application, Prentice - Hall, Inc., pp. 98 - 108, 408 - 413;

Moore, G. R., (1959) Vaporization of superheated drops in liquids, AIChE J., Vol. 5, pp. 458;

Niaz, R. H. and de V. Davis, (1969) Adiabatic two phase flow in a capillary tube, Concurrent Gas-Liquid Flow, Symposium of the Canada Society of Chemical Engineers, University of Waterloo, Canada, Vol. 1, pp. 259 - 269;

Pasqua, P. F., (1953) Metastable flow of Freon-12, Refrigerant Engineering, Vol. 61, No. 10, pp. 1084 - 1088;

Pate, M. B. and D. R. Tree, (1984) A linear quality model for capillary tube-suction line heat exchanger, ASHRAE Transactions, Vol. 90, part. 2A, pp. 3 - 17;

Pate, M. B. and D. R. Tree, (1984) An analysis of pressure and temperature measurements along a capillary tube - suction line heat exchanger, ASHRAE Transactions, Vol. 90, part. 2A, pp. 291 - 301;

Pate, M. B. and D. R. Tree, (1983) An experimental analysis of a capillary tube-suction line heat exchanger, Proc. of the 16th Int. Congr. of Refrig., Comm. 132, Paris, France, pp. 709 - 715;

Pate, M. B., (1982) A theoretical and experimental analysis of capillary tube-suction line heat exchanger, Ph. D. Thesis, Purdue University;

Qian, B. J., Y. W. Wu, J. F. Chang and Y. M. Ding, (1984) Handbook on heat transfer, HD-JY Publications, Beijing;

Rezk, A. M. A. and A. G. Awn, (1979) Investigation on flow of R-12 through capillary tubes, XIIth International Congress of Refrigeration, Venice, Proceedings Vol. II, pp. 443 - 452;

Richter, H.J., (1983) Separated two-phase flow model: application to critical two-phase flow, Int. J. Multiphase flow, Vol. 9, No. 5, pp. 511-530;

Riznic J. R. and M. Ishii, (1989) Bubble number density and vapor generation in flashing flow, Int. J. Heat Mass Transfer, Vol. 32, No. 10, pp. 1821 - 1833;

Schulz, U. W., (1985) State of the art: the capillary tube for, and in, vapor compression systems, ASHRAE Trans., Vol. 91, Part 1, pp. 92 - 105;

Skripov, L. A., (1974) Metastable liquid, John Wiloy and Sons, New Your;

Spiegel, M. R., (1968) Mathematical handbook of formulas and tables, McGraw - Hill Book company, New York;

Swart, R. H., (1946) Capillary tube heat exchangers, (1946) Refrigerating Engineering, September, pp. 221 - 224, 248, 249;

Sweedyk, J. M., (1981) Capillary tube - their standardization and use, ASHRAE Trans., Vol. 87, part 1, pp. 1069 - 1076;

Whitesel, H. A., (1957) Capillary two-phase flow-part II, Refrigerating Engineering, Vol. 65, No. 9, pp. 35-40;

Wijaya, M., (1992) Adiabatic capillary tube test data for HFC-134a, Proceedings 1992 International Refrigeration Conference, pp. 63-71;

Yan, Q. S. and X. L. Wang, (1991) Studies on the behavior of a capillary tube in a small refrigeration system, The XVIIIth International Congress of Refrigeration, Montreal, Canada.

IMAGE EVALUATION TEST TARGET (QA-3)

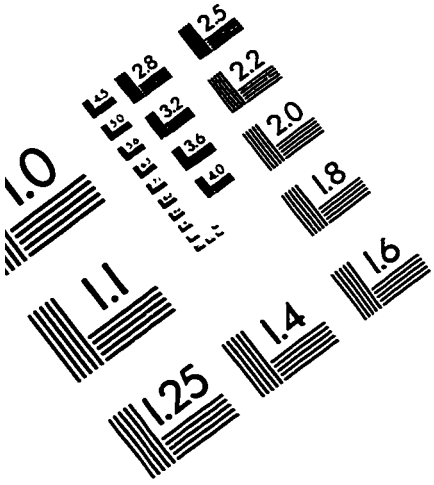

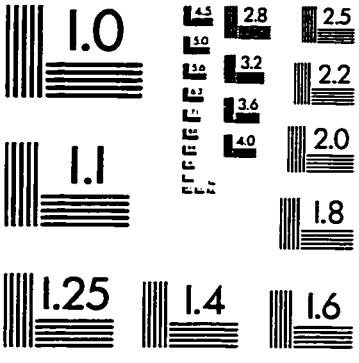

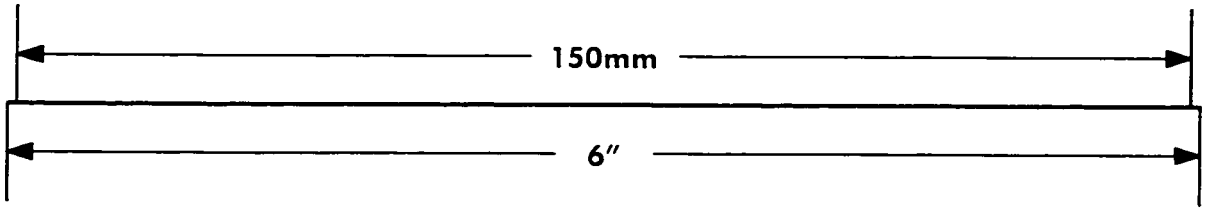

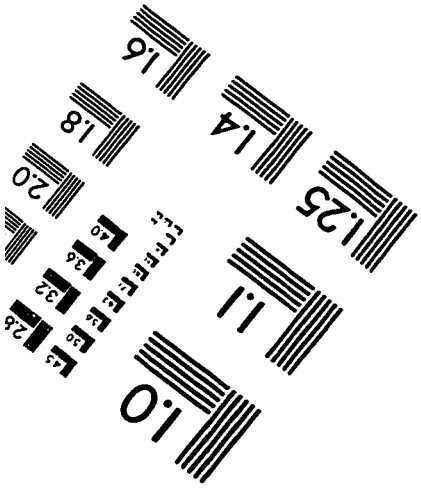

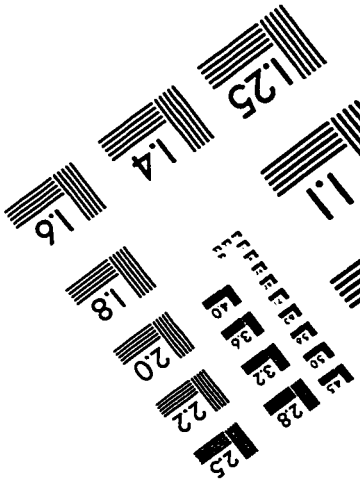

APPLIED IMAGE, Inc
1653 East Main Street
Rochester, NY 14609 USA
Phone: 716/482-0300
Fax: 716/288-5989